New Jersey Institute of Technology
Digital Commons @ NJIT

Dissertations | Theses and Dissertations

Fall 1997

Automobile air bag inflation system based on fast combustion reaction

Yacoob Tabani
New Jersey Institute of Technology

Follow this and additional works at: https://digitalcommons.njit.edu/dissertations

 Part of the Mechanical Engineering Commons

Recommended Citation
Tabani, Yacoob, "Automobile air bag inflation system based on fast combustion reaction" (1997). *Dissertations*. 1051.
https://digitalcommons.njit.edu/dissertations/1051

This Dissertation is brought to you for free and open access by the Theses and Dissertations at Digital Commons @ NJIT. It has been accepted for inclusion in Dissertations by an authorized administrator of Digital Commons @ NJIT. For more information, please contact digitalcommons@njit.edu.

Copyright Warning & Restrictions

The copyright law of the United States (Title 17, United States Code) governs the making of photocopies or other reproductions of copyrighted material.

Under certain conditions specified in the law, libraries and archives are authorized to furnish a photocopy or other reproduction. One of these specified conditions is that the photocopy or reproduction is not to be "used for any purpose other than private study, scholarship, or research." If a, user makes a request for, or later uses, a photocopy or reproduction for purposes in excess of "fair use" that user may be liable for copyright infringement,

This institution reserves the right to refuse to accept a copying order if, in its judgment, fulfillment of the order would involve violation of copyright law.

Please Note: The author retains the copyright while the New Jersey Institute of Technology reserves the right to distribute this thesis or dissertation

Printing note: If you do not wish to print this page, then select "Pages from: first page # to: last page #" on the print dialog screen

NJIT
New Jersey's Science &
Technology University

The Van Houten library has removed some of the personal information and all signatures from the approval page and biographical sketches of theses and dissertations in order to protect the identity of NJIT graduates and faculty.

ABSTRACT

AUTOMOBILE AIR BAG INFLATION SYSTEM BASED ON FAST COMBUSTION REACTIONS

by
Yacoob Tabani

Current automobile air bag inflator technology is complex, expensive and environmentally unsafe. A new and novel air bag inflator based on fast combustion reactions of methane-oxygen mixtures has been developed and studied. The thermodynamics and mass flow parameters of this new inflator have been modeled and found to be in agreement with experimental results.

The performance of the fast combustion inflator was evaluated in terms of pressure-time relationships inside the inflator and in a receiving tank simulating an air bag as well as the temperature-time relationship in the tank.

In order to develop this fast combustion inflator, several critical issues were studied and evaluated. These included the effects of stoichiometry, initial mixture pressure and extreme hot and cold conditions. Other design and practical parameters, such as burst disk thickness and type, ignition device, tank purging gas, concentration of carbon monoxide produced and severity of temperature in the tank were also studied and optimized. Several inflator sizes were investigated and found to meet most of the requirements for a successful air bag inflator.

A theoretical and integrated model has been developed to simulate the transient pressure and temperature as well as the mass flow rate from the inflator to the tank. The model is based on the change in the internal energy inside the inflator and the receiving

tank as the mass flows from the inflator to the tank. The model utilizes the Chemical Equilibrium Compositions and Applications code developed by NASA to estimate the equilibrium conditions in the inflator. A large volume of experimental results made at different conditions were found to be in agreement with the integrated model.

The fast combustion inflator developed during this research is simple in principle and construction and is environmentally attractive.

AUTOMOBILE AIR BAG INFLATION SYSTEM BASED ON FAST COMBUSTION REACTIONS

by
Yacoob Tabani

A Dissertation
Submitted to the Faculty of
New Jersey Institute of Technology
in Partial Fulfillment of the Requirements for the Degree of
Doctor of Philosophy

Department of Mechanical Engineering

October 1997

Copyright © 1997 by Yacoob Tabani

ALL RIGHTS RESERVED

APPROVAL PAGE

AUTOMOBILE AIR BAG INFLATION SYSTEM BASED ON FAST COMBUSTION REACTIONS

Yacoob Tabani

Dr. Mohamed E. Labib, Dissertation Advisor — Date
Professor of Civil and Environmental Engineering, New Jersey Institute of Technology

Dr. Rong Y. Chen, Committee Member — Date
Professor of Mechanical Engineering, New Jersey Institute of Technology

Dr. John V. Droughton, Committee Member — Date
Professor of Mechanical Engineering, New Jersey Institute of Technology

Dr. Pasquale J. Florio, Committee Member — Date
Associate Professor of Mechanical Engineering, New Jersey Institute of Technology

Dr. Ralph Hensler, Committee Member — Date
Director of Engineering Technology, Breed Technologies, Inc., Boonton, New Jersey

BIOGRAPHICAL SKETCH

Author : Yacoob Tabani

Degree : Doctor of Philosophy

Date : October 1997

Undergraduate and Graduate Education :

- Doctor of Philosophy in Mechanical Engineering,
  New Jersey Institute of Technology, Newark, New Jersey, 1997

- Master of Science in Mechanical Engineering,
  New Jersey Institute of Technology, Newark, New Jersey, 1993

- Bachelor of Engineering in Mechanical Engineering,
  N. E. D. University of Engineering and Technology, Karachi, Pakistan, 1989

Major : Mechanical Engineering

To Dr. M. E. Labib and my beloved family

ACKNOWLEDGMENT

I would like to thank a few of those who aided in the completion of this work : Dr. Labib for his inspiration, encouragement and patience; Dr. Florio for serving as the chairman of the committee and also for his copious assistance; Dr. Chen, Dr. Droughton and Dr. Hensler for actively participating in my committee; Bart Adams for his help throughout this work and for taking the pictures of my experimental set-up; the entire staff of Breed Technologies, Inc., Boonton, New Jersey for their assistance and support.

Thanks also to Breed Technologies, Inc. for financially supporting this work.

TABLE OF CONTENTS

TABLE OF CONTENTS
(Continued)

TABLE OF CONTENTS
(Continued)

TABLE OF CONTENTS
(Continued)

TABLE OF CONTENTS
(Continued)

LIST OF TABLES

LIST OF TABLES
(Continued)

LIST OF FIGURES

LIST OF FIGURES
(Continued)

LIST OF FIGURES
(Continued)

LIST OF FIGURES
(Continued)

CHAPTER 1

INTRODUCTION

1.1 Objective

The objective of this dissertation is to develop and study a new automobile air bag inflator based on fast combustion reactions of methane-oxygen mixtures. The combustion is performed by forced ignition using an electric match as a source of ignition.

The performance of the inflator is evaluated in terms of pressure-time relationships inside the inflator and in a receiving tank simulating an air bag as well as the temperature-time relationship in the tank. Several important issues related to inflator design are studied and evaluated. These include the effects of stoichiometry, initial mixture pressure and extreme hot and cold conditions. Other practical issues, such as the concentration of carbon monoxide produced and the severity of temperature in the tank are also studied and optimized.

A theoretical model has been developed to simulate the experimental results and to calculate the mass flow rate from the inflator to the tank. The model is based on the change in the internal energy inside the inflator and the tank as the mass flows from the inflator to the tank.

In this chapter, some general information about air bags is given first. This includes the safety aspect, brief history, elements and types of air bags as well as the types and design requirements of air bag inflators. This is followed by a discussion on current commercial inflator system and the novel combustion approach of this research. In the

end, a description of previous relevant work in this field is given and the present work is discussed.

1.2 General Information about Air Bags

Automobile safety is among the major concerns in present day society. Present day automobiles are equipped with a variety of passive safety systems. These systems do not require any intervention of the occupant to be activated. Figure 1.1 shows different types of passive safety systems. Air bags belong to the class of passive restraint systems or supplemental restraint systems (SRS).

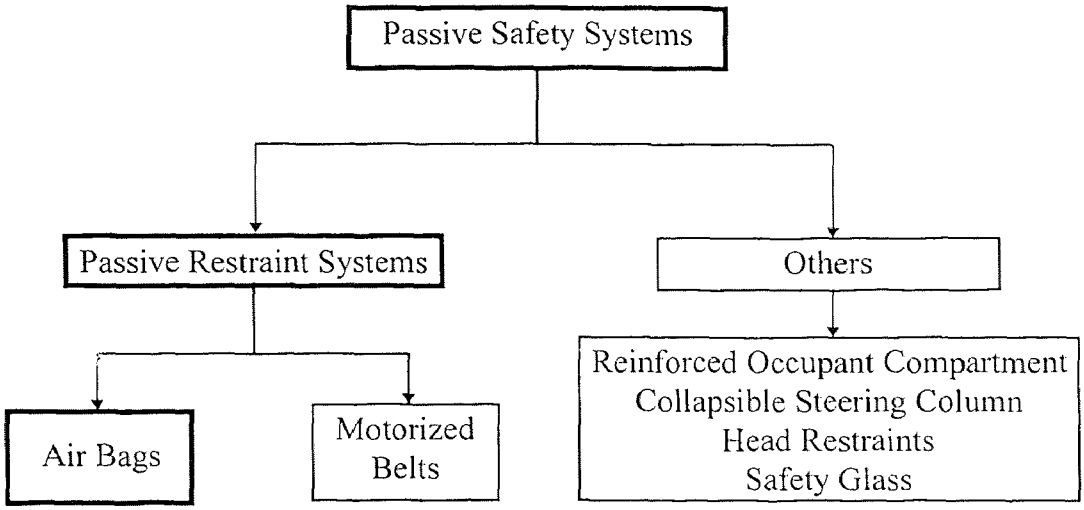

Figure 1.1 Types of passive safety systems

Air bags or supplemental inflatable restraints (SIR) are designed to supplement the protection offered by seat belts. Although seat belts should always be used as the primary means of protection, air bags are necessary because belts allow some occupant movement as they pull tightly around their reels. In addition, there is some stretch designed into seat belts to keep people from stopping abruptly in crashes [1]. Because of this combination of looseness and stretch, belted front-seat occupants can still move

forward enough in crashes to hit the steering wheel, instrument panel or windshield. Air bags reduce the level of the chest's and head's acceleration due to inertia incurred by the occupant during the collision. The air bags perform this function by creating energy-absorbing buffers between the occupants and the hard interior surfaces of vehicles [2].

Most air bags are designed to inflate in crashes equivalent to hitting a solid barrier at 10-12 miles per hour (mph). Mercedes and BMW use different inflation thresholds depending on whether or not people are using their seat belts. In these cars, thresholds of 10-12 mph are used for unbelted occupants but thresholds are higher (about 16 mph) for people with belts because they are unlikely to be injured in crashes at slower speeds [2].

1.2.1 Safety Aspect of Air Bag

Air bags have proven to be highly effective in reducing fatalities from frontal crashes. Frontal crashes result in 64 percent of all driver and right front passenger fatalities [3]. As of year-end 1996, air bags had inflated in about 1.2 million vehicles involved in crashes. In most of these crashes, there were only driver side air bags, but in about 150,000 vehicles passenger side air bags also inflated. Driver side air bags reduce deaths by about 14 percent in all kinds of crashes. Deaths in frontal crashes where air bags have inflated are reduced by about 26 percent among drivers using seat belts and by about 32 percent among drivers without belts. Passenger side air bags are reducing deaths among front-seat passengers by about 11 percent in all kinds of crashes. Deaths in frontal crashes where air bags have inflated are reduced by about 15 percent among right front passengers using their belts and about 22 percent among passengers without belts [4]. The National Highway Traffic Safety Administration (NHTSA) estimates that, between 1986 and

June 1 , 1997, air bags have saved 2,050 drivers and passengers (1,830 drivers and 220 passengers) [9]. Based on current levels of effectiveness, air bags will save more than 3,000 lives each year when all the passenger cars and light trucks and vans are equipped with dual air bags. This estimate is based on the current safety belt usage rate of about 68 percent [3].

At the same time, air bags are causing fatalities in some situations, especially to children. As of June 9, 1997, sixty seven deaths reportedly have been caused by air bags inflating in low severity crashes. These deaths include 24 adult drivers, 3 adult passengers (a 98-year-old woman, an unbelted 57-year-old man, and an unbelted 66-year-old woman), 30 children between the ages of 1 and 9, and 10 infants in rear-facing restraints [4]. Most of these people are believed to be unbelted.

The energy required to inflate air bags can injure people on top of, or very close to, air bags as they begin to inflate. In the first few milliseconds of inflation, the forces can seriously injure anyone struck by an inflating bag. Most air bag deaths involve people who were not using belts, were improperly belted, or were positioned improperly. Unbelted people, especially passengers, are at risk because they are likely to move forward if there is hard braking or other violent maneuvers before a crash. Then they can get too close to their air bags and be injured. Improperly positioned people at risk include drivers who sit very close to the steering wheel (less than 10 inches away) and infants in rear-facing restraints positioned in front of passenger air bags [2].

In March 1997, the National Highway Traffic Safety Administration (NHTSA) released a new regulation that will allow automobile manufacturers to install air bags in

new cars that deploy with 20 to 35 percent less force than the current air bags. Air bags now deploy at up to 200 mph [5].

The National Highway Traffic Safety Administration recognized that while depowered air bags would provide immediate benefits in a number of situations, they would not fully solve the problem of adverse effects from air bags and could also reduce protection to unbelted occupants in higher speed crashes. The ultimate solution to the problem of adverse effects from air bags is the implementation of smart air bags. Smart air bags will reduce the injury risk even among people who have moved forward before their air bags inflate. For example, sensors will detect rear-facing infant restraints and automatically switch off air bags on the passenger side. Rates of air bag inflation will be tailored to crash severity so inflation forces will be lower in less serious crashes than in ones at higher speeds. Smart air bags could even recognize people's positions just before inflation and reduce the force if anyone is in a position to be harmed by the air bag [2].

Air bag-equipped vehicles represent an increasing proportion of cars on U.S. roads. In 1990, less than 2 percent of cars on U. S. roads were equipped with air bags [6]. As of July 1, 1997, about 32 percent (62 million) cars in the United States were equipped with driver side air bags. About 17 percent (33 million) also had passenger side air bags [9].

1.2.2 Brief History of Air Bag

Historical references to air bag concepts date back to the 1920s [7]. Patents for air bags began to be issued in the 1950's [1]. General Motors was the first domestic automobile manufacturer to offer air bags commercially. Driver side air bags were optional on

several of General Motors's high end vehicles starting with the 1974 model year [7]. Mercedes was the first to reintroduce air bags, offering them for sale in the 1984 model year. They were optional on the driver's side on several models and became standard equipment across the line two years later [8].

Air bags received serious public attention in the late 1980s. Yet, in a relatively short period of time, the market for air bags has experienced extremely rapid growth [7]. In September 1993, the U.S. Congress and the National Highway Traffic Safety administration adopted a rule requiring air bags for both driver and the front-seat passenger in all passenger cars by 1998 and in all light trucks and vans by 1999 [13].

1.2.3 Basic Elements of an Air Bag System

An automobile air bag system consists of three main elements or subsystems : the crash sensing equipment, the inflator and the inflatable bag. These elements are shown in Figure 1.2.

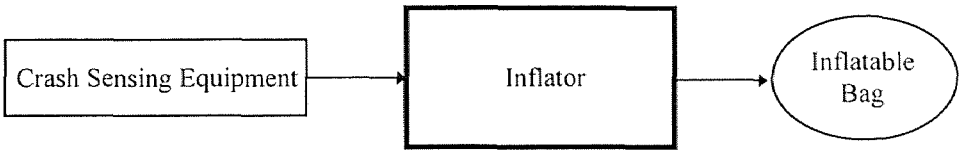

Figure 1.2 Basic elements of an air bag system

When a crash occurs, the rapid deceleration of the car causes the sensors to supply a firing signal to a pyrotechnic squib. The squib ignites the propellant in the inflator and the expanding gas deploys and inflates the air bag. The inflator is responsible for deployment of the air bag to a prescribed pressure and temperature over a period of up to approximately 100 msec [10].

1.2.4 Types of Air Bags

Three types of air bags are used in commercially available vehicles : the driver side and the passenger side air bags for frontal crashes (defined as initial and/or principal impact at 10 to 2 o'clock position), and the side impact air bags for side crashes. Figure 1.3 shows the different types of air bags.

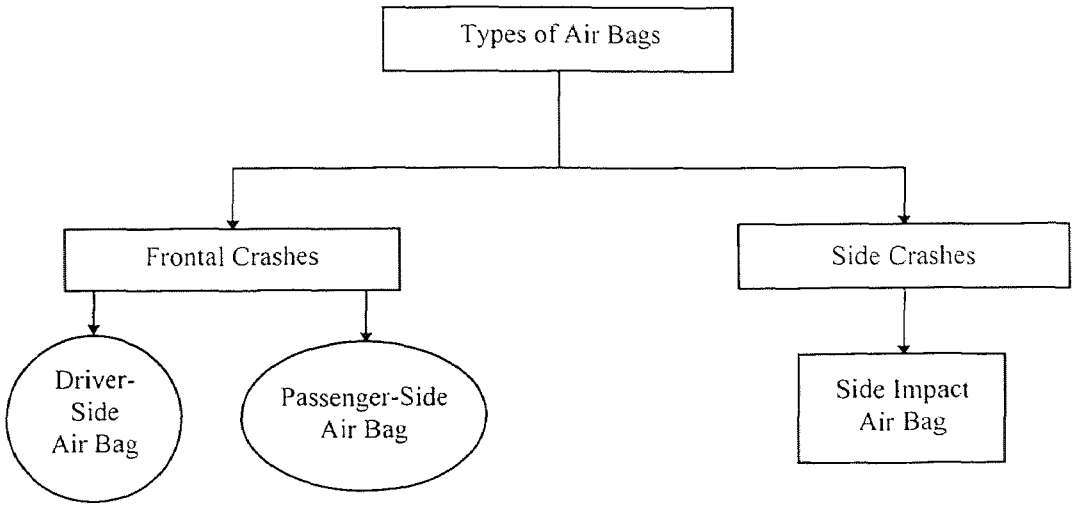

Figure 1.3 Types of air bags

The frontal impact air bags are designed to absorb the vehicle occupant's kinetic energy during a crash so that the occupant comes to rest without sustaining injury. Energy absorption occurs when the occupant contacts and compresses the air bag, forcing gas to escape the bag. The side impact air bags, on the other hand, are not intended to absorb energy but to exert force and move the occupant away from the actual crash location. Side impact air bags are designed to protect occupants' chests, and they are likely to provide some head protection, too. Some side air bags are designed specifically to protect the head [2].

1.2.4.1 Driver Side Air Bag : Driver side air bags are stored in the hub of the steering wheel. Driver side air bags inflate more quickly than its companion passenger side air bag. This is a design requirement due to the shorter distance between the driver and the steering column (versus passenger and the instrument panel). The entire inflation sequence takes place within 30 - 45 msec. Typical driver side air bags measure approximately 714 mm (28 in) in diameter, are 152 mm (6 in) deep [7]. A driver side air bag usually has a volume of approximately 60 - 70 liters when inflated to its normal pressure of 2 to 3 psig and is roughly spherical in shape [11].

Driver side air bags are coated (impermeable) to increase fabric slip, facilitate deployment, protect the nylon fabric from hot gases, and precisely control gas escape during deployment. If for example, gas were to escape excessively, pressure in the bag would be lowered and inflation times would be extended, reducing the effectiveness of the cushion during the ride-down sequence [7].

1.2.4.2 Passenger Side Air Bag : Passenger side air bags are mounted near the top of the instrument panel. The passenger side air bags must be designed to protect a broad range of occupant sizes and ages. In addition, the area covered by passenger side systems is more than twice that of the driver side units, and the distance between the dashboard and a passenger's head is twice that between the driver's head and the steering wheel. Finally, whereas drivers generally sit in the same position, front seat passengers ranging in size from children to adults ---- sit in many different positions. Passenger side air bags are fully inflated in 50-65 msec. Passenger side air bags measure approximately 280 mm (11 in), 100 mm (4 in) and 130 mm (5 in) in width, depth and height respectively [7]. A

passenger side air bag usually has a volume of about 150 liters when inflated to a pressure of 1 to 2 psig and is roughly tear-drop shaped [11].

Passenger side air bags are frequently left uncoated (permeable) because they do not have to inflate as rapidly and because the inside surface of the bag does not receive the high temperatures, high pressures, or hot particulate exposure of the driver side air bag, owing to the larger volume of the passenger side bag and the greater distance from the inflator [7].

1.2.4.3 Side Impact Air Bag : Side impact air bags are mounted either in the door (Mercedes and BMW) or in the seat (Volvo). Door-mounted systems designed primarily to protect the thorax or chest were the main goal when side air bags were being developed in the early 1990s. But now most of the side bags are seat-mounted [12]. In seat mounted systems, the bag moves with the seat and stays with the occupant. Therefore, seat-mounted bags do not have to cover as wide of an area as the door-mounted bags do.

The sensors for side impact air bag are located in the crush zone to trigger deployment. Because there is not much space between the door frame, where crash sensors typically are located, and occupants, the sensors for side impact air bags must detect an impact within 4-5 milliseconds compared with 15-20 milliseconds in a frontal crash. They also must inflate faster – within 20 milliseconds after initial impact. Side impact air bags are smaller than frontal bags. They usually have a volume of 6 to 20 liters [12]. Like the driver side air bags, side impact air bags are also coated to precisely control gas escape during deployment.

1.2.5 Air Bag Material and Packing

Nowadays, most of the air bags are made of Nylon 6 and Nylon 6.6 materials in 420, 630, or 840 denier [13]. Denier is the weight, in grams, of 9,000 meters of a given constant-density yarn. Nylon is strong and abrasion-resistant and ages well under a wide range of environmental conditions.

Many driver side and side impact air bags are coated with neoprene or silicone to seal the bag and protect it from the heat of product gases. Neoprene is not fully compatible with nylon and is prone to heat-aging effects from temperature cycling, ozone, and other agents that can reduce the service life of the air bag fabric. In contrast, silicone coatings used in some applications have extended the fabric's service life to 15 years, as opposed to the 10-year life of neoprene. Further, silicone coatings are more compatible with air bag fabric recycling efforts because silicone polymers can tolerate the high heat required to melt and reprocess the air bag fabric. The major drawback of silicone coatings is their higher cost in comparison with neoprene [14].

Air bags are packed into inflator modules like parachutes. Popular folding patterns include accordion fold, reversed accordion fold, pleated accordion fold, and overlapped folds [13]. The gas that inflates air bags must be vented immediately so that occupants can ride the bag down. The gas is vented through openings located in the rear of the bags or through porous bag fabric.

1.2.6 Types of Inflators

There are currently three major types of inflator systems either under development or commercially available.

1.2.6.1 Pyrotechnic Inflator : This type of inflator is in predominant use today. It consists of an igniter, a booster compound, a solid propellant (generally sodium azide plus an oxidizer) and a metal chamber housing the propellant, igniter and filter. Advantages of this type of inflator are small size and low weight. Disadvantages include cost, difficulty in handling and disposal of sodium azide which is toxic [14].

1.2.6.2 Stored Gas Inflator : This type of inflator involves the utilization of a quantity of stored compressed gas such as argon or nitrogen which is selectively released to inflate the air bag. Advantages of this type of system are greater environmental compatibility. Disadvantages are the significant additional space and weight of the cylinder required for safe storage of this highly pressurized gas [14].

1.2.6.3 Hybrid or Augmented Inflator : Hybrid inflators use a combination of gaseous combustion products and stored pre-pressurized gas to inflate the air bag. Advantages of hybrid inflators are more reliable air bag deployment at unusually high or low ambient temperatures and higher thermodynamic efficiency (defined as the percentage of propellant chemical energy that is converted into useful work i.e. pressurizing the bag) than conventional pyrotechnic inflators. The main disadvantage associated with hybrid models has been their larger size due to the necessity of storing pressurized gas at 10-20 MPa (1450-2900 psi) for an extended period of time [14].

1.2.7 Design Requirements of an Inflator

Although each type of inflator has its own set of requirements, there are some general design requirements for all types of inflators, independent of the type of air bag. Some of these requirements are :

1. ***Cost :*** The downsizing of air bag inflators can play an important role in reducing the cost. Smaller, more compact inflators can provide greater design flexibility, lower raw material cost, simplified assembly, improved visibility of instrument panel and control levers for safety and reduced potential for incidental injuries [14].
2. ***Emissions :*** The inflator should produce negligible particulate and toxic emissions.
3. ***Power Consumption :*** The power needed to activate the device should be small.
4. ***Recycling :*** The inflator should be recyclable after deployment of the bag and also at the end of car's service life.
5. ***Longer Service Life :*** The inflator should be able to withstand large thermal and mechanical stresses and should be operational for at least 15 years with a minimal or no change in performance.
6. ***Hot to Cold Performance Variation :*** There should not be more than 10% hot to cold performance variation (-40 °C to 90 °C).

1.2.8 Tank Tests

The most common way to evaluate the performance of an air bag inflator is to release the product gases into a Receiving Tank usually 20 to 120 liters in volume and observe the pressure-time relationship, the temperature-time relationship and the final product composition. Such investigations are commonly called tank tests and are widely used in

the automotive industry to test and validate inflator performance. Usually, the bag tests are performed in the very last stages of inflator development because they are more expensive and more time consuming. Figure 1.4 shows typical pressure-time curves inside the receiving tank for driver side, passenger side and side impact air bag inflators.

Nowadays, air bag inflators are specified by the outer envelope (module) size, number of moles of gas produced and the time during which 80 percent of the mass comes out of the inflator ($t_{80\%}$). Table 1.1 shows these parameters for the driver side, the passenger side and the side impact air bag inflators [48].

Table 1.1 Envelope sizes, number of moles of gas produced and $t_{80\%}$ for different types of inflators [48]

Type of Inflator	Envelope Size (mm)	Moles of Gas Produced	$t_{80\%}$ (msec)
Driver Side	240 x 165 x 80	1.0	40
Passenger Side	395 x 22 x 125	2.0 - 2.5	60
Side Impact	-------	0.5 - 0.6	10

1.3 Current Commercial Inflator System

Currently, almost all commercially available air bag inflators contain sodium azide (NaN_3) as the primary propellant. The oxidizing agent in these inflators may be copper oxide, molybdenum disulphide, iron oxide or silicon dioxide and varies with the manufacturer. A small quantity of a second substance called the enhancer such as potassium nitrate or boron potassium nitrate is added to facilitate ignition. For a typical composition consisting of sodium azide (NaN_3), potassium nitrate (KNO_3) and silicon dioxide (SiO_2), the chemical reaction is given as :

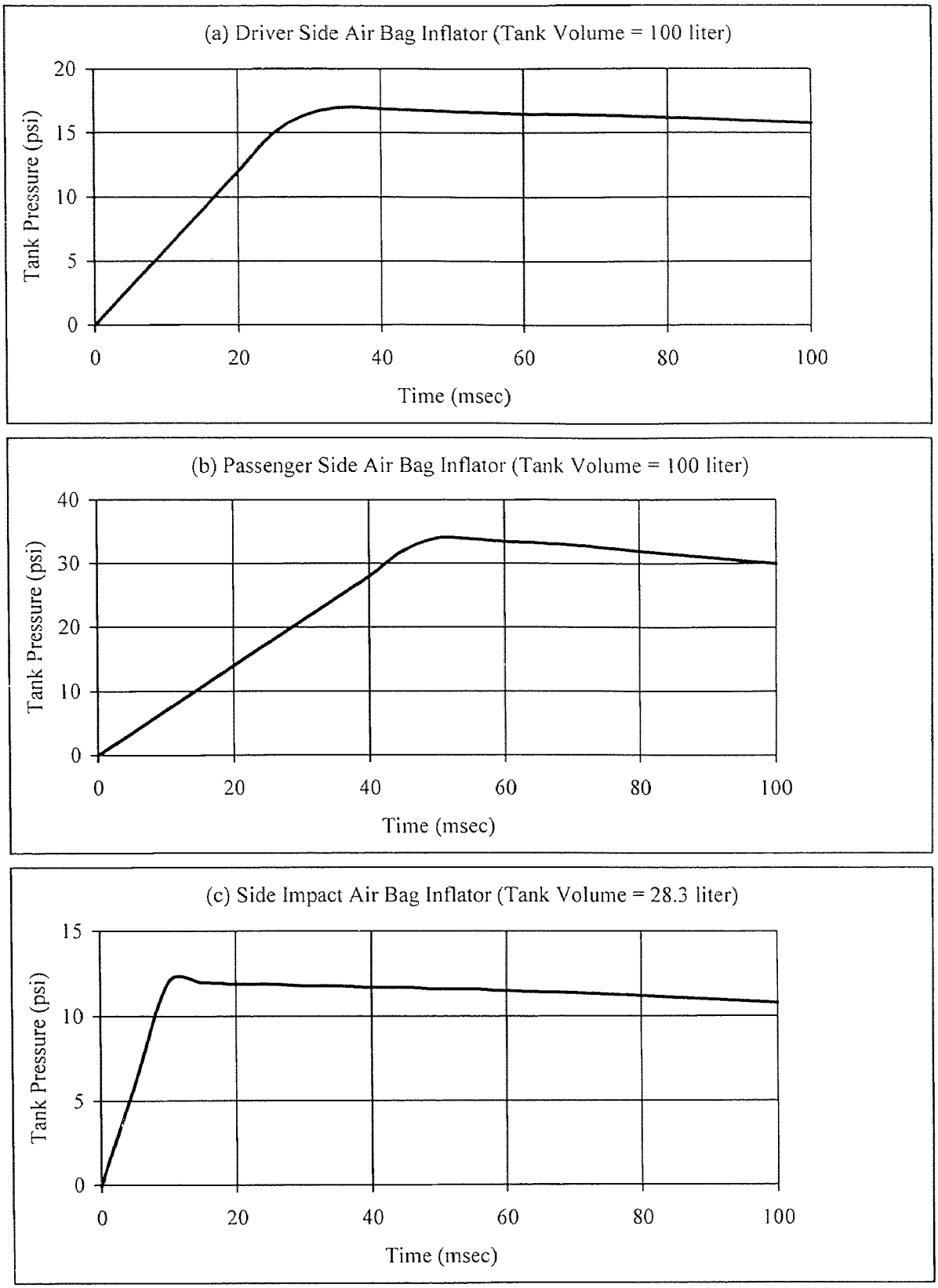

Figure 1.4 Pressure-time curves in the receiving tank for different types of inflators

$$10NaN_3 + 2KNO_3 + 5SiO_2 \rightarrow 5Na_2O \,.\, K_2O \,.\, 5SiO_2 + 16N_2$$

solid pellets slag nitrogen

Although, the sodium azide system produces a breathable nitrogen gas, it has some negative aspects. Sodium azide is highly toxic to humans and the environment in its condensed form. Contact of an occupant's skin with a water/azide mixture tends to lower blood pressure. Also, if a water-azide mixture contacts metals particularly copper, it can form primary explosives. There is a concern for automobiles that are scrapped at the end of their lives without removal of the inflators. NaN_3 propellants also produce solid reaction products (slag) which must be filtered, and the combustion process itself is relatively inefficient. In the combustion of sodium azide, the products of combustion are N_2 (99.2%), H_2O (0.6%) and H_2 (0.1%). Other gases such as CO, CO_2, NO_x, NH_3 and SO_2 are also formed along with aerosols containing sodium hydroxide, sodium carbonate and other metallic oxides. Some of these gases like CO, NO_x are not good for the environment.

In the sodium azide system, the pressure in the combustion chamber varies from initial atmospheric (14.7 psi) to 10 MPa (1450 psi) or more after combustion [23]. The pressure in the discharge tank is usually between 172 kPa (25 psi) and 242 (35 psi). Usually, a driver side air bag is fully inflated in about 45 to 50 msec. In about 85 to 100 msec after the impact the driver rides the bag down, unharmed as the air bag cushion deflates.

1.4 Novel Combustion Approach

In this research, we have developed and studied a new technology for air bags using fast combustion reactions of methane and oxygen. The reaction between methane (CH_4) and oxygen (O_2) occurs as follows :

$$CH_4 + 2O_2 \rightarrow CO_2 + 2H_2O$$

1 mole 2moles 1 mole 2 moles

If the reaction is complete, methane is totally converted to carbon dioxide (CO_2) and water (H_2O). Both of these products are environmentally safe. Using the Chemical Equilibrium Compositions and Applications Code [15,16] and the model of Hanna & Karim [52], the major species formed in the reaction of methane and oxygen are CO_2, H_2O, H, H_2, O, O_2, CO, OH, HCO, HO_2 and H_2O_2. We have selected methane because it has simple structure and chemistry and also it has unusually high auto-ignition temperature.

The fast combustion inflator is expected to be cheaper than the sodium azide system because methane is cheaper and easily available as compared to sodium azide. Also, the equipment cost is expected to be much less than the sodium azide system because the equipment is relatively simple. In addition we do not require the expensive mechanism of filtration here, since we do not produce particulates.

The immediate goal of the industry is to use this combustion-based device for side impact air bags; however, the technology is not restricted only to side impact air bags. It can be applied to driver side and passenger side air bags also.

1.5 Previous Relevant Work in this Field

There is no published literature on the forced ignition of methane-oxygen mixtures in connection with air bags. Previously, work on forced ignition of methane and oxygen mixtures was performed by Steinle et al. [17] and Di Blasi et al. [53]. Steinle et al. performed forced ignition experiments by using heated wires located within the spherical combustion chamber having an inside volume of about 21 cc. The chrome-nickel wires of 10 ohm and of about 3cm length and 0.06 mm diameter, wound in coils of 1 by 2 mm, were heated electrically. The temperature at ignition was measured from the temperature-dependent resistance with a limited accuracy of about $\pm$ 50 K at about 1100 K (800°C). Di Blasi et al. performed numerical simulation of forced ignition of methane-oxygen mixtures. In their work, a methane-oxygen mixture of mole ratio 1:10 initially at rest at one bar pressure and 300 K temperature was considered. They compared a simple model proposed by Dryer and Glassman [18], containing two reactions and five chemical species with a detailed model of Westbrook [19], comprising 56 reactions and 18 chemical species. In both cases the ignition source was located on the vertical wall. Their relevance to the present work is due to their investigation of the forced ignition of methane and oxygen system.

Most of the work published in the field of air bag has been for pyrotechnic inflators or pyrotechnic in combination with stored gas [20-24,42-44]. The initial work on pyrotechnic inflator modeling was performed by Stevens et al. [20]. They have developed a computer program to simulate the performance of pyrotechnic inflator. However, there were many parameters involved in modeling the complex transient chemical thermodynamics of the burning igniter and propellant pellets, and the gas dynamics and

heat transfer associated with the internal combustion chamber and diffuser components. The uncertainty of many values of the input parameters, which must be provided by the users of the program, may affect the accuracy of the simulation results.

Wang [21,42] developed a semi-analytical model to calculate the transient gas temperature and mass flow rate from the inflator. He treated the inflator as a single element generating gas at certain mass flow rate for the purpose of modeling the air bag inflation process. The author did not model the individual internal processes of the inflator.

Butler et al. [22,43] developed a mathematical model to simulate the transient, thermochemical events associated with ignition and combustion of a pyrotechnic inflator. Two series of calculations were presented. The first was for a baseline test case of a conventional pyrotechnic inflator. The second series of calculations illustrated the influence of pre-pressurized inert gas on the performance of a pre-pressurized pyrotechnic inflator system. Performance of the inflators was measured in terms of the pressure-time and the temperature-time profiles in the inflator and the receiving tank as well as the pressure-time integrals at specified times after ignition.

Materna [23,44] presented an analytical model which predicts the peformance of a pyrotechnic air bag inflator by accounting for the heat transfer, filtration, combustion, fluid flow and thermodynamic processes occurring during the inflation event. He considered all the essential aspects of the inflator, especially the details of the clogging of the filter. However, there were no mathematical details given in Materna's paper.

The most comprehensive published model for a pyrotechnic air bag inflator was that presented by Chan [24] in which the propellant combustion, filter pressure drop and

cooling, nozzle and receiving tank behavior were all explicitly modeled. In addition to sodium azide system, a handful of work is also published on non-azide inflators [10,45,46].

1.6 Present Work

The present work is based on the fast combustion reactions of methane-oxygen mixtures. The forced ignition of the mixture was performed experimentally by using an electric match as a source of ignition.

The performance of the inflator is evaluated in terms of pressure-time relationships inside the inflator and in the tank as well as the temperature-time relationship in the tank. Several important issues related to inflator design are studied and evaluated. These include the effects of stoichiometry, initial mixture pressure and extreme hot and cold conditions. Other practical issues, such as the concentration of carbon monoxide produced and the severity of temperature in the tank are also studied and optimized.

A theoretical model has been developed to simulate the experimental results and to calculate the mass flow rate from the inflator to the tank. The model is based on the change in the internal energy inside the inflator and the tank as the mass flows from the inflator to the tank.

In Chapter 2, the experimental set-up is discussed and the experimental procedures are given.

In Chapter 3, the experimental results are given. First, the design requirements for different types of air bag inflators are given. The pressure and temperature results of a

typical experiment are discussed next. This is followed by a discussion of the major critical issues and other important requirements needed for the development of the inflator. Lastly, the application of fast combustion to different inflator sizes is discussed and the conclusions are formulated.

In Chapter 4, a description of the theoretical model is given along with a comparison with the experimental results. Prior to discussing the model, the applicability of an ideal gas assumption is justified and the mass flow rate equation for one-dimensional isentropic flow is given. This is followed by a complete discussion of the model and a demonstration of the model by several experimental examples.

In Chapter 5, the fast combustion inflator has been evaluated with the sodium azide inflator currently used in industry. A set of standards and criteria is used to measure and access the performance of the fast combustion inflator.

In Chapter 6, the conclusions drawn from the above work are formulated.

CHAPTER 2

EXPERIMENTAL SET-UP AND PROCEDURES

2.1 Introduction

In this chapter, the experimental set-up is discussed and the experimental procedures are given. In the beginning, a brief description of each component of the experimental set-up is given. This is followed by the experimental procedures for the tank testing of combustion and ideal gas experiments. In the end, a brief description of gas chromatography and the procedure for gas chromatography is given.

2.2 Experimental Set-up

The experimental set-up is shown in Figure 2.1 and the schematic layout of the experimental set-up is shown in Figure 2.2.

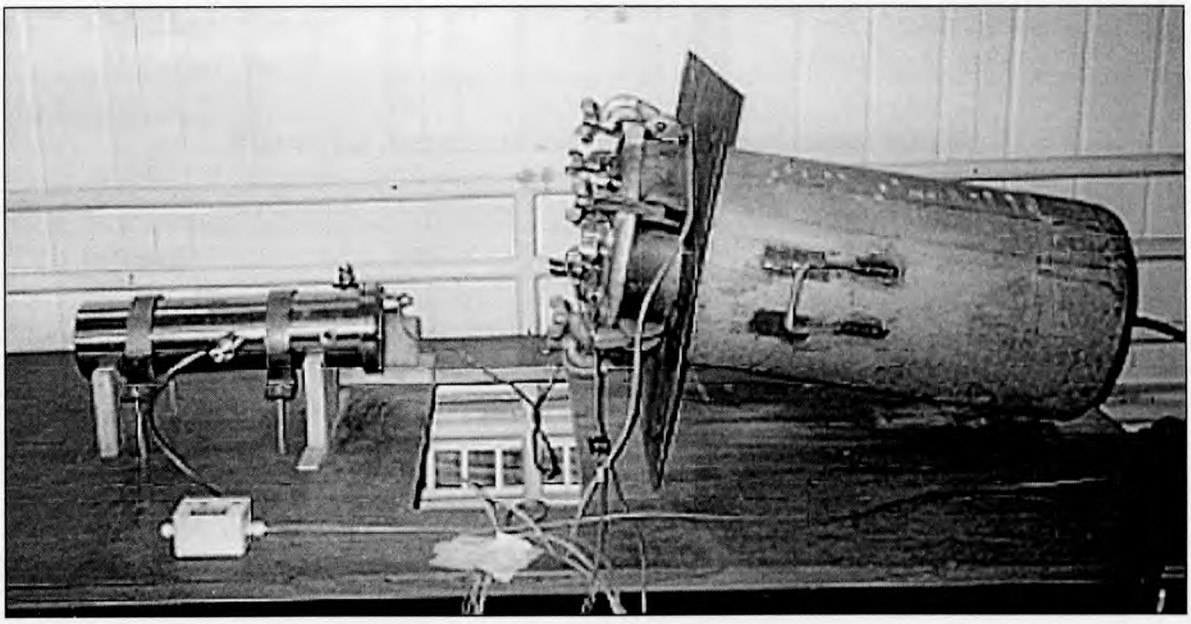

Figure 2.1 Experimental set-up

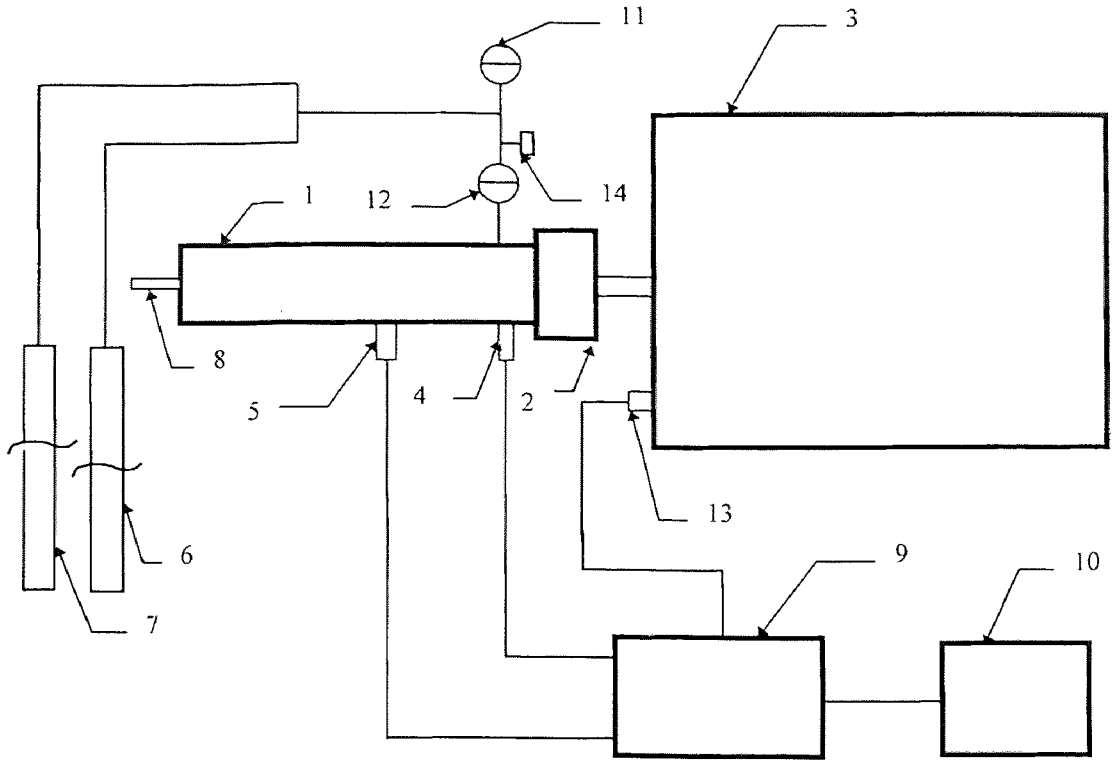

1	Inflator	8	Inflator's thermocouple
2	Burst disk mechanism	9	Data acquisition box
3	Receiving tank	10	Computer
4	Igniter	11	Release valve
5	Inflator's pressure transducer	12	Inlet valve
6	Methane cylinder	13	Tank pressure transducer
7	Oxygen cylinder	14	Metering transducer

Figure 2.2 Schematic layout of the experimental set-up

2.2.1 Inflator

The gases (methane and oxygen) from the individual cylinders are mixed and ignited inside a stainless steel inflator. The inflator is a cylindrical vessel with 3 in. inside diameter, 5 in. outside diameter and 18 in. length. The original inflator has a volume of 2.085 liter. To perform experiments with different sizes of inflator, three different aluminum volume fillers are added inside the original inflator to make the inflator volume as 0.067 liter, 0.0246 liter, and 0.250 liter. One end of the inflator is closed while the

other end contains a burst disk arrangement (Figure 2.3). The burst disk mechanism is covered by two semi-circular flanges and a circular ring (Figure 2.4). Each of these flanges has five bolts. The burst disk mechanism is attached to the inflator by tightening these bolts. The flanges are covered by a circular ring which has a bolt to tighten it. Figure 2.5 shows the schematic of inflator and burst disk mechanism. The inflator has an inlet/exit port, a port for holding the igniter and several other ports for transducers and a thermocouple.

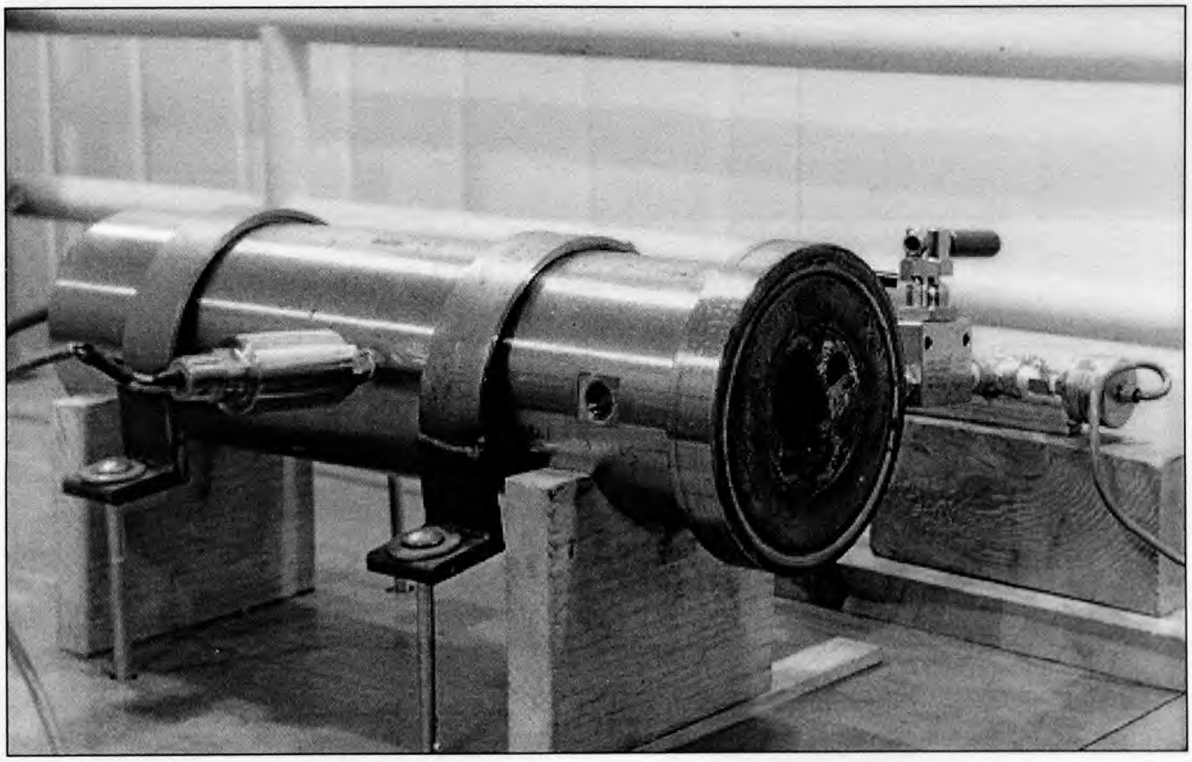

Figure 2.3 Inflator

In some of the experiments for side impact air bags, a small inflator, 0.0146 liter in volume is used. Table 2.1 shows all the inflator volumes used in this study.

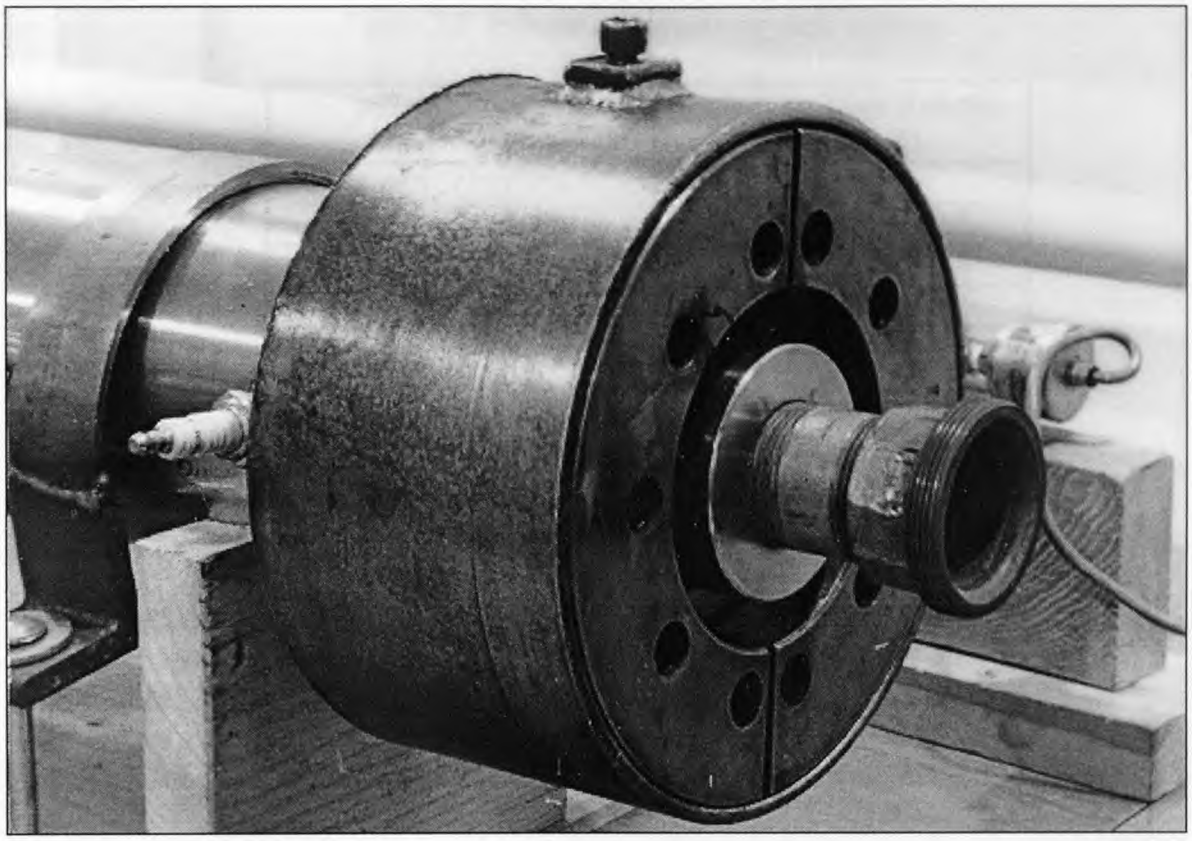

Figure 2.4 Inflator and burst disk mechanism

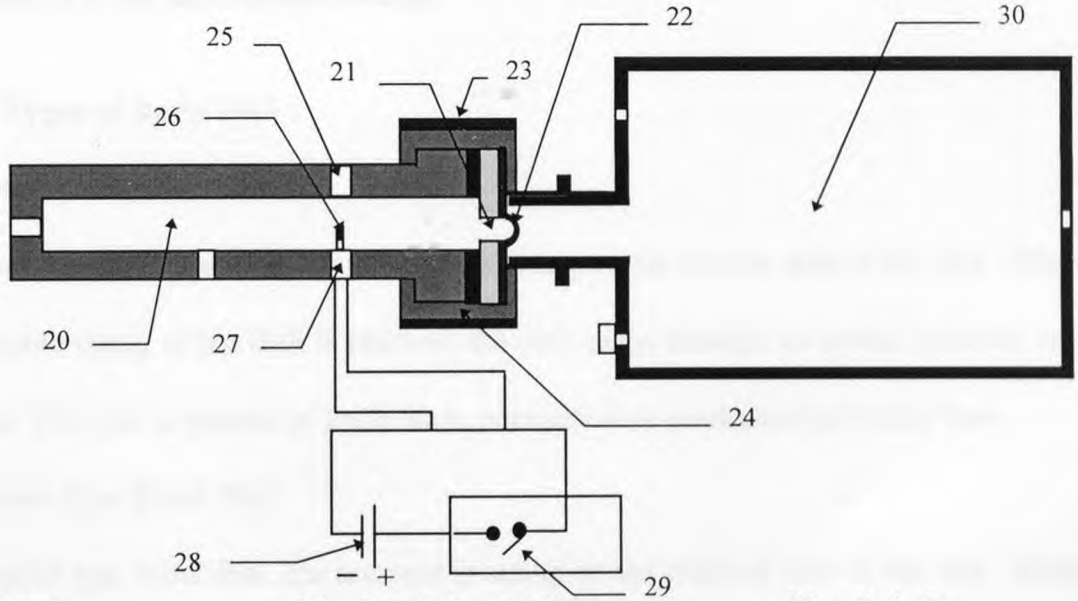

20	Inflator	24	Semi-circular flange	28	Switch
21	Orifice	25	Inlet/exit port	29	Battery
22	Burst disk	26	Igniter	30	Receiving tank
23	Circular ring	27	Adapter		

Figure 2.5 Schematic illustration of inflator and burst disk mechanism

Table 2.1 Inflator and receiving tank volumes

Inflator Volume Liter (cu.in)	Receiving Tank Volume Liter (cu.ft)
2.085 (127.23)	70.0 (2.5)
0.250 (15.25)	70.0 (2.5)
0.067 (4.10)	70.0 (2.5)
0.0246 (1.50)	70.0 (2.5)
0.0146 (0.89)	28.3 (1.0)

2.2.2 Burst Disk Mechanism

The burst disk mechanism has an orifice of 0.75 in. The burst disk blocks the flow of gas from the inflator and through the orifice into a receiving tank or an air bag. A burst disk is a solid metal, differential pressure relief device with an instantaneous full-opening, non-reclosing design. The burst disk ruptures in 1 to 3 milliseconds upon the application of a predetermined level of pressure in the inflator. This level of pressure is only available after ignition of the combustible mixture.

2.2.2.1 Types of Burst Disk :

1. Reverse Acting Burst Disk

In a reverse acting burst disk, the pressure is acting on the convex side of the disk. When the pressure rating of the disk is reached, the disk snaps through its neutral position and reverses. The disk is opened by knife blade penetration or predetermined score lines.

2. Tension Type Burst Disk

In a tension type burst disk, the pressure is acting on the concave side of the disk. When the pressure increases beyond the allowable operating pressure, the disk starts to grow. This growth will continue as the pressure increases, until the tensile strength of the

material is reached and rupture occurs. The two types of burst disks are shown in Figure 2.6 [25].

2.2.2.2 Materials of Burst Disk : The most commonly used materials for burst disks are aluminum, silver, nickel, monel, inconel and 316 stainless steel. Sometimes, liners such as Teflon or lead and coatings such as vinyl or Teflon are used to protect the disks in corrosive applications.

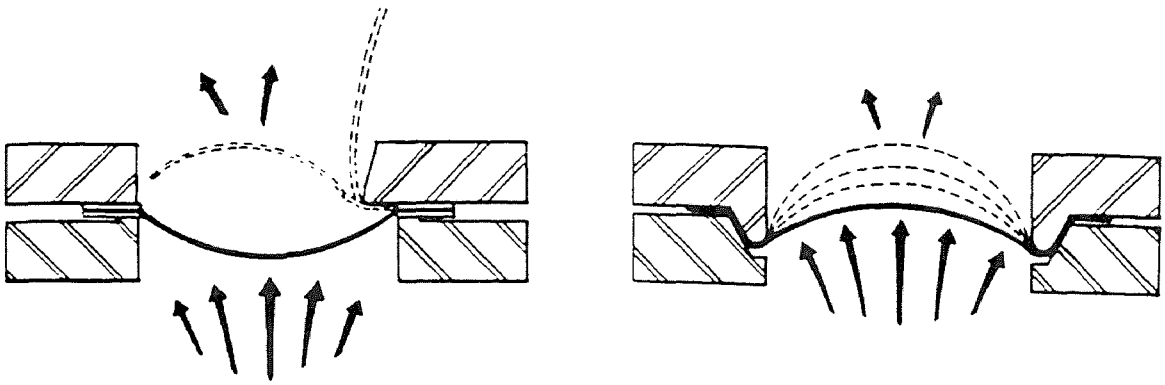

(a) Reverse acting burst disk (b) Tension type burst disk

Figure 2.6 Types of burst disk

2.2.2.3 Effect of Temperature on Burst Disk : The burst pressures decrease as operating temperatures increase. Table 2.2 shows the maximum temperatures for burst disk materials, liners and coatings [26].

The thicknesses of burst disk used in this study and their pressure ratings are given in Table 2.3. The material of all burst disks is 316 stainless steel. The disks are 1 in. in diameter with an opening of 0.75 in. except the burst disk for the 0.0146 liter inflator which is 0.670 in. in diameter and has an opening of 0.25 in.

Table 2.2 Maximum temperatures for burst disk materials, liners and coatings

Material	Maximum Temperature, °F (°C)
Aluminum	260 (126.7)
Silver	260 (126.7)
Nickel	800 (426.7)
Monel	800 (426.7)
Inconel	1000 (537.8)
316 SS	900 (482.2)
Lead	250 (121.1)
Polyvinylchloride	180 (82.2)
Teflon	400-500 (204.4-260.0)

Table 2.3 Pressure ratings of different thicknesses of burst disks

Thickness of Burst Disk (in.)	Pressure Rating (psi)
0.002	900 - 1050
0.003	1400 - 1500
0.004	1900 - 2000
0.010	6000 - 7000
0.012	Not rated
0.015	Not rated
0.020	10300 - 10600
0.025	16300 - 17000

The fully-hardened or annealed burst disks are sometimes used in industry. Annealed burst disks have uniform properties and give more consistent results. To compare the performance of annealed burst disks with the regular burst disks, some experiments are performed with annealed burst disks. These annealed burst disks are 0.004", 0.010", 0.012" and 0.015" in thickness.

2.2.3 Igniter

The combustible mixture in the inflator is ignited with the help of an electric match or a pyrofuze wire. During the course of this research, three different types of electric matches

are used, M100 with 4 in. duplex lead wires, M103 with 18 in. lead wires and EL fuse V with 1.8 m duplex lead wires. These matches are manufactured by ICI and contain up to 0.030 gram of lead mononitroresorcinate (LMNR) oxidizer mixture [27].

The pyrofuze wire used has a diameter of 0.020 in. and is manufactured by Pyrofuze Corporation. The pyrofuze wire consists of two metallic elements in intimate contact with each other. When these elements are brought to the initiating temperature (about 650 °C), they alloy rapidly resulting in flame and high temperature (about 2800 °C). About 1360 Joules/gm (325 calories/gram) of thermal energy is released during this reaction. The outer jacket of pyrofuze wire consists of 5% Ruthenium and 95% Palladium whereas, the inner core consists of aluminum [28].

The igniter in our experimental set-up is powered by a 12 volt vehicle battery. An adapter is used to hold the igniter (Figure 2.7). A pair of electrical lead wire extends from

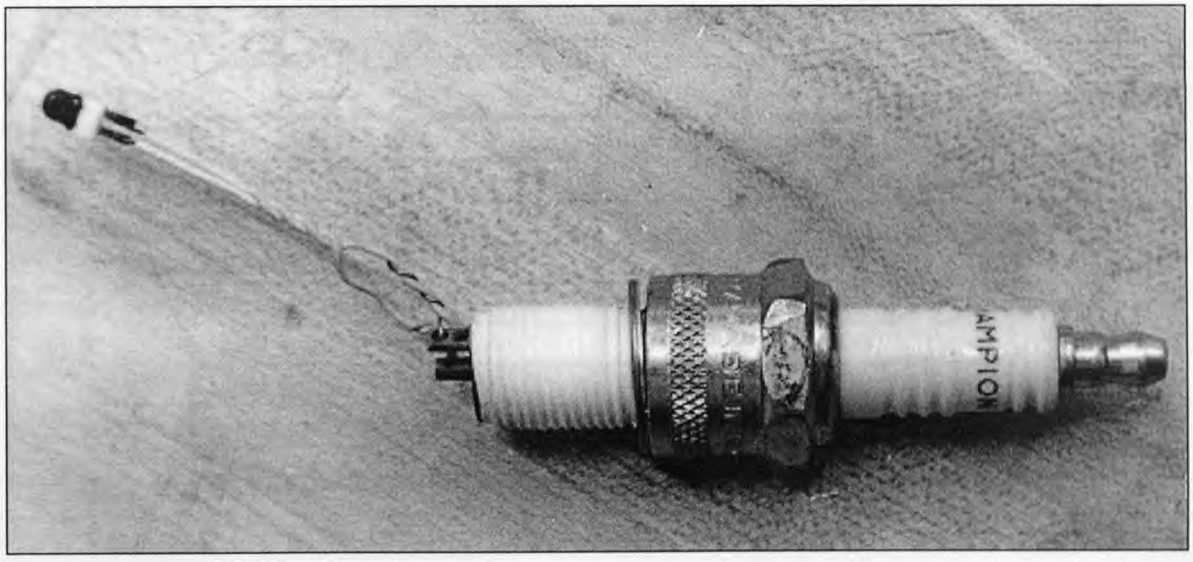

Figure 2.7 Electric match and adapter

the adapter to the battery. The ignition of electric match or pyrofuze wire is controlled by a switch which is normally open. When the switch is closed, ignition occurs and the electric match or pyrofuze wire is ignited to initiate the combustion reaction (Figure 2.5).

2.2.4 Pressure Transducers

In this study, the pressure transducers are used for three purposes :

1. To measure pressure inside the inflator,
2. To measure pressure inside the receiving tank, and
3. To meter the gases entering the inflator.

The transducers used are either strain gage or piezoelectric. In the receiving tank, Data Instrument XPRO transducer with a pressure rating of 0 - 100 psi (or 0 - 200 psi) is used. To meter the gases, Data Instrument XPRO transducer with a pressure rating of 0-3000 psi is used. Table 2.4 shows the different transducers used in the inflator. All pressure transducers have a response time of less than 1 msec.

Table 2.4 Transducers used to measure pressure in the inflator

Type	Pressure Range (psi)
Kistler 6730	0 - 15,000
Kistler 217C	0 - 75,000
Data Instrument XPRO	0 - 3,000, 0 - 5,000
Barksdale 403-09-O	0 - 10,000
Data Instrument AB	0 - 20,000
Data Instrument BF	0 - 20,000
Sensotec Z/4834-01ZG	0 - 30,000
Sensotec Z/a356-01	0 - 60,000

2.2.5 Thermocouples

The thermocouples are used to measure temperatures inside the inflator and the receiving tank. In the receiving tank, three different types of thermocouple are used : a NANMAC

E12-3-E-U thermocouple and two OMEGA E type bare thermocouples (0.005" and 0.0005" in diameter). These thermocouples are used in combination with NANMAC cold junction compensator and OMEGA signal conditioner which amplifies the voltage to 0-5 V. The signal is sampled at a rate of about 2500 Hz (or 2500 points per sec).

2.2.6 Data Acquisition System

The data acquisition system consists of a data acquisition box and a computer. The data acquisition system converts the millivolt and milliampere output of the transducers into digital pressure. The data acquisition box provides the required voltage for igniting the electric match or pyrofuze wire. The data acquisition software 'NJIT' [29] allows us to take data with a variable sampling rate and to view the pressure and temperature data in real time. The data files from various experiments are used to analyze the results and to compare them with the theoretical model.

2.2.7 Receiving Tank

As mentioned in Section 1.2.8, the most common way to evaluate the performance of an air bag inflator system is to release the products of combustion from the inflator into a receiving tank. Once the required conditions for pressure, temperature and mass flow are satisfied in the tank, then the final testing is done with air bags. Nowadays, the testing for driver and passenger side air bags is usually done in 60 to 100 liter tank whereas, the testing for side impact air bag is usually done in 28.3 liter tank. In this study two different sizes of receiving tank are used, a 28.3 liter tank for 0.0146 liter inflator and a 70 liter tank for all other inflator sizes. The receiving tank has ports for transducers and thermocouples and also a purge valve to purge the tank with an inert gas (helium or

nitrogen). The gas sampling cylinder can also be attached to the tank to take samples of gas for gas chromatography analysis. Figure 2.8 shows the inflator and the tank connection together with the ports for transducer, thermocouple and the purging gas.

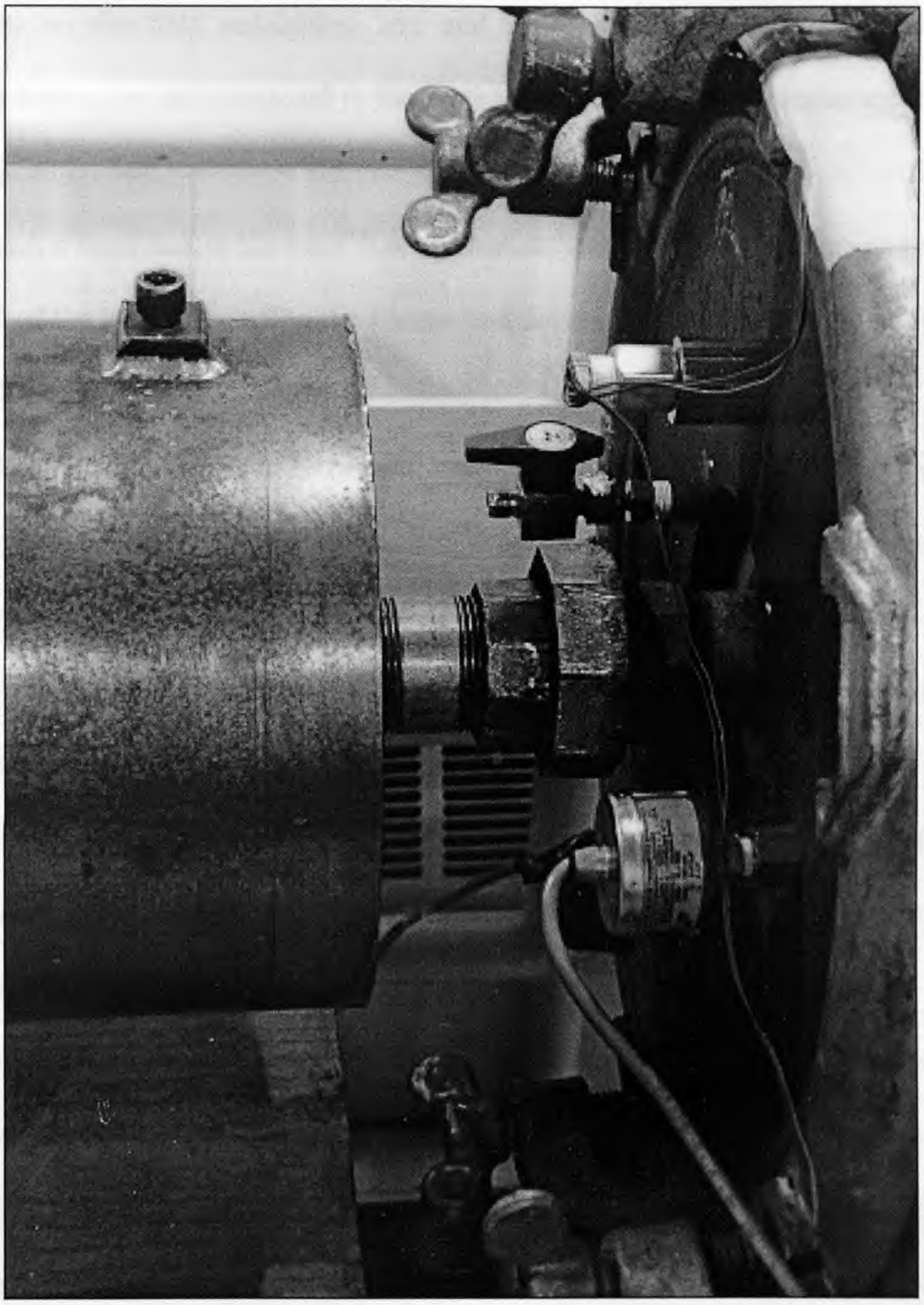

Figure 2.8 Inflator and tank connection showing the ports for tank transducer, thermocouple and the purging gas.

2.3 Experimental Procedures

2.3.1. Procedure for Combustion Experiments

Following is the tank testing procedure for combustion experiments :

1. Turn on the data acquisition box and make sure that all the transducers and thermocouples are connected to the system and their leads are connected to the data acquisition box.
2. Attach a burst disk to the burst disk mechanism and attach this mechanism to the open end of the inflator by using the flanges and the ring. Attach the receiving tank to the inflator.
3. If the receiving tank is to be purged, open the purging gas supply valve at the inlet of the tank and subsequently release the gas by opening the discharge valve attached to the tank.
4. Cut the pyrofuze wire or the lead wire of the electric match to the required length and connect it to the adapter. Attach the adapter to the inflator.
5. Open the inlet valve to the inflator. Purge the inflator with oxygen by connecting the oxygen hose to Quick Connect fitting located just before the inlet valve. Release oxygen by using the release valve. Repeat the purging process once more.
6. Zero all the channels of the software again by pressing the key 'Z' from the keyboard.
7. Disconnect the oxygen hose and attach the methane hose to the same Quick Connect fitting. Put a measured quantity of methane inside the inflator. In this study, the gas quantity is metered by measuring the gas pressure inside the inflator. The pressure is measured by a pressure transducer attached just upstream of the inlet valve and can be read from the computer screen.

8. Close the inlet valve to the inflator. Open the release valve and remove any excess methane from the fittings. Close the release valve.
9. Disconnect the methane hose and attach the oxygen hose to the Quick Connect fitting. Build a pressure equal to or greater than the pressure of methane and open the inlet valve. Put a measured quantity of oxygen inside the inflator.
10. Close the inlet valve again. Open the release valve and remove any excess oxygen from the fittings. Remove the methane hose and keep the release valve open.
11. Start the data acquisition software by pressing the key 'S' from the keyboard and select a sampling rate.
12. Measure the voltage in the lead to be connected to the igniter adapter with the help of a voltmeter. If there is no voltage, connect the lead to the igniter adapter.
13. Ignite the electric match or pyrofuze wire by pressing any key of the keyboard.
14. Take data for about 200 milliseconds, or any other required duration.
15. Open the inlet valve to the inflator and the discharge valve of the receiving tank to release any product gas left in the system.

2.3.2 Procedure for Ideal Gas Experiments

Some of the experiments are done with an ideal gas (nitrogen) to assess the accuracy of measured data. Following is the procedure for tank testing of ideal gas experiments :

1. Turn on the data acquisition box and make sure that all the transducers are connected to the system and their leads are connected to the data acquisition box.
2. Attach a burst disk (0.004") to the burst disk mechanism and attach this mechanism to the open end of the inflator by using the flanges and the ring.

3. Attach a gas motor (a device used to rupture the burst disk on command) to the tank side of the burst disk mechanism with the help of a rubber stopper. Attach the receiving tank to the inflator.
4. Purge the receiving tank with nitrogen by opening the supply valve at the inlet of the tank and subsequently release the gas by opening the discharge valve attached to the tank.
5. Open the inlet valve to the inflator. Purge the inflator with nitrogen by connecting the nitrogen hose to Quick Connect fitting located just before the inlet valve. Release nitrogen by using the release valve. Repeat the purging process once more.
6. Zero all channels of the software by pressing the key 'Z' from the keyboard.
7. Put a measured quantity of nitrogen inside the inflator. The quantity of nitrogen is metered by using the pressure transducer attached just upstream of the inlet valve. When the pressure in the inflator is equal to the nitrogen bottle (cylinder) pressure, further increase in inflator pressure is achieved by using a booster pump.
8. Close the inlet valve to the inflator and remove any excess nitrogen from the fittings by opening the release valve. Remove the nitrogen hose.
9. Start the data acquisition software by pressing the key 'S' from the keyboard and select a sampling rate.
10. Measure the voltage in the lead to be connected to the gas motor wires with the help of a voltmeter. If there is no voltage, connect the lead to the gas motor wires.
11. Activate the gas motor by pressing any key of the keyboard. Take data.
12. Open the inlet valve to the inflator and the discharge valve of the receiving tank.

2.3.3 Other Procedures

The following procedures and precautions for the calibration and testing of instrumentation are given in Appendix A :

A1. Procedure for the calibration of pressure transducers.

A2. Procedure for the calibration of thermocouple.

A3. Testing the burning time of electric matches.

A5. Precautions, handling of electric matches and procedures for safety.

2.4 Gas Chromatography

The analysis of product gases from the tank is performed by using gas chromatography. A sample is collected in a sampling cylinder just after firing the shot. The sample is then analyzed for carbon monoxide (CO) by using gas chromatograph.

2.4.1 Gas Chromatograph

The GOW-MAC Series 550P Thermal Conductivity Gas Chromatograph is used to perform gas analysis of the product gases [31]. The CTR I column [32] is used in the analysis. This column can separate Air, CO, CH_4, CO_2, O_2, and N_2. The calibration for CO is done by using three CO standards, 100 ppm, 1000 ppm and 1% in helium. The results from the chromatograph are plotted on HP3396 Series II Integrator [33]. The following parameters are used in the analysis :

Flow rate column A = 60.0 ml/min (30.0 ml/min)

Flow rate column B = 25.5 ml/min

Current = 150 mA

Detector temperature = 200°C

Injector temperature = 45°C

2.4.2 Procedure for Gas Chromatography

1. The tank testing is performed as described above but the receiving tank is not purged with helium. A sample of product gases is taken from the receiving tank in a 50 ml. sampling cylinder.
2. Set the current and the injector and detector temperatures of the Gas Chromatograph.
3. Adjust the flow rate of column A (working column) and column B (reference column) of the chromatograph with the help of a flowmeter.
4. A 10 ml sample is taken in a syringe from the sampling cylinder. The sample is injected in the chromatograph and the area of CO peak is noted using the HP3396 Series II Integrator. The concentration of CO is obtained by using this area and the calibration curve from CO standards.
5. Repeat step 4 three or four times and take the average of CO concentration.

The procedure for the calibration of carbon monoxide is given in Appendix A4.

CHAPTER 3

EXPERIMENTAL RESULTS FOR THE DEVELOPMENT OF A FAST COMBUSTION INFLATOR

3.1 Introduction

The performance of an air bag inflator is customarily evaluated by observing the pressure-time relationship in the inflator and the tank, the temperature-time relationship in the tank and the final combustion product composition [sections 1.2.8. and 2.2.7]. The tank pressure simulates the effect of gas volume required to fill an air bag. The tank temperature can be used to calculate thermal stresses and to assess the temperature in the bag. The inflator pressure is useful to determine the strength of an inflator, to guide in its design and to calculate the mass flow rate from the inflator to the bag. The product composition is useful to assess the gases formed in the reaction and to determine their toxic effects, if any. During this research, the inflator pressure, tank pressure and tank temperature were measured. Also, tank gas samples have been analyzed to determine the concentration of carbon monoxide. In this research, about 250 experiments were performed to develop and investigate this novel fast combustion inflator.

In order to utilize the fast combustion inflator, there are several critical issues which need to be addressed. These include the effects of stoichiometry, initial mixture pressure and effects of extreme hot and cold operating conditions. Other design and practical parameters such as burst disk thickness and type, ignition device, tank purging gas and severity of temperature in the tank are also important to design an inflator successfully. It should be noted that this type of inflator is different than the sodium azide inflator, as described in Chapter 1.

In this chapter, the design requirements for different types of air bag inflator are given. The temperature and pressure results of a typical experiment are given next, and discussed in the light of the design requirements. This is followed by the discussion of the major critical issues and other important requirements needed for the development of the fast combustion inflator. Lastly, the application of fast combustion to different inflator sizes is discussed and the conclusions are formulated. In this chapter, the experimental results are discussed in reference to the development of a fast combustion inflator – i.e., the technology aspects of the development. More detailed discussions of the results based on thermodynamics and a comparison with the theoretical model are given in Chapter 4.

3.2 Design Requirements for Different Inflator Types

One of the objectives of this study was to optimize the pressure-time behavior in the receiving tank. Table 3.1 shows the design requirement for driver side, passenger side and side impact air bags [34]. Note that $t_{80\%}$ is the time when 80% of the mass should have come out the inflator.

A driver side inflator for a 60 liter bag, needs to create a pressure of 50.75 psi in a 28.3 liter tank in less than 50 msec. This inflator should produce a total of 1.0 mole of gas and 80% of this amount should come out of the inflator in less than 40 msec. A passenger side inflator for a 150 liter bag, needs to create a pressure of 84.10 psi in a 60 liter tank in less than 70 msec. The passenger side air bag inflator should produce about 2.0 - 2.5 moles of gas and 80% of this amount should come out in less than 60 msec. A side impact air bag for a 12 liter bag, needs to create a pressure of 13.05 psi in a 28.3 liter tank in less than 15 msec. The side impact inflator should produce 0.5 - 0.6 moles of gas

and 80% of this amount should come out in less than 10 msec. The pressure in psi is always a gage pressure unless otherwise indicated and the time to attain the required pressure is the time after the ignition.

Table 3.1 Design requirements for different types of air bag inflators [34]

Type	Driver Side	Passenger Side	Side Impact
Bag volume, liter	60	150	12
Inflator size (dia x length), mm	95 x 40	61 x 250	25 x 135
Inflator volume, liter	0.2835	0.7306	0.0662
Tank volume, liter	28.3	60.0	28.3
Tank pressure required, psi	50.75	84.10	13.05
Time to attain the reqd. pressure, msec	50	70	15
No. of moles of gas reqd., #	1.0	2.0 - 2.5	0.5 - 0.6
$t_{80\%}$, msec	40	60	10

3.3 Results and Discussion of a Typical Experiment

Consider an experiment with a 150/300 (methane = 150 psi, oxygen = 300 psi) mixture inside a 0.250 liter inflator. This inflator volume is about 10% smaller than the volume of driver side air bag inflator. The mixture is ignited with an electric match. The thickness of the burst disk used in the experiment is 0.010". The receiving tank (70 liter) is purged with nitrogen. The pressure and temperature curves for this experiment are shown in Figure 3.1. The figure shows that in about 7.5 msec after the current is supplied, ignition occurs and the pressure in the inflator increases very quickly. In the air bag industry, this time of sudden increase in pressure is referred to as the initial time (or t = 0). In our

device, the pressure in the inflator increases beyond the pressure rating of the burst disk. Normally, this takes place within 1 - 3 msec from ignition. Thus, about 10 msec after the ignition, the burst disk ruptures and the products of combustion flow into the receiving tank. The pressure curve in the tank is not smooth in the beginning. This is due to the fact that in the tank, the product gases undergo expansion, until the pressure equals the equilibrium pressure.

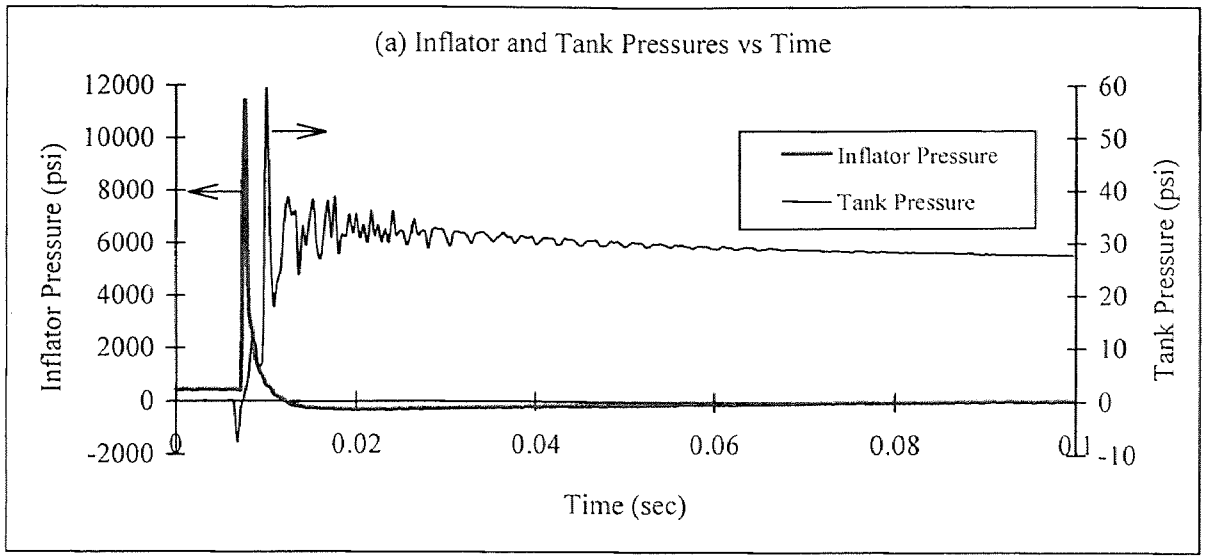

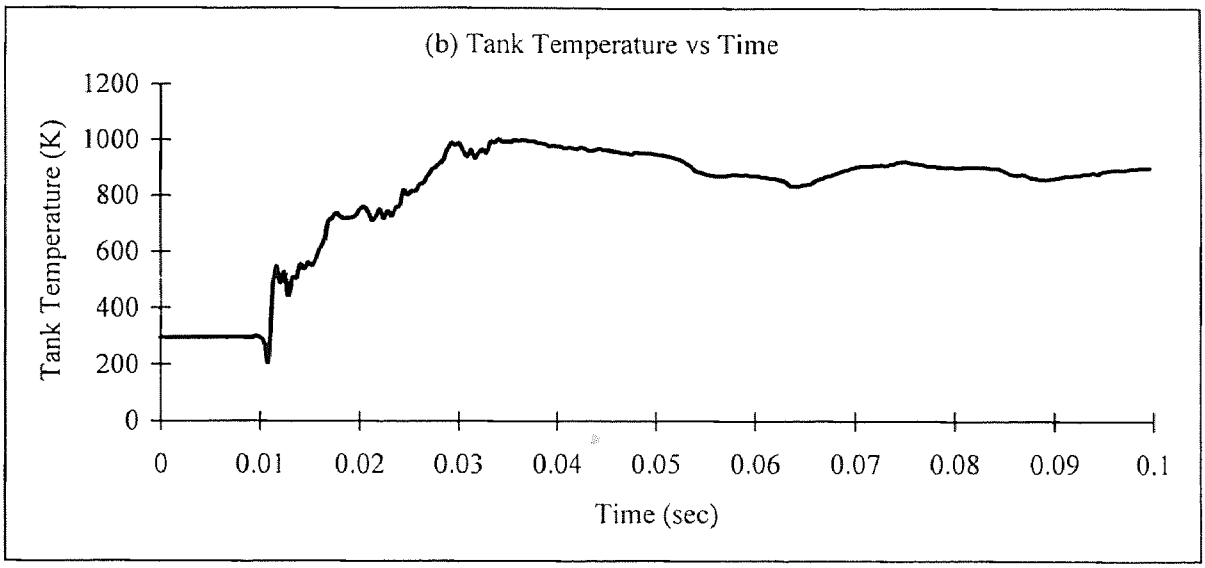

Figure 3.1 Pressure and temperature curves for a typical experiment

The maximum pressure in the inflator shown in Figure 3.1(a), is usually not the actual peak pressure developed inside the inflator. The reason for this is that in most of the experiments, the data was sampled after every 0.4 msec and if the peak pressure occurred between two sampling events, it is not captured by the data acquisition system. Also, the inflator pressure goes negative after reaching the peak. This is due to the fact that after a sudden rise and drop of pressure, the beams in the strain gage transducers do not come back to their original shape in such a short time and it takes some time for them to come back to their original shape.

Figure 3.1(a) shows that the maximum average tank pressure for this experiment is about 34 psi and it drops to 30 psi in 50 msec. According to Table 3.1, we need a pressure of 50.75 psi in a 28.3 liter tank. Since, the volume of our tank (70 liter) is about 2.5 times of this tank volume, we need a pressure of 20.30 (=50.75/2.5) psi in our tank. This shows the pressure that we are getting experimentally is sufficient to inflate an air bag.

The total number of product moles for this composition is about 0.4. This is about 60% lower than the number of moles required for the driver side air bag inflator. The number of product moles can be increased by increasing the number of moles of the initial mixture or by using a hybrid inflator, as will be discussed in Chapter 5. Also, Figure 3.1 shows that most of the mass leaves the inflator in less than 5 msec. Based on such results, the requirement of $t_{80\%}$ is also met.

Figure 3.1(b) shows that the maximum temperature in the inflator is about 1000 K and it drops to about 850 K in 65 msec. This temperature is higher than the temperature

of 600 K [10] or 700 K [22] used in the literature for the azide inflator; however, these temperatures are not uncommon for combustion-based inflators [35,49].

3.4 Major Critical Issues in the Development of Fast Combustion Inflator

In order to develop the fast combustion inflator, several critical issues were studied and evaluated. These included the effects of stoichiometry, initial mixture pressure and extreme hot and cold operating conditions (-40 °C and +90 °C).

3.4.1 Effect of Stoichiometry

During this research, the experiments were performed for stoichiometric, oxygen-rich, and methane-rich mixture compositions. The objective was to study the effect of stoichiometry on the dynamics inside the inflator and the tank, and to determine the final products' composition and their concentration. The corressponding experiments are summarized in Table 3.2.

Table 3.2 Experiments to assess the effect of stoichiometry

Stoichiometric		Oxygen-Rich		Methane-Rich	
Methane (psi)	Oxygen (psi)	Methane (psi)	Oxygen (psi)	Methane (psi)	Oxygen (psi)
20	40	20	60	30	40
30	60	20	70	30	55
40	80	20	80	35	40
90	180	30	70	40	40
100	200	120	360	120	120
125	250	150	350		
135	270				
150	300				
155	310				
210	420				

3.4.1.1 Stoichiometric Mixtures : The reaction between methane and oxygen occurs as follows :

$$CH_4 + 2O_2 \rightarrow CO_2 + 2H_2O$$

A stoichiometric mixture means that the components of the gaseous mixture (methane and oxygen) were charged into the inflator in the stoichiometric ratio (1:2) for the methane-oxygen reaction. Since the inflator was purged with oxygen before the mixture was charged into it, a small quantity of oxygen is always present and it is to be added when making calculations.

For stoichiometric mixtures, the peak pressure in the inflator increases with the initial pressure of the methane-oxygen mixture. Also, the pressure in the receiving tank increases with the initial pressure of the methane-oxygen mixture. Figure 3.2 compares the tank pressure curves for 20/40 (methane = 20 psi, oxygen = 40 psi) and 30/60 (methane = 30 psi, oxygen = 60 psi) mixtures. Figure 3.2 shows that the tank pressure in the 30/60 case is about 15% higher than in the 20/40 case.

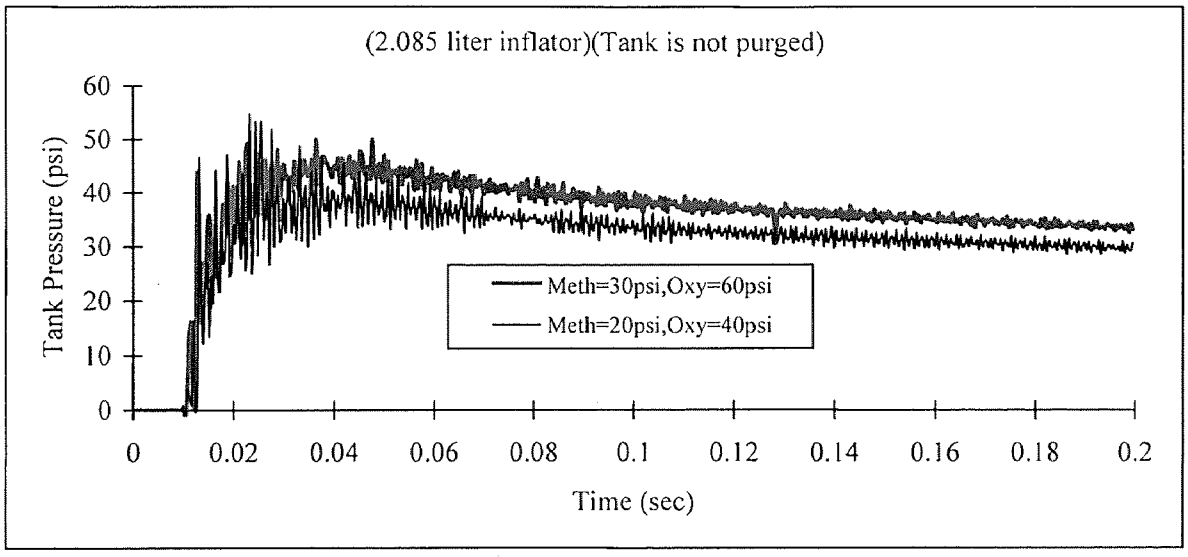

Figure 3.2 Tank pressure curves for different initial pressures of stoichiometric mixtures

3.4.1.2 Oxygen-Rich Mixtures : In this case, like the stoichiometric mixtures, the pressure in the tank increases with the initial pressure of methane-oxygen mixture. Figure 3.3 compares the tank pressure curves for different oxygen-rich mixtures. The average increase in tank pressure is about 10% for the 20/60 case compared with the 20/80 case.

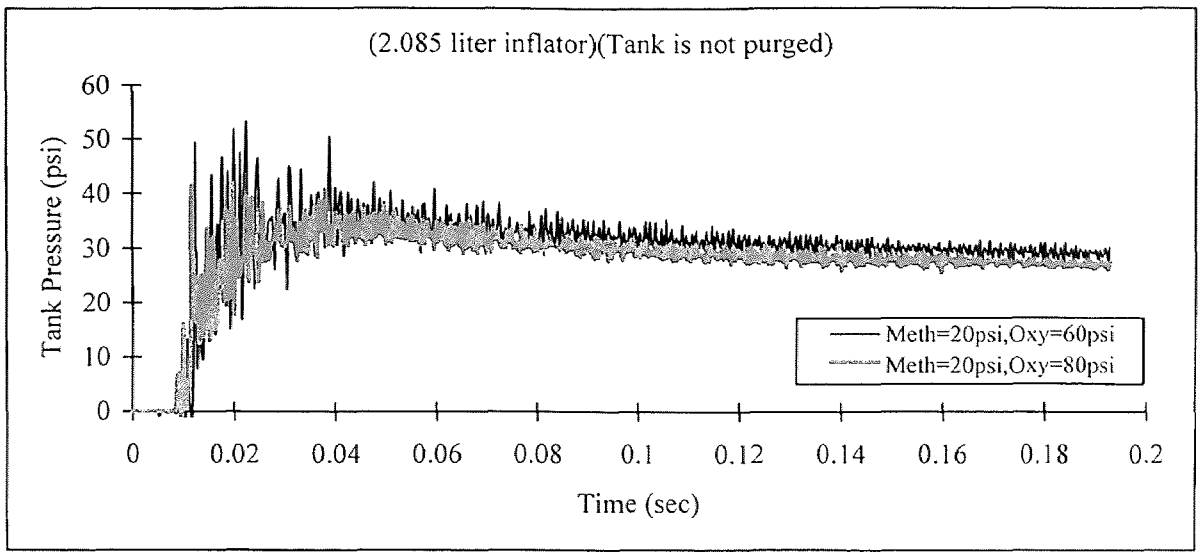

Figure 3.3 Tank pressure curves for different initial pressures of oxygen-rich mixtures

3.4.1.3 Methane-Rich Mixtures : Like the stoichiometric and oxygen-rich mixtures, the maximum pressure in the tank increases with the initial pressure of methane-oxygen mixture. Figure 3.4 compares the results of stoichiometric (methane = 30 psi, oxygen = 60 psi), oxygen rich (methane = 30 psi, oxygen = 70 psi) and methane rich (methane = 30 psi, oxygen = 40 psi) mixtures. Figure 3.4 shows that for the same amount of methane, the tank pressure for the oxygen-rich mixture is slightly lower (less than 10%) than the tank pressure for stoichiometric mixture. Also, the tank pressure for the methane-rich

mixture is slightly higher (less than 10%) than the tank pressure for the stoichiometric mixture.

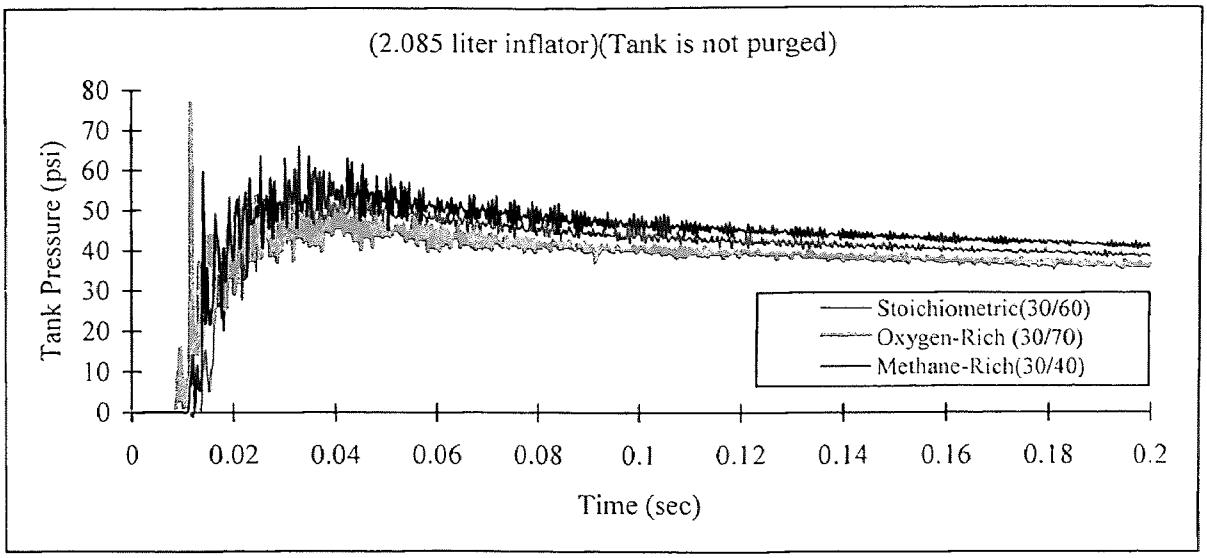

Figure 3.4 Comparison of stoichiometric, oxygen-rich and methane-rich mixtures

These results indicate that the dynamics inside the inflator and the tank are not affected significantly by the stoichiomety of methane-oxygen mixtures. Based on these results, it was decided that the stoichiometric mixture is an ideal selection for the remainder of experimentation in this research. So, most of the testing was done with stoichiometric mixtures in order to get complete combustion of the reactants.

3.4.2 Effect of Initial Mixture Pressure

As mentioned above, most of the experiments in the later part of this research were performed with stoichiometric mixtures. The peak pressure in the inflator and the pressure in the tank increases with the initial mixture pressure. Also, the tank temperature increases with the initial mixture pressure.

Figure 3.5 compares the inflator and tank pressures and the tank temperature for three different initial mixture pressures : 30/60, 90/180 and 125/250 in a 0.250 liter inflator. Figure 3.5(a) shows that the peak pressure in the inflator increases with the initial

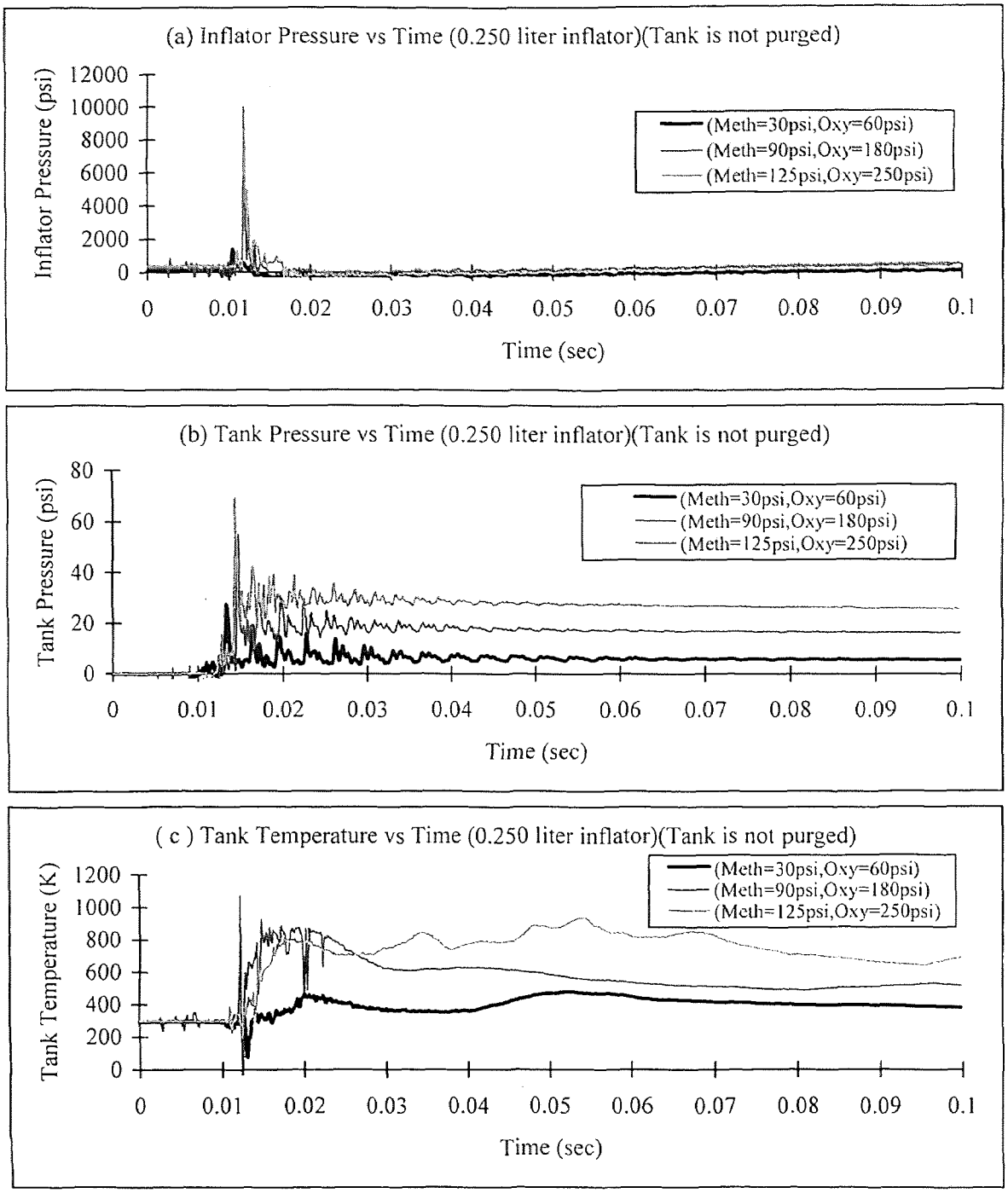

Figure 3.5 Comparison of pressure and temperature curves for different initial mixture pressures

mixture pressure. For a 30/60 mixture, the peak inflator pressure is 1380 psi, for a 90/180 mixture, it is 6210 psi, and for a 125/250 mixture, it is 9960 psi. Figure 3.5(b) shows that the tank pressure also increases with the initial mixture pressure. For a 30/60 mixture, the maximum average tank pressure is about 8 psi, for a 90/180 mixture, it is about 20 psi, and for a 125/300 mixture, it is about 30 psi. Figure 3.5(c) shows that the tank temperature also increases with the initial mixture pressure. For a 30/60 mixture, the maximum tank temperature is about 475 K, for a 90/180 mixture, it is about 850 K and for a 125/250 mixture, it is about 900 K.

Figure 3.6 compares the experimental values of peak inflator pressure, the maximum average tank pressure and the maximum tank temperature for different initial mixture pressures. All these values are for a 0.250 liter inflator. The figure shows that the peak inflator pressure, the maximum average tank pressure and the maximum tank temperature increase with the initial mixture pressure. These values are in close agreement with our model --- see Chapter 4.

3.4.3 Effect of Hot and Cold Ambient Conditions

One of the requirements for commercial inflators is that they should operate equally well for ambient temperatures in the range from -40 °C to +90 °C. Their performance should not vary by more than ±10% from hot to cold [36].

To test the performance of the fast combustion inflators, some experiments were performed at hot and cold conditions. The experiments were performed for a stoichiometric mixture (methane = 210 psi, oxygen = 420 psi) in a 0.067 liter inflator. In

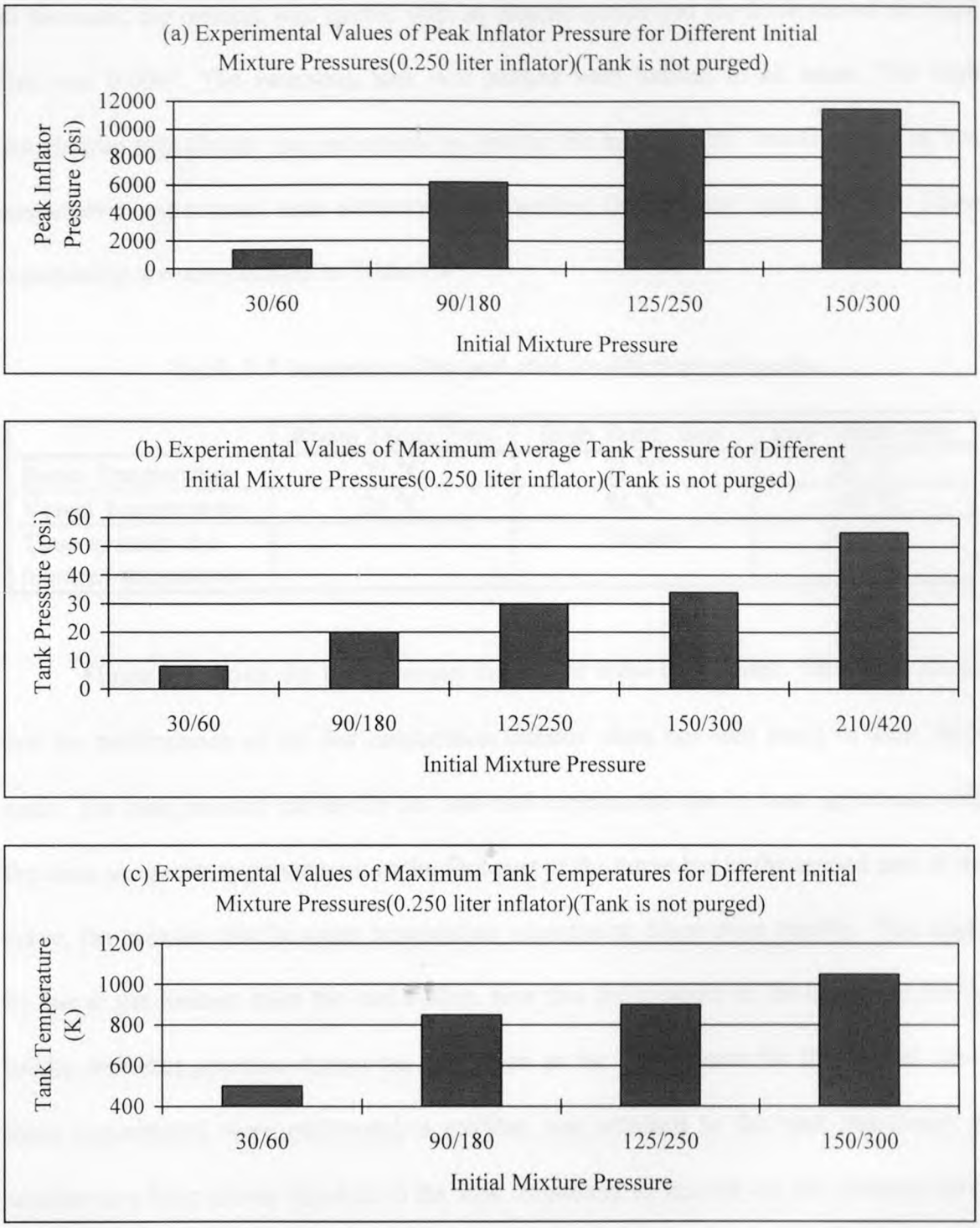

Figure 3.6 Experimental values of pressure and temperature for different initial mixture pressures

all the cases, the mixture was ignited with an electric match and the thickness of the burst disk was 0.004". The receiving tank was purged with helium in all cases. The high temperature experiment was performed by heating the inflator with heater tape. The low temperature experiment was performed by cooling the inflator with dry ice. These experiments are summarized in Table 3.3.

Table 3.3 Summary of hot and cold condition experiments

	Room Temp. Exp.	High Temp. Exp.	Low Temp. Exp.
Room Temperature	21 °C	21 °C	20 °C
Vessel Temperature	21 °C	84 °C	-20 °C
Time to attain the required temperature		5 hours	3 hours

Figure 3.7 shows the tank pressure curves for these three cases. The figure shows that the performance of the fast combustion inflator does not vary much in these three cases. The tank pressure curves for hot and cold experiments are in close agreement with the room temperature experiment in the first part of the curve but in the second part of the curve, the pressure for the room temperature experiment drops more rapidly. This might be due to gas leakage from the tank. Also, note that the pressure in the tank rises slowly unlike the other pressure curves we have seen so far. The reason for this is that when these experiments were performed, a snubber was attached to the tank transducer. A snubber is a filter device attached to the tank transducer to smooth out the pressure curve in the tank.

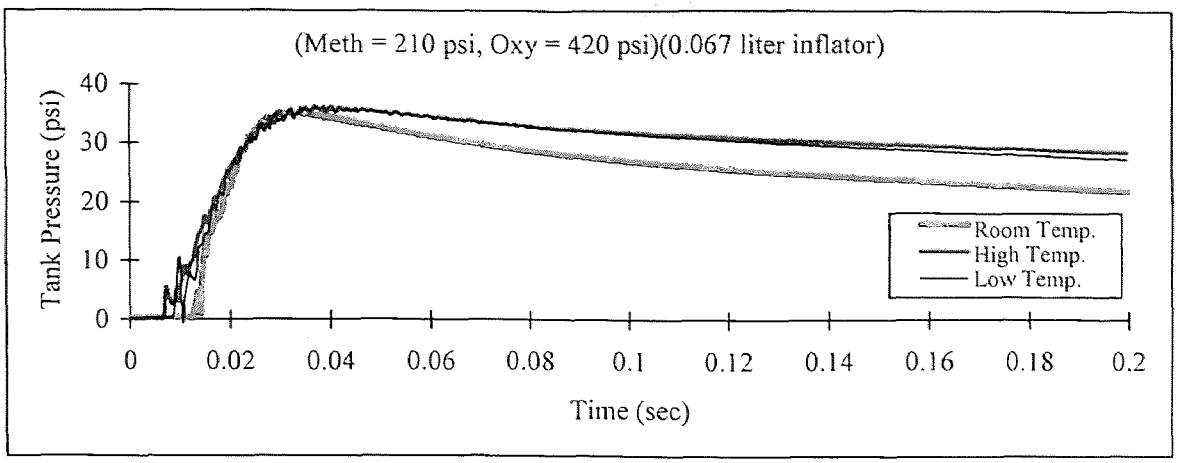

Figure 3.7 Tank pressure curves for room, high and low temperature experiments

3.5 Satisfaction of Other Important Requirements

In addition to the critical issues discussed above, there are other design and practical parameters, such as burst disk type and thickness, ignition device, tank purging gas, concentration of carbon monoxide produced and the severity of temperature in the tank which need to be studied and optimized.

3.5.1 Effect of the Burst Disk Type and Thickness

The burst disk is an important component of a fast combustion inflator and to study the influence of the burst disk thickness and type on the dynamics in the inflator and the tank was an important aspect of this research.

A number of experiments were performed with burst disks of different thicknesses. Figure 3.8 compares the tank pressure traces obtained by using three different burst disk thicknesses.

It is clear from Figure 3.8 that the thickness of the burst disk has no significant effect on the dynamics in the tank or on the time at which the disk ruptures.

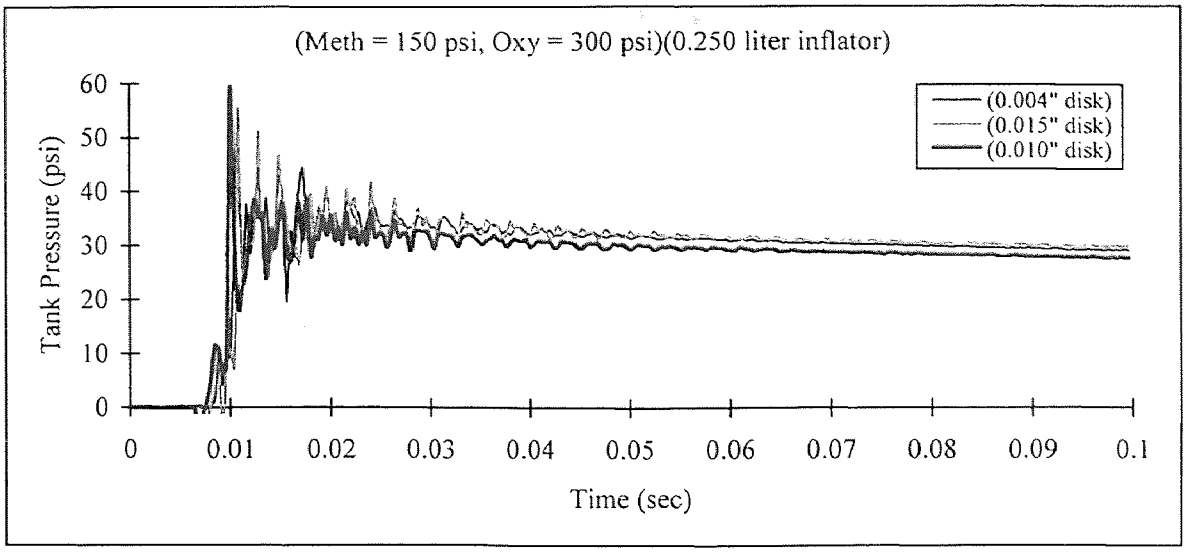

Figure 3.8 Comparison of tank pressure curves for different thicknesses of burst disk

A series of experiments was performed with annealed burst disks to see whether the type of burst disk has an effect on the dynamics in the inflator and the tank. Figure 3.9 compares the pressure traces in the inflator using a regular and an annealed burst disk. Again, there is no significant difference in the tank pressure in the case of an annealed burst disk.

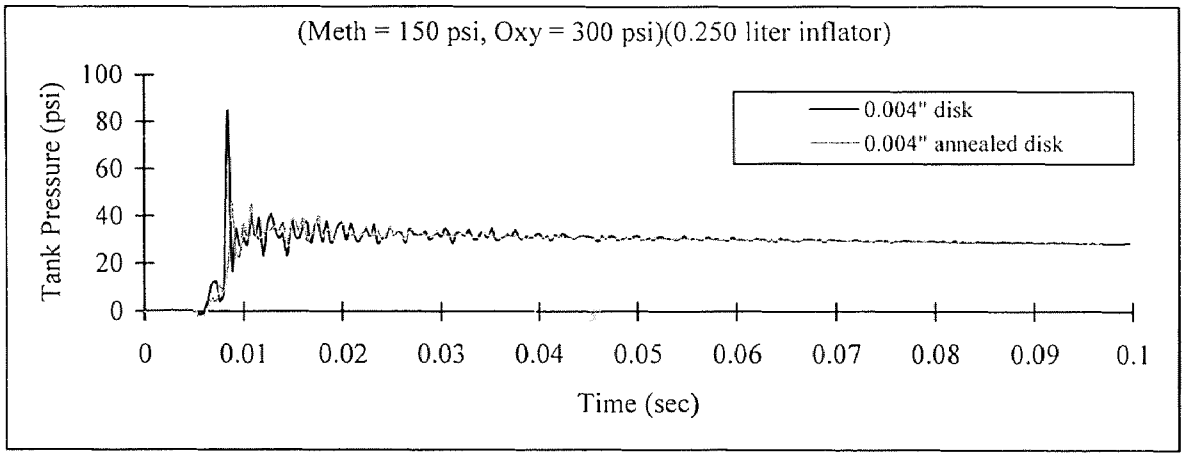

Figure 3.9 Comparison of regular and annealed burst disks

In the beginning of this research, it was thought that the pressure peak in the inflator might not be real. In order to verify that the peak pressure developed in the inflator was indeed real, we did some experiments with rated burst disks to see whether these disks would be ruptured by the pressure developed in the inflator. Table 3.4 shows the burst pressures for the rated burst disks that were used in this research.

Table 3.4 Burst pressures for rated burst disks

Burst Disk Thickness (in)	Burst Pressure (psi)
0.01	6,000 - 7,000
0.02	10,000
0.025	17,000

Figure 3.10 shows the tank pressure curves for two experiments performed with 0.025" burst disk. These experiments were performed for a 210/420 mixture (methane = 210 psi, oxygen = 420 psi) in a 0.250 liter inflator with a 70 liter receiving tank. Since the burst disks were ruptured in both the cases, it can be concluded that the pressure peak in the inflator is real. This pressure should be considered while designing the fast combustion inflator.

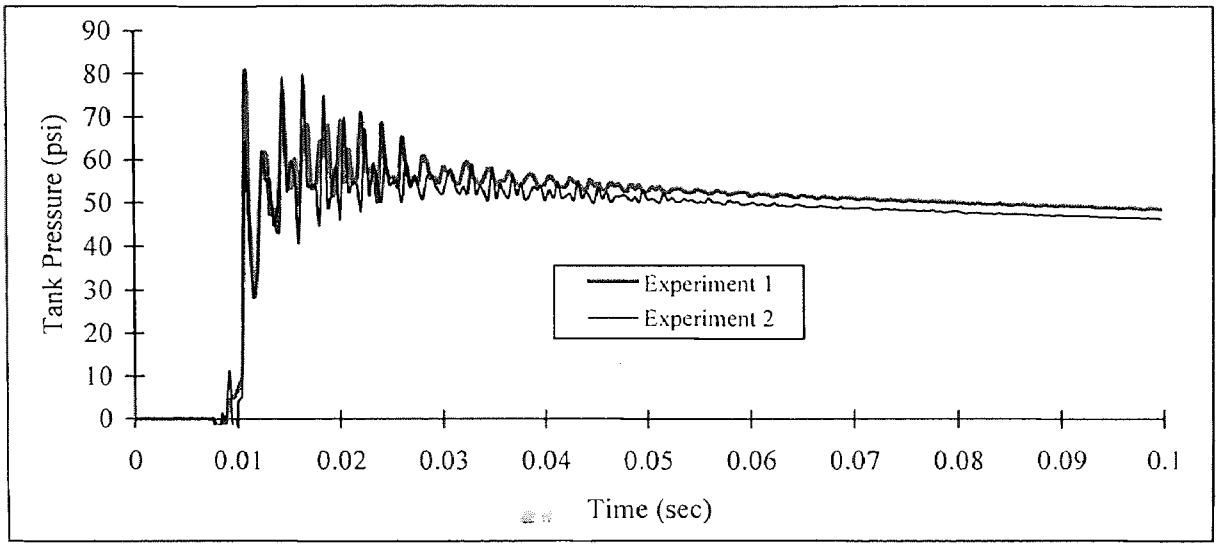

Figure 3.10 Tank pressure curves for experiments performed with rated burst disks

3.5.2 Effect of the Ignition Device

During this research, two different ignition devices were used to perform ignition : an electric match and a pyrofuze wire. Although, some of the experiments were performed with pyrofuze wire, electric matches proved to be more reliable. They gave a higher consistency of the results and were easier to use.

A number of experiments were performed by placing the electric match at different positions inside the inflator to study the effect of the position of the match on the dynamics inside the inflator, but no significant difference in the dynamics were observed.

3.5.3 Effect of the Tank Purging Gas

To study the effect of the purging gas on the pressure trace in the tank, experiments were performed with three different purging gases : atmospheric air, helium and nitrogen. Figure 3.11 compares the tank pressure curves with helium and air as the purging gas. The figure shows that the tank pressure is slightly higher with helium than with air.

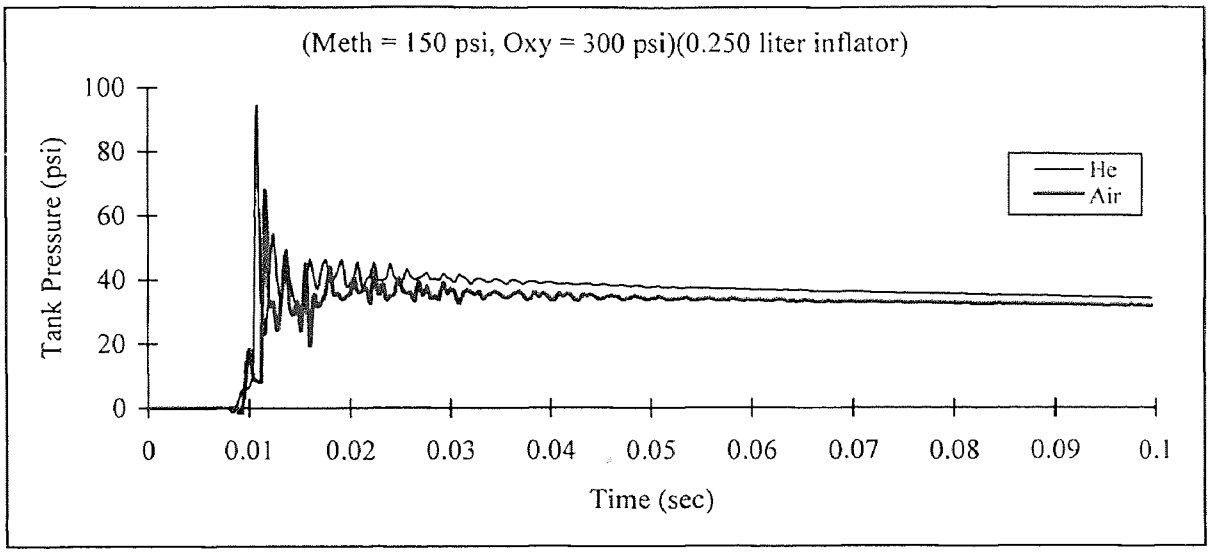

Figure 3.11 Comparison of tank pressure curves with helium and nitrogen as the purging gas

Figure 3.12 compares the pressure curves with nitrogen and air as the purging gas. The figure shows that the tank pressure is slightly lower with nitrogen than with air. These results are in agreement with our model given in Chapter 4.

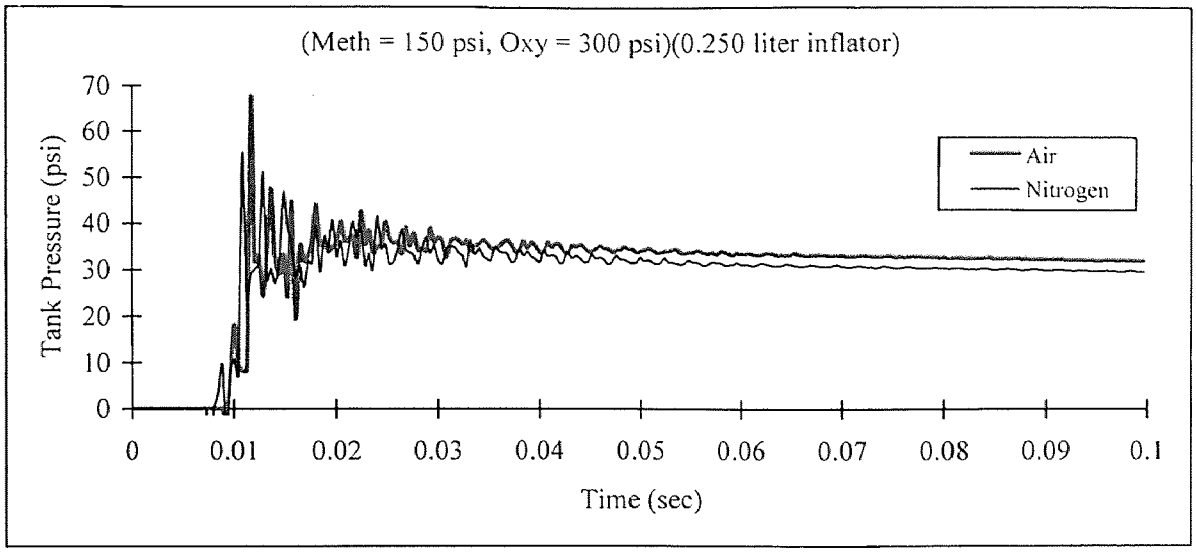

Figure 3.12 Comparison of tank pressure curves with nitrogen and air as the purging gases

3.5.4 Concentration of Carbon Monoxide

The chemical composition of the combustion products is also important in the design of an air bag inflator. In the fast combustion inflator, the major products of combustion are carbon dioxide (CO_2) and water (H_2O) but other gases such as carbon monoxide (CO) and oxygen (O_2) are also formed in small quantities. During this research, the concentration of carbon monoxide in the tank was measured. This was done by collecting a sample of gas from the receiving tank and analyzing it for carbon monoxide using Thermal Conductivity Gas Chromatograph. In the carbon monoxide analysis, the tank was not purged because this simulates very closely to an actual air bag inflation. In an actual air bag inflation, as the bag inflates, some air enters the bag from outside.

Some of the results of the CO analysis for stoichiometric, oxygen-rich and methane-rich mixtures are given in examples 1, 2 and 3 respectively.

Example 1 : The inflator was filled with a stoichiometric mixture (methane = 30 psi, oxygen = 60 psi). The four samples of the products of combustion from the receiving tank were analyzed for CO. The concentrations of CO obtained are shown in Table 3.5. The chromatograph for sample 3 is shown in Figure 3.13(a).

Example 2 : The inflator was filled with an oxygen-rich mixture (methane =30psi, oxygen = 70 psi). The three samples of the products of combustion from the tank were analyzed for CO. The concentrations of CO obtained are shown in Table 3.5. The chromatograph for sample 1 is shown in Figure 3.13(b).

Example 3 : The inflator was filled with a methane-rich mixture (methane = 30 psi, oxygen = 40 psi) at room temperature. The four samples of the products of combustion were analyzed for CO. The concentrations of CO obtained are shown in Table 3.5. The chromatograph for sample 1 is shown in Figure 3.13(c).

Table 3.5 Concentration of CO for different mixtures

Sample No.	Concentration of CO (ppm)		
	30/60 Mixture	30/70 Mixture	30/40 Mixture
1	536	473	250
2	525	550	248
3	456	474	199
4	357	----	173
Average :	469	499	218

According to General Motors (all other vehicle manufacturers have similar criteria), a total emission of 500 ppm of CO from all air bag sources in a 100 CFM volume is allowable. Typically, it is desired that one third of this level is produced by the

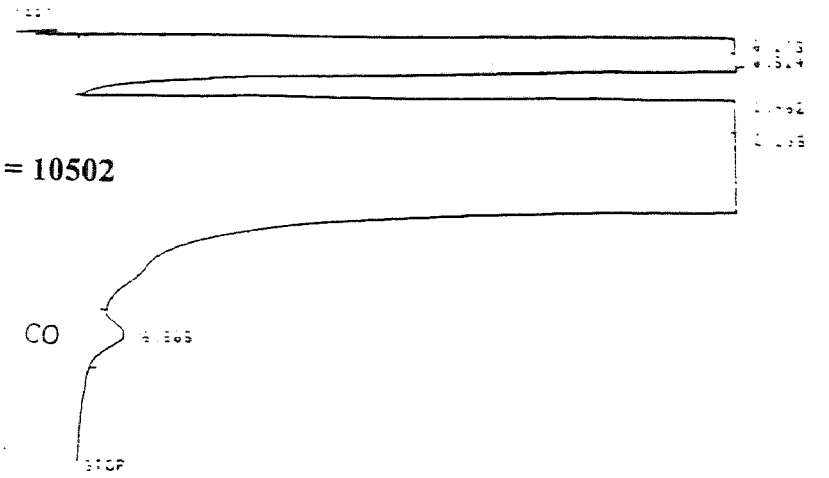

(a) **CO Area = 10502**

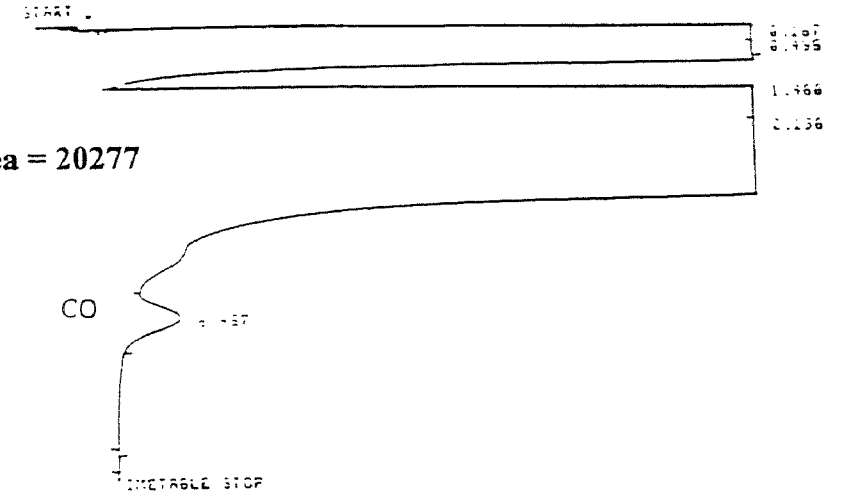

(b) **CO Area = 20277**

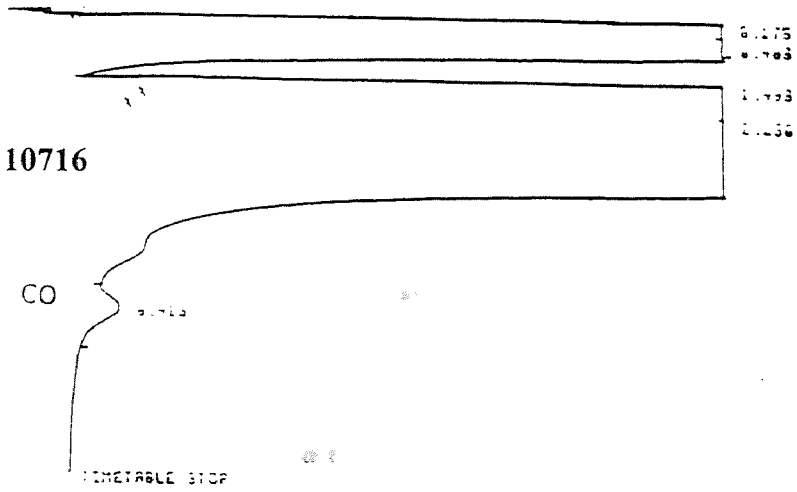

(c) **CO Area = 10716**

Figure 3.13 Chromatographs for different gas samples

driver side unit and two thirds by the passenger side unit. One eighth of the total is also allowed for a side impact air bag, should a side impact system deploy. Should the quantity of CO2 released exceed 2 percent of the gas in the 100 CFM volume then the CO limit is dropped to 450 ppm [37].

According to the American Conference of Industrial Hygienists, the short term exposure level (STEL) value for carbon monoxide is 400 ppm. This value times 5.5 (i.e. 2200 ppm) is considered appropriate guidelines for air bag deployment conditions [50].

3.5.5 Severity of the Temperature in the Receiving Tank

The temperature measurement in the tank is an important design parameter in the development of any air bag inflator because it reflects the temperature in the bag. The measurement of temperature in the tank is not easy because the response time of thermocouples are high if the flow rates involved are small. The only successful work on experimental measurement of tank temperature was published by Chan [24]. Although three different types of thermocouples were used to measure the tank temperature : a NANMAC E12 thermocouple and two OMEGA E type bare thermocouples (0.005" and 0.0005" in diameter), the only accurate temperature measurements were done with the OMEGA 0.0005" bare thermocouple.

Figure 3.14 shows the temperature traces inside the tank for two experiments performed with a 150/300 methane-oxygen mixture in a 0.250 liter inflator. In both cases, the tank was purged with nitrogen. The maximum temperature in the tank is about 1050 K and it drops to 800 K in 200 msec. This temperature is higher than the temperature of 600 K [10] or 700 K [22] for the pyrotechnic (sodium azide) inflators usually found in

the literature. However, no experimental measurement of temperature magnitude is published to date. Also, the temperature of 1000 K are not uncommon in combustion based inflators [35,49].

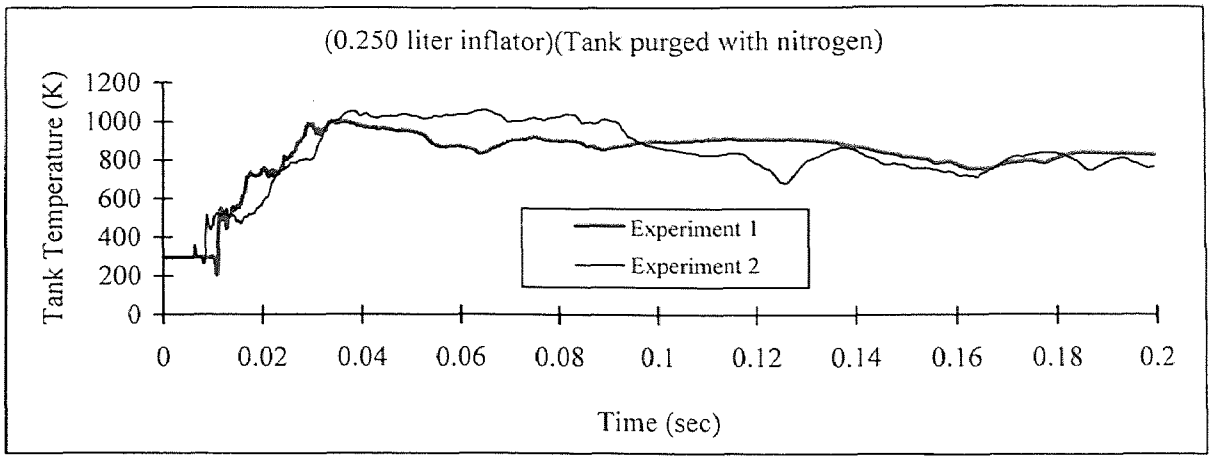

Figure 3.14 Tank temperature curve for a 150/300 mixture

Figure 3.15 shows the temperature curve inside the tank for a 30/60 mixture ignited in a 0.250 liter inflator. In this case the tank was not purged. We get a maximum temperature of about 480 K and it drops to 380 K in about 100 msec.

So, the conclusion is that at lower initial mixture pressures, the tank temperatures are lower than at higher initial mixture pressures.

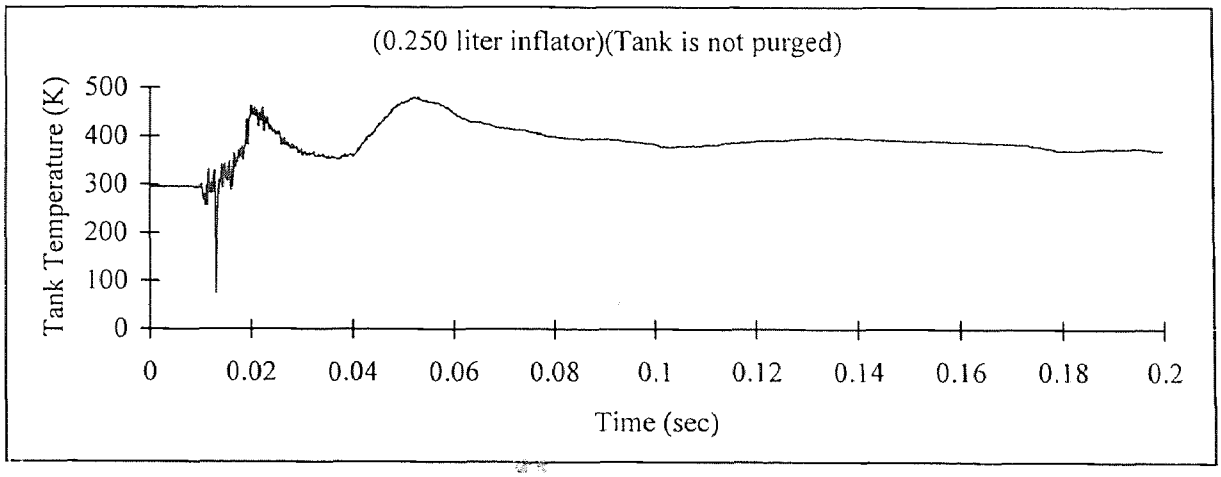

Figure 3.15 Tank temperature curve for a 30/60 mixture

3.6 Application to Different Inflator Sizes

As mentioned earlier, during this research, five different inflator sizes were used. The inflator and tank pressure increase with the increase in the inflator size for the same initial mixture pressure.

2.085 Liter Inflator : The initial experiments of this research were done in 2.085 liter inflator. Most of the experiments to study the effects of stoichiometry and to measure the concentration of carbon monoxide in the tank were done with this inflator. Most of the experiments with this inflator were performed at initial pressures of 100 psi or less and in all the experiments, 70 liter receiving tank was used. Figure 3.16 shows the inflator and tank pressure curves for a 30/60 mixture.

0.067 Liter Inflator : The volume of this inflator is about 2.7 times the volume of side impact air bag inflators commercially used at this time. In all the experiments, 70 liter receiving tank was used. The experiments with higher initial pressures started with this inflator. Figure 3.17 shows the inflator and tank pressure curves for a 150/350 mixture.

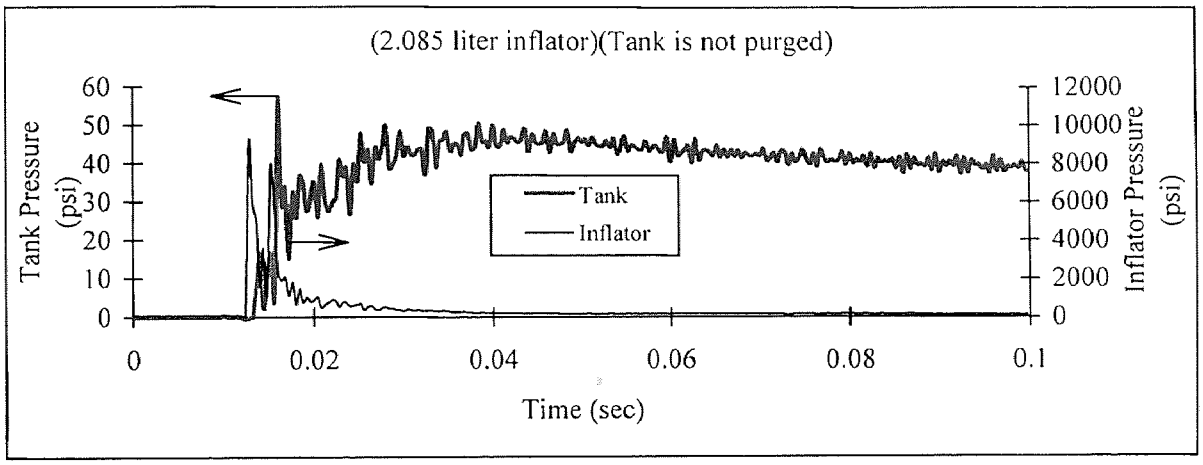

Figure 3.16 Inflator and tank pressure curves for a 30/60 mixture (2.085 liter inflator)

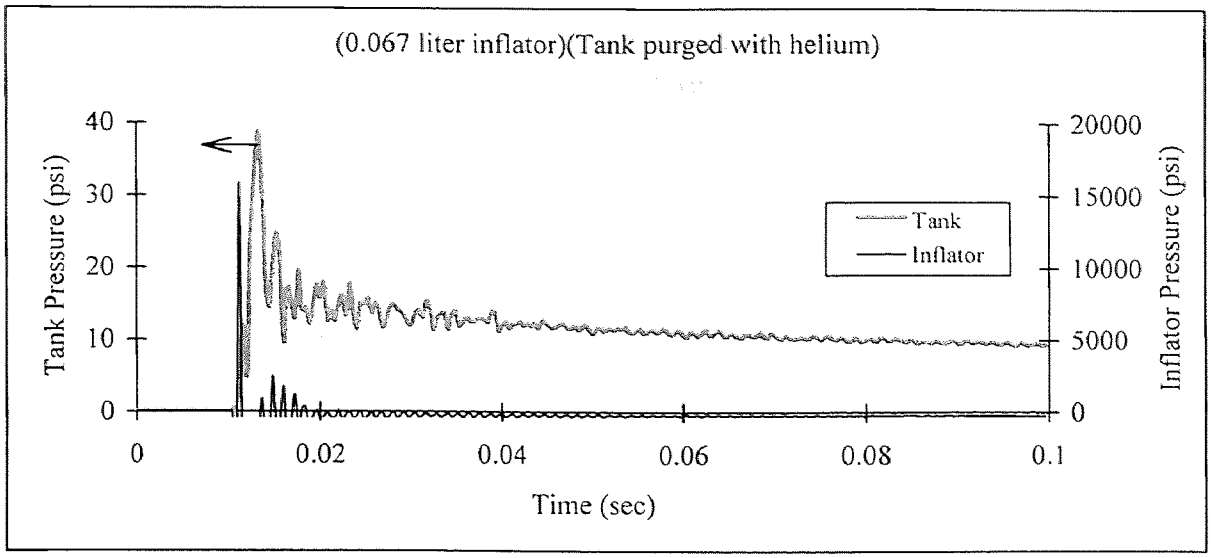

Figure 3.17 Inflator and tank pressure curves for a 150/350 mixture (0.067 liter inflator)

0.0246 Liter Inflator : The volume of this inflator is equal to the volume of commercially used side impact air bag inflators. The experiments with this inflator were only performed for stoichiometric, 150/300 (methane = 150 psi, oxygen = 300 psi) mixture. In all the experiments, 70 liter receiving tank was used.

0.0146 Liter Inflator : The volume of this inflator is about 50% smaller than the volume of commercially used side impact air bag inflators. Again, most of the experiments were performed with stoichiometric mixtures. Figure 3.18 shows the inflator and the tank pressure curves for a 150/300 mixture. A 28.3 liter receiving tank was used in all the experiments.

0.250 Liter Inflator : This inflator is about 10% smaller than the present size of the commercially used driver side inflator. Most of the experiments performed with this inflator were for stoichiometric mixture and in all the experiments, a 70 liter receiving tank was used. Figure 3.19 shows the inflator and tank pressure curves for a 150/300 mixture.

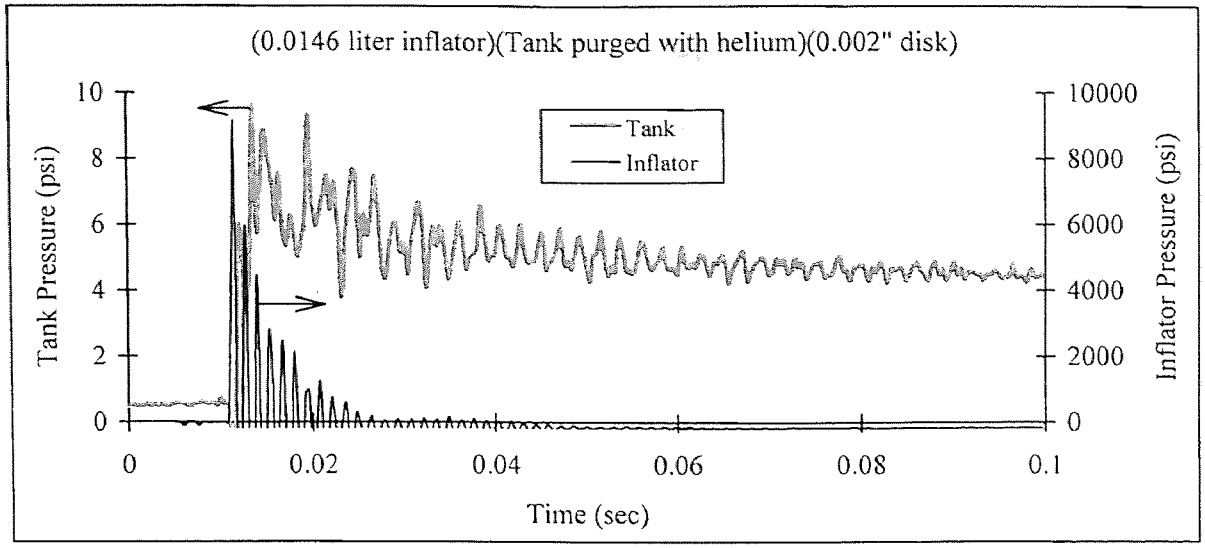

Figure 3.18 Inflator and tank pressure curves for a 150/300 mixture (0.0146 liter inflator)

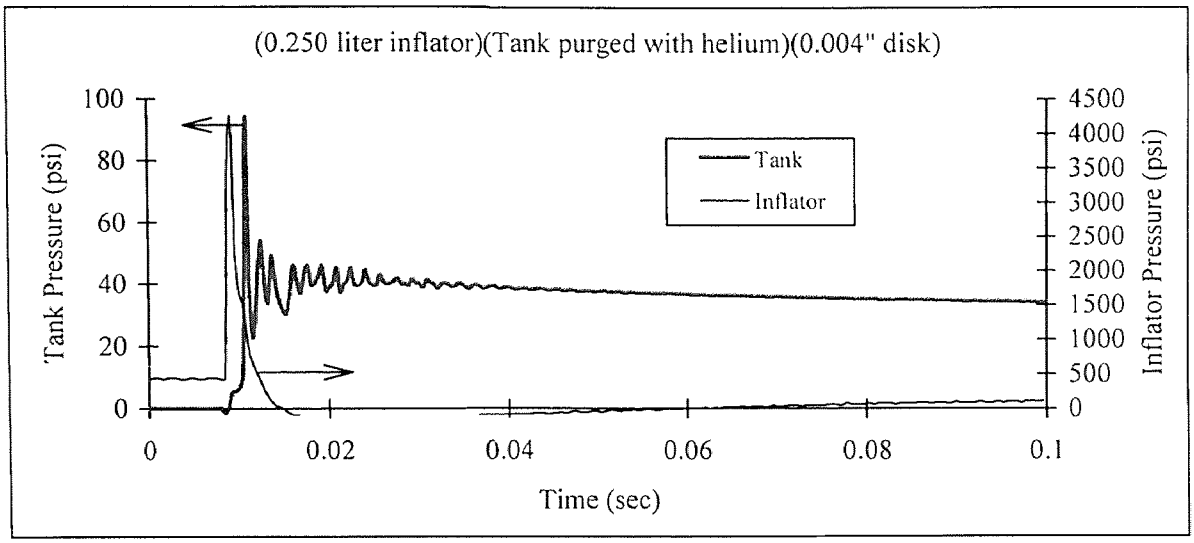

Figure 3.19 Inflator and tank pressure curves for a 150/300 mixture (0.250 liter inflator)

From the above discussion, it is clear that the dynamics inside the inflator and the tank and the shapes of pressure-time curves inside the inflator and the tank are consistent for all inflator sizes.

3.7 Conclusions

The experimental results were discussed for the development of fast combustion inflator. The following conclusions can be drawn from the discussion :

1. The dynamic condition with respect to pressure variation with time (P-t) i.e., with respect to inflating an air bag in the required time is satisfied.
2. Most of the design requirements are satisfied such as hot and cold operating conditions, concentration of carbon monoxide produced and the effect of burst disk.
3. The experimental results are in agreement with the thermodynamics and mass flow model as discussed in Chapter 4.
4. One main requirement that needs additional consideration is the number of moles and we propose to operate the system at high initial pressures or use it as hybrid system as discussed in Chapter 5.

CHAPTER 4

DEVELOPMENT OF THEORETICAL MODEL AND COMPARISON WITH EXPERIMENTAL RESULTS

4.1 Introduction

In this chapter, a description of the theoretical model called the fast combustion model is given along with a comparison with the experimental results. The model is based on the change in the internal energy inside the inflator and the receiving tank as the mass flows from the inflator to the tank. To simplify the model, it is assumed that :

1. the gases inside the inflator and the tank behave as ideal gases.
2. the mass flow from the inflator to the tank behave as one-dimensional isentropic flow.

Prior to discussing the model, we first present and justify the applicability of an ideal gas assumption and give the mass flow rate equation for one-dimensional isentropic flow. This discussion is followed by a complete discussion of the fast combustion model and a demonstration of the model by several experimental examples.

4.2 Development of Theoretical Model

As presented above to simplify the model, it is assumed that the gases inside the inflator and the tank behave as ideal gases and the mass flow from the inflator to the tank behaves as one-dimensional isentropic flow. In this section we demonstrate and justify the applicability of these assumptions for the system and set-up of this research.

4.2.1 Ideal Gas Assumption and Justification

The assumption of ideal gas is justified based on the analysis of gases and their thermodynamic properties. The reaction between methane (CH_4) and oxygen (O_2) occurs as follows :

$$CH_4 + 2O_2 \rightarrow CO_2 + 2H_2O$$

The products of combustion from the above reaction are carbon dioxide (CO_2) and water (H_2O) but other gases such as carbon monoxide (CO), oxygen (O_2) and hydrogen (H_2) are also formed in small quantities. In the inflator, the mixture is mostly composed of methane (CH_4) and oxygen (O_2) before combustion and carbon dioxide (CO_2), water vapor (H_2O), carbon monoxide (CO), oxygen (O_2) and hydrogen (H_2) after combustion. In the tank, the mixture is mostly composed of carbon dioxide (CO_2), water vapor (H_2O) and oxygen (O_2). Other gases such as nitrogen (N_2) and helium (He) are also present when the tank is purged with nitrogen (or air) and helium respectively. Table 4.1 gives the mass fractions of the primary inflator and tank gases for a 150/300 (methane = 150 psi, oxygen = 300 psi) case. In this case, the tank is not purged, i.e. it is in equilibrium with atmospheric air. These mass fractions are calculated by using the CEA program. The gases shown in Table 4.1 form the majority of constituents.

Table 4.1 Mass fractions of primary inflator and tank gases

Gas	Mass Fraction (Inflator)	Mass Fraction (Tank)
CO_2	0.264	0.050
H_2O	0.343	0.041
CO	0.168	---
O_2	0.117	0.213
H_2	0.004	---
N_2	---	0.684

We will justify that the ideal gas assumption can be used for both the inflator and the tank. Before we proceed, it seems reasonable to give a definition for some of the terms used later :

1. ***Reduced Temperature :*** The ratio, T/T_c is called the reduced temperature denoted by T_r; where T_c is the critical temperature.
2. ***Reduced Pressure :*** The pressure ratio, P/P_c is called the reduced pressure denoted by P_r; where P_c is the critical pressure.
3. ***Fugacity Coefficient :*** The fugacity coefficient, f/P measures the departure from ideal gas behavior. For an ideal gas, f/P = 1.0, i.e. the fugacity of an ideal gas is equal to the pressure of the ideal gas system.
4. ***Compressibility Factor :*** The compressibility factor, Z defined as :

$$Z = \frac{Pv}{RT}$$

where P, v, R and T are the pressure, specific volume, ideal gas constant and temperature respectively. The compressibility factor measures the departure from ideal gas behavior, which is represented by Z = 1.

The critical temperatures and pressures of inflator and tank gases are given in Table 4.2 [38,39]. First we look at the gases in the inflator, then at the tank. The maximum temperature and pressure in the inflator are 4215 K and 726 atm respectively [15,16]. Based on these values, the reduced temperature (T_r) and reduced pressure (P_r) are calculated and the corresponding values for fugacity coefficient (f/P) and compressibility factor (Z) are calculated. The values of the fugacity coefficient are calculated from the generalized Honari-Brown Fugacity Coefficient Charts [40] and the values of

compressibility factor are calculated from the generalized Nelson-Obert Compressibility Charts [40]. These values are given in Table 4.3.

Table 4.2 Critical temperatures and pressures of gases

Gas	Critical Temperature, °C (K)	Critical Pressure, atm
Methane (CH_4)	- 82.5 (190.5)	45.8
Oxygen (O_2)	-118.8 (154.2)	49.7
Carbon dioxide (CO_2)	31.1 (304.1)	73.0
Water (H_2O)	374.1 (647.1)	218.4
Carbon monoxide (CO)	-139.0 (134.0)	35.0
Hydrogen (H_2)	-239.9 (33.1)	12.8
Nitrogen (N_2)	-147.0 (126.0)	33.5
Helium (He)	-267.9 (5.1)	2.26

Table 4.3 Fugacity coefficients and compressibility factors for the inflator gases

Gas	P_r	T_r	(f/P)	Z
CH_4	15.8	22.1	~1.0*	~1.0*
O_2	14.6	27.3	~1.0*	~1.0*
CO_2	9.9	13.8	1.04	1.08
H_2O	3.3	6.5	1.02	1.03
CO	20.7	31.4	~1.0*	~1.0*
H_2	56.7	127.3	N/A	N/A

The values indicated by '*' in Table 4.3 are extrapolated from the charts. Also, the values for (f/P) and Z for hydrogen are not available (N/A) from the charts. But since the temperature in the inflator is much higher than the critical temperature of hydrogen, it can be assumed that hydrogen behaves as an ideal gas inside the inflator.

The maximum temperature and pressure in the tank are 1500 K and 6.10 atm respectively [15,16]. Table 4.4 shows the values of P_r, T_r, (f/P) and Z for tank gases.

Table 4.4 Fugacity coefficients and compressibility factors for the tank gases

Gas	P_r	T_r	(f/P)	Z
CO_2	0.08	4.93	1.0	1.0
H_2O	0.03	2.32	1.0	1.0
O_2	0.12	9.73	1.0	1.0
N_2	0.18	11.90	1.0	1.0
He	2.70	294.12	N/A	N/A

The values of (f/P) and Z for helium are not available (N/A) at these P_r and T_r. Again, since the temperature in the tank is much higher than the critical temperature of helium, it can be assumed that helium behaves as an ideal gas inside the tank.

It is clear from Tables 4.3 and 4.4 that all the major gases in the inflator and the tank behave as ideal gases. Therefore, it seems reasonable to assume that the mixtures of gases in the inflator and the tank behave as ideal gas mixtures.

4.2.2 Description of One-dimensional Isentropic Mass Flow Rate Model

The mass flow rate from the inflator to the tank, $\dot{m}$ calculated using the one dimensional laws for the isentropic flow of an ideal gas. The inflator and tank system is shown schematically in Figure 4.1. The following assumptions are made:

1. Frictional effects are small and there is no heat transfer with the surroundings, thus the flow may be considered as reversible adiabatic or isentropic.
2. One-dimensional flow and therefore, uniform fluid properties over any cross-section.
3. Quasi-steady approximation holds. We neglect transient effects. This assumption will be justified by the agreement of the model and experiments.

The equation for mass flow rate is derived from the continuity equation which is given as [41] :

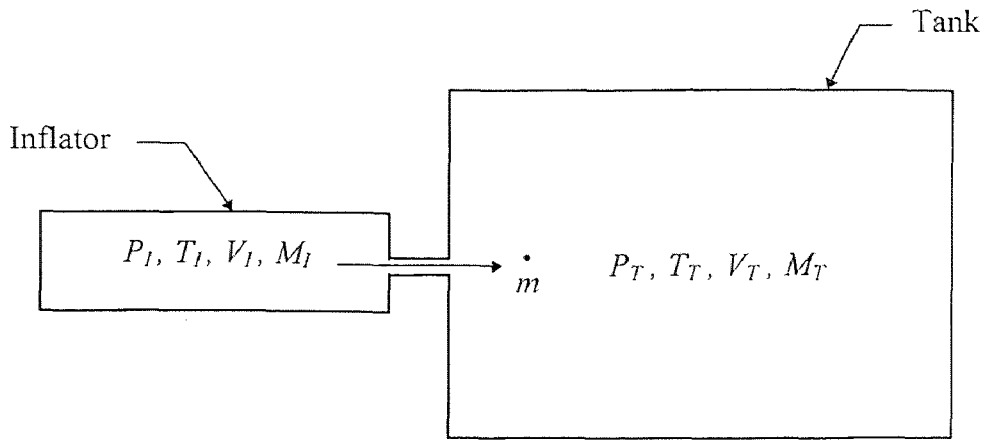

Figure 4.1 Schematic of inflator and tank system

$$\dot{m} = \rho_T A C_T \tag{1}$$

The equation is as follows :

$$\dot{m} = A \frac{P_I}{\sqrt{T_I}} \sqrt{\frac{\gamma}{R}} \frac{M}{\left[1 + \left(\frac{\gamma - 1}{2}\right) M^2\right]^{\frac{(\gamma+1)}{2(\gamma-1)}}} \tag{2}$$

where ;

$$M = \sqrt{\left[\frac{2}{(\gamma - 1)}\right]} \sqrt{\left[\frac{P_T}{P_I}\right]^{(1-\gamma)/\gamma} - 1} \tag{3}$$

and

$\dot{m}$ = mass flow rate (kg/s)

A = area of the orifice (m^2)

P_I = pressure in the inflator (Pa)

P_T = pressure in the tank (Pa)

T_I = temperature in the inflator (K)

T_T = temperature in the tank (K)

ρ_I = density of inflator gases (kg/m^3)

ρ_T = density of tank gases (kg/m^3)

V_I = volume of the inflator (m^3)

V_T = volume of the tank (m^3)

M_I = mass inside the inflator (kg)

M_T = mass inside the tank (kg)

C_T = velocity of tank gases (m/s)

R = universal gas constant (J/kg K)

γ = ratio of specific heats

M = Mach number

If the pressure ratio (P_T/P_I) is smaller than the critical pressure ratio (P_C/P_I), which is defined as :

$$\frac{P_C}{P_I} = \left[\frac{2}{(\gamma+1)}\right]^{\gamma/(\gamma-1)} \tag{4}$$

the flow is choked and the mass flow through the orifice is maximum. The mass flow rate in this case is given as :

$$\dot{m} = A\frac{P_I}{\sqrt{T_I}}\sqrt{\frac{\gamma}{R}\left[\frac{2}{(\gamma+1)}\right]^{(\gamma+1)/(\gamma-1)}} \tag{5}$$

4.2.2.1 Validation of the One-dimensional Model Using an Ideal Gas : An ideal gas was used in the inflator to access the accuracy of the measured data by comparing simulated and experimental data. In this case, nitrogen was selected as the ideal gas to

validate the model. A FORTRAN program 'FASTN2' was written to simulate the experimental data. The program is based on the assumptions described in section 4.2.2. In addition, it is assumed that the specific heats of nitrogen are constant. The program calculates the mass flow rate from the inflator to the tank and also calculates the temperature and pressure inside the inflator and the tank as a function of time. The program and a typical output from the program are given in Appendix B.2.

Validation Example 1 : Consider the expansion of nitrogen at 849.54 psi (5960248.3 Pa) from a 0.250 liter inflator to a 70 liter tank. The burst disk (0.004" thick) was ruptured on command and nitrogen flows from the inflator to the tank. The tank was purged with nitrogen before the experiment. The input parameters for the program 'FASTN2' are shown in Table 4.5. In this case the ruptured area of the burst disk is 0.8 times the area of the orifice so the area is taken as 0.000228 m^2 instead of 0.0002850 m^2, which is the area of the complete orifice.

Table 4.5 Input parameters for the ideal gas model (Example 1)

Parameter	Inflator	Tank
Pressure (Pa)	5960248.3	101351.7
Temperature (K)	298.15	298.15
Volume (m^3)	0.000250	0.07
Mass (kg)	0.01684	0.08020

Figure 4.2 shows the pressure and the temperature curves inside the inflator and the tank. Figure 4.2 (a) and (b) show that the experimental pressure curves are in close agreement with the model. Figure 4.2 (a) shows that in the inflator pressure starts to drop at 13.5 msec when the burst disk is ruptured and at 33.5 msec, the inflator pressure is in equilibrium with the tank pressure. Figure 4.2 (b) shows that the experimental pressure

trace in the tank is not smooth in the beginning. This is due to the expansion when nitrogen enters the tank until the pressure equals the equilibrium pressure. The maximum pressure in the tank obtained from the model is 3.03 psi. From the experiment, the maximum average pressure in the tank is 3.20 psi. So, the difference is about 6%, which is acceptable. Figure 4.2 (c) contains the inflator and tank temperatures obtained from the model. It can be seen that the temperature in the inflator drops continuously from 298.15 K to 95.3 K whereas the temperature in the tank increases from 298.15 K to 305.3 K and then it drops to 300.4 K.

Figure 4.3 compares the mass flow rate from the inflator to the tank for the experiment and the model. The experimental mass flow rate is in close agreement with the model. The maximum difference between the experiment and the model is about 10%. The experimental mass flow rate is calculated from the inflator and tank pressure curves using the FORTRAN Program 'MFLOW'. The program and a typical output from the program are given in Appendix B.3. The figure shows that nitrogen starts to enter the tank at 13 msec and within another 20.5 msec, the whole mass of nitrogen is inside the tank. The pressure in the tank is maximum at this time (Figure 4.2(b)). Since the tank to inflator pressure ratio is less than the critical pressure ratio up to 28.4 msec, the flow is choked up to that time.

Validation Example 2 : In this example, two experiments with the expansion of nitrogen at 877.12 psi (6150455.2 Pa) are considered. The inflator and tank volumes are 0.250 liter 70 liter tank respectively. Again, the burst disk (0.004" thick) is ruptured on command and the tank is purged with nitrogen. In the inflator, two transducers are used to measure

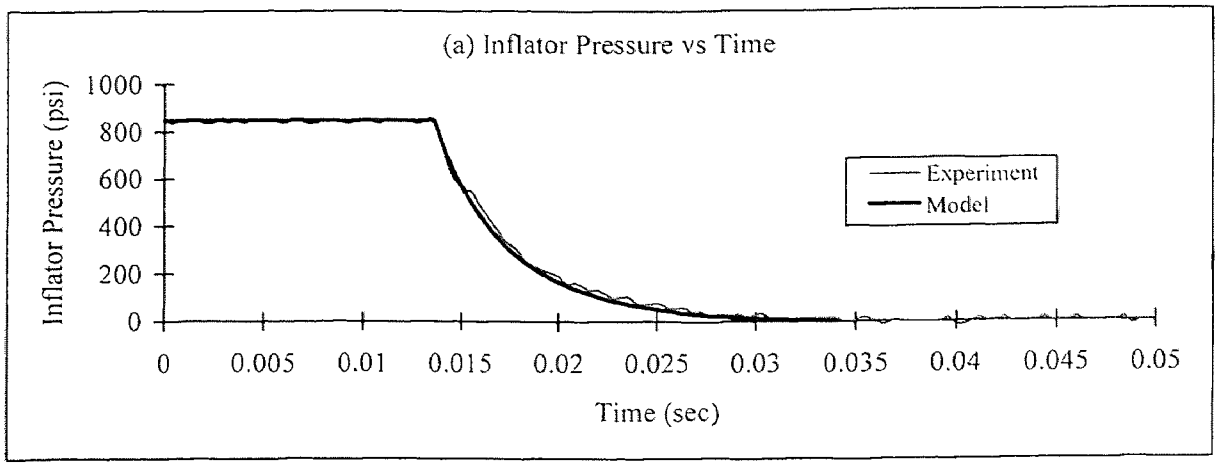

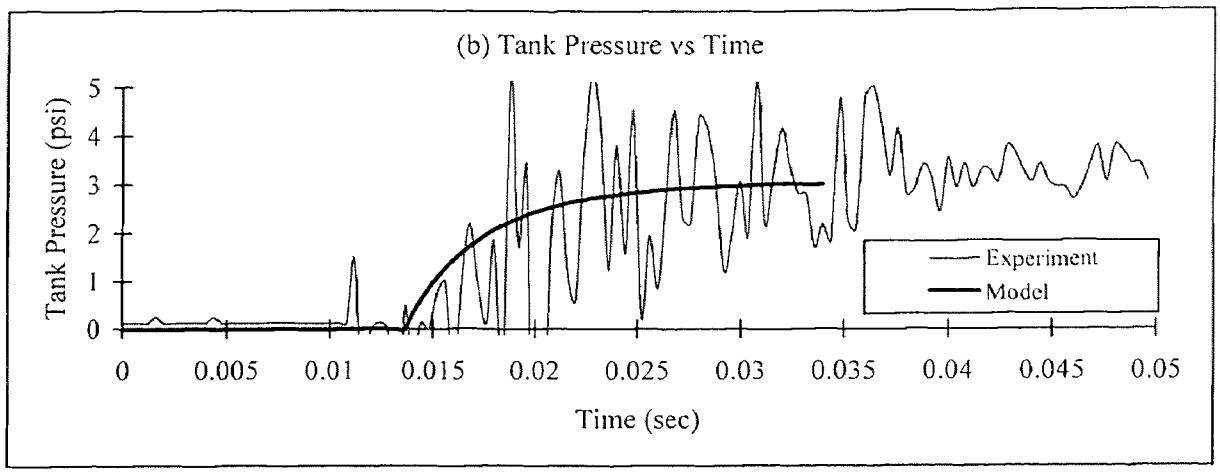

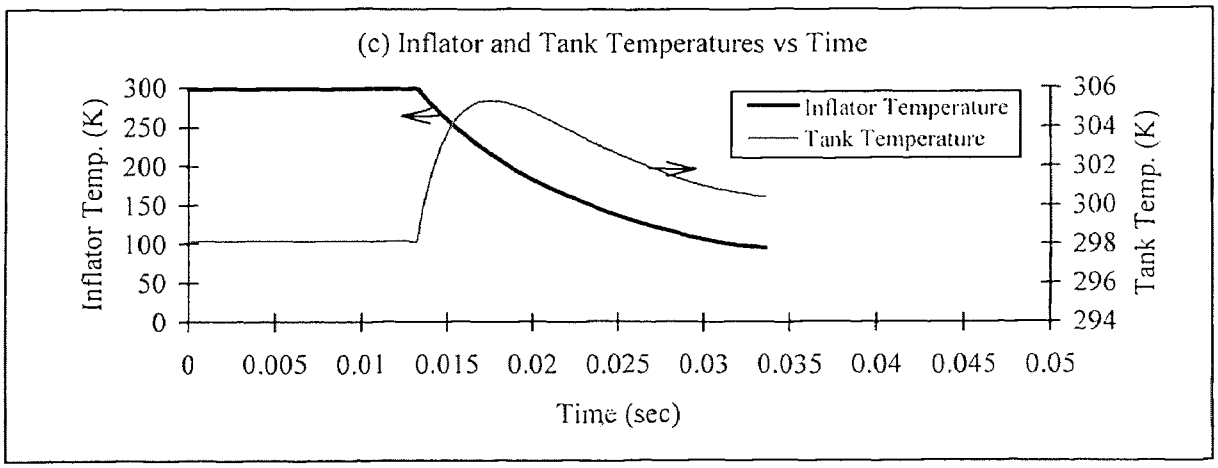

Figure 4.2 Pressure and temperature curves inside the inflator and the tank demonstrating the applicability of the one dimensional model

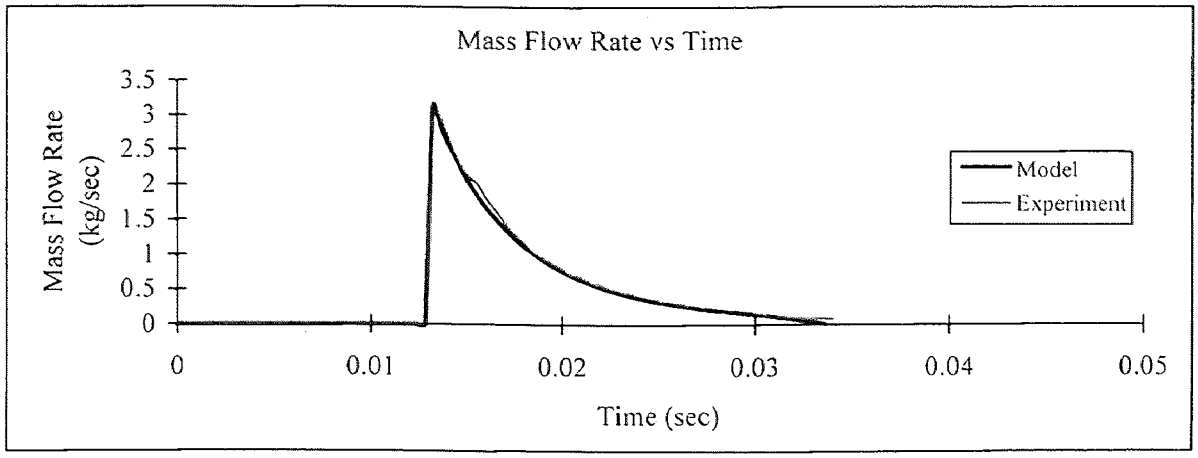

Figure 4.3 Comparison of theoretical and experimental mass flow rates

the pressure : a Data Instrument's 3000 psi transducer (Trans. 1) and a Sensotec's 30,000 psi transducer (Trans. 2). The input parameters for the program 'FASTN2' are shown in Table 4.6. In this case the ruptured area of the burst disk is 0.75 times the area of the orifice so the area is taken as 0.0002138 m^2 instead of 0.0002850 m^2, which is the total area of the orifice.

Table 4.6 Input parameters for the ideal gas model (Example 2)

Parameter	Inflator	Tank
Pressure (Pa)	6150455.2	101351.7
Temperature (K)	298.15	298.15
Volume (m^3)	0.000250	0.07
Mass (kg)	0.01738	0.08020

Figure 4.4 gives the pressure curves inside the inflator and the tank. Figure 4.4 (a) shows that the experimental pressure curves in the inflator, obtained from two different pressure transducers located at different positions in the inflator, are in close agreement with each other and they agree very well with the model. The pressure in the inflator starts to drop after about 12.0 msec when the burst disk is ruptured and after about 31.0 msec, the inflator pressure is in equilibrium with the tank pressure. Figure 4.2 (b) shows

that the maximum pressure in the tank obtained from the model is 3.12 psi. From the experiment, the maximum average pressure in the tank is about 3.30 psi. So, the difference is again about 6%.

From the above examples, it is clear that curves generated by the nitrogen experiments are in good agreement with the model. In the next section, we will describe the fast combustion model.

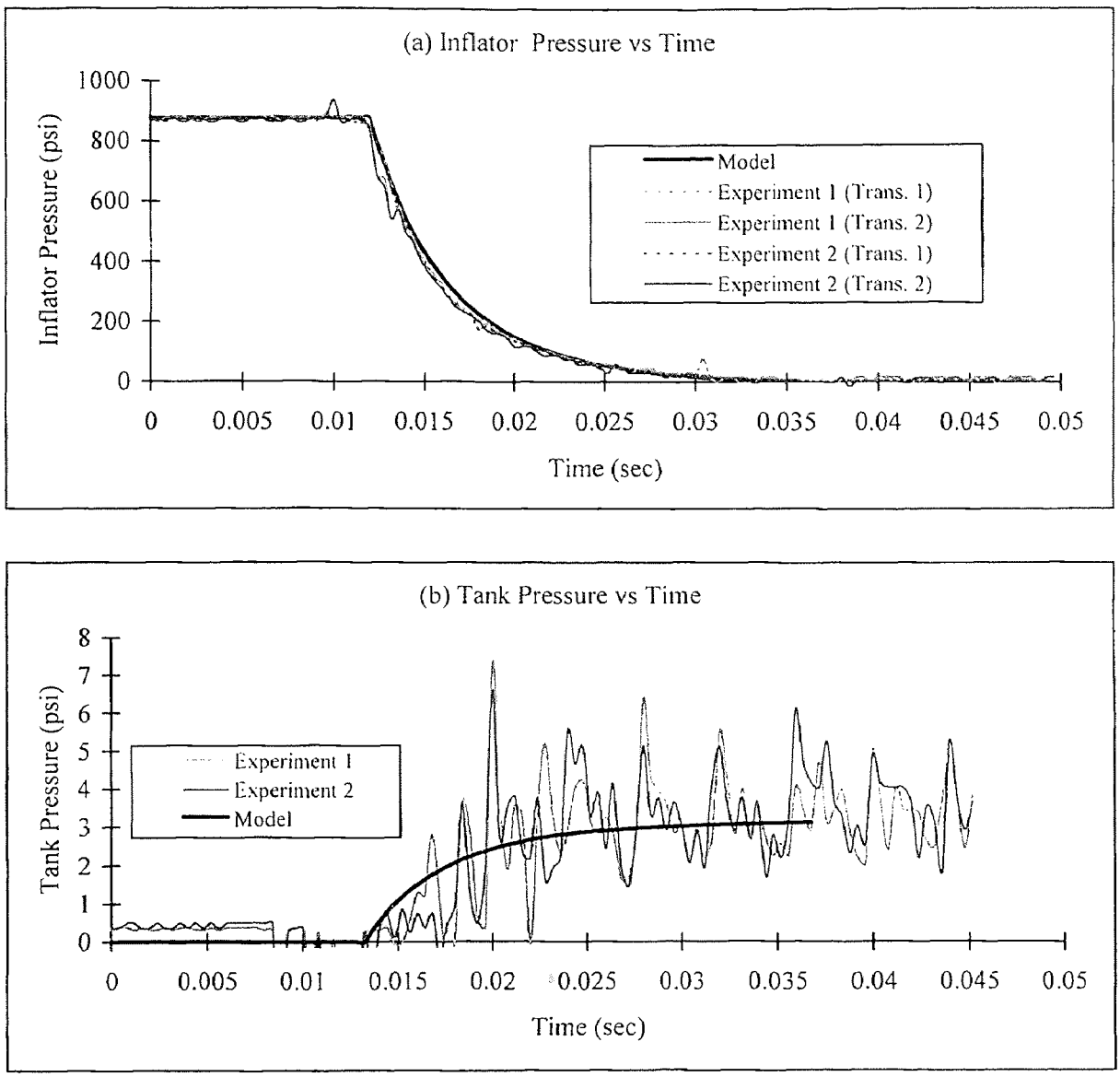

Figure 4.4 Comparison of inflator and tank pressure curves using nitrogen as an ideal gas

4.2.3 Description of Fast Combustion Model

A theoretical model, called fast combustion model was developed to simulate the experimental results for the fast combustion inflator. The model is based on the change in the internal energy of the inflator and the tank as the mass flows from the inflator to the tank. The model is based on the assumptions described in section 4.2.2. In addition, it is assumed that the specific heats vary as a function of temperature. The specific heats are specified as polynomials of the form :

$$C_p/R = a_1 + a_2T + a_3T^2 + a_4T^3 + a_5T^4 \qquad (6)$$

The values of a_1, a_2, a_3, a_4 and a_5 are taken from the Chemkin Thermodynamic Database [47]. The polynomial fit of equation (6) span for two temperature ranges : 300-1000 K and 1000 - 5000 K. In the inflator, specific heats are calculated for the 1000 - 5000 K temperature range and in the tank, specific heats are calculated for the 300 - 1000 K temperature range. Also, it is assumed that the mass fractions of different species are constant. The model uses the Chemical Equilibrium Compositions and Applications (CEA) code developed by NASA [15,16] to calculate the equilibrium conditions in the inflator.

4.2.3.1 Chemical Equilibrium Compositions and Applications (CEA) Program : The program CEA is used to obtain the chemical equilibrium compositions of gas mixtures for assigned thermodynamic states. These states may be specified by assigning two thermodynamic state functions as follows :

a. temperature and pressure, tp

b. enthalpy and pressure, hp

c. entropy and pressure, sp

d. temperature and volume (or density), tv

e. internal energy and volume (or density), uv

f. entropy and volume (or density), sv

Chemical equilibrium is usually described by either of two equivalent formulations – equilibrium constants or minimization of free energy. However, with the minimization of free energy method each species can be treated independently without specifying a set of reactions a priori, as is required with equilibrium constants. Therefore, the minimization of free energy formulation is used in the CEA program.

The conditions of equilibrium can be stated in terms of any of several thermodynamic functions, such as the minimization of Gibbs or Helmholtz energy or the maximization of entropy. Gibbs energy is most easily minimized if the thermodynamic state is characterized by temperature and pressure whereas, Helmholtz energy is most easily minimized if one wishes to use temperature and volume (or density) to characterize a thermodynamic state.

The following assumptions are made in the CEA program :

1. All gases are ideal
2. All condensed phases are pure
3. The interactions among phases can be neglected

The equation of state for the mixture is :

$$Pv = n\,R\,T$$

where;

P = pressure (Pa)

v = specific volume (m^3/kg)

n = moles per unit mass of mixture (kg-mole/kg)

R = universal gas constant (J/kg-mole.K)

T = temperature (K)

An internal energy and volume (or density), uv problem is solved to find the equilibrium conditions in the inflator. A typical input and output of this problem for a 150/300 (methane = 150 psi, oxygen = 300 psi) case is given in Figure 4.5.

The results of CEA program are in close agreement (±10%) with the CHEETAH code [51]. CHEETAH is a thermochemical code that solves thermodynamic equations between product species to find chemical equilibrium.

A FORTRAN program 'FASTCOMB' was written to simulate the experimental results for the fast combustion inflator. The program calculates the mass flow rate from the inflator to the tank. It also calculates the pressure and temperature variation with time inside the inflator and the tank. The flow chart for the program is given in Figure 4.6. The program and a typical output from the program are given in Appendix B.4.

In the fast combustion model, a uv problem is first solved by using the CEA program. The output from this program and the other parameters such as volume, mass

INPUT

```
reac  fuel  = CH4  mole = 0.104  t = 298
      oxid  = O2   mole = 0.219  t = 298
prob   uv   rho (g/cc) = 0.0347
output cal massf
end
```

OUTPUT

Pressure, atm	516.19
Temperature, K	4148.77
Density, g/cc	3.4709E-02
Mol. Wt.	22.891
Gamma	1.1409
Mass Fractions :	
CO	0.16848
CO2	0.26413
COOH	0.00015
H	0.00087
HCO	0.00006
HO2	0.00141
H2	0.00426
HCOOH	0.00003
H2O	0.34353
H2O2	0.00027
O	0.01741
OH	0.08171
O2	0.11769
O3	0.00001

Figure 4.5 Input and output for a uv problem

etc. are used as input for the FASTCOMB program. Based on the initial mass in the inflator and the tank, the initial internal energy is calculated. The inflator and tank pressures are then compared. If the inflator pressure is smaller than the tank pressure then the program stops. Otherwise, it calculates the specific heats, the mass flow rate and the fraction of mass going from the inflator to the tank. Based on this change in mass in the inflator and the tank, the new internal energies, temperatures, molecular weights and

pressures in the inflator and the tank are calculated. Then the time is updated and the whole procedure is repeated until the inflator pressure is less than or equal to the tank pressure.

4.3 Comparison of Experimental Results with the Fast Combustion Model

The experimental results are compared with the fast combustion model in the following examples :

Example 1 : An experiment with 30/60 mixture inside a 0.250 liter inflator. A 0.004" thick burst disk is used and the tank is not purged so it is in equilibrium with atmospheric air. The experimental pressure and temperature curves are compared with the model.

Example 2 : An experiment with 90/180 mixture inside a 0.250 liter inflator. A 0.004" thick burst disk is used and the receiving tank is not purged. The experimental pressure and temperature curves are compared with the model.

Example 3 : An experiment with 125/250 mixture inside a 0.250 liter inflator. A 0.004" thick burst disk is used and the receiving tank is not purged. The experimental pressure and temperature curves are compared with the model.

Example 4 : An experiment with 150/300 mixture inside a 0.250 liter inflator. A 0.015" thick burst disk is used and the tank is purged with nitrogen. The experimental pressure and temperature curves are compared with the model and the theoretical mass flow rate and the mass percentage out of the inflator as a function of time are presented. Also, the tank pressure and temperature curves obtained from the model are compared if the tank is not purged instead of purging it with nitrogen.

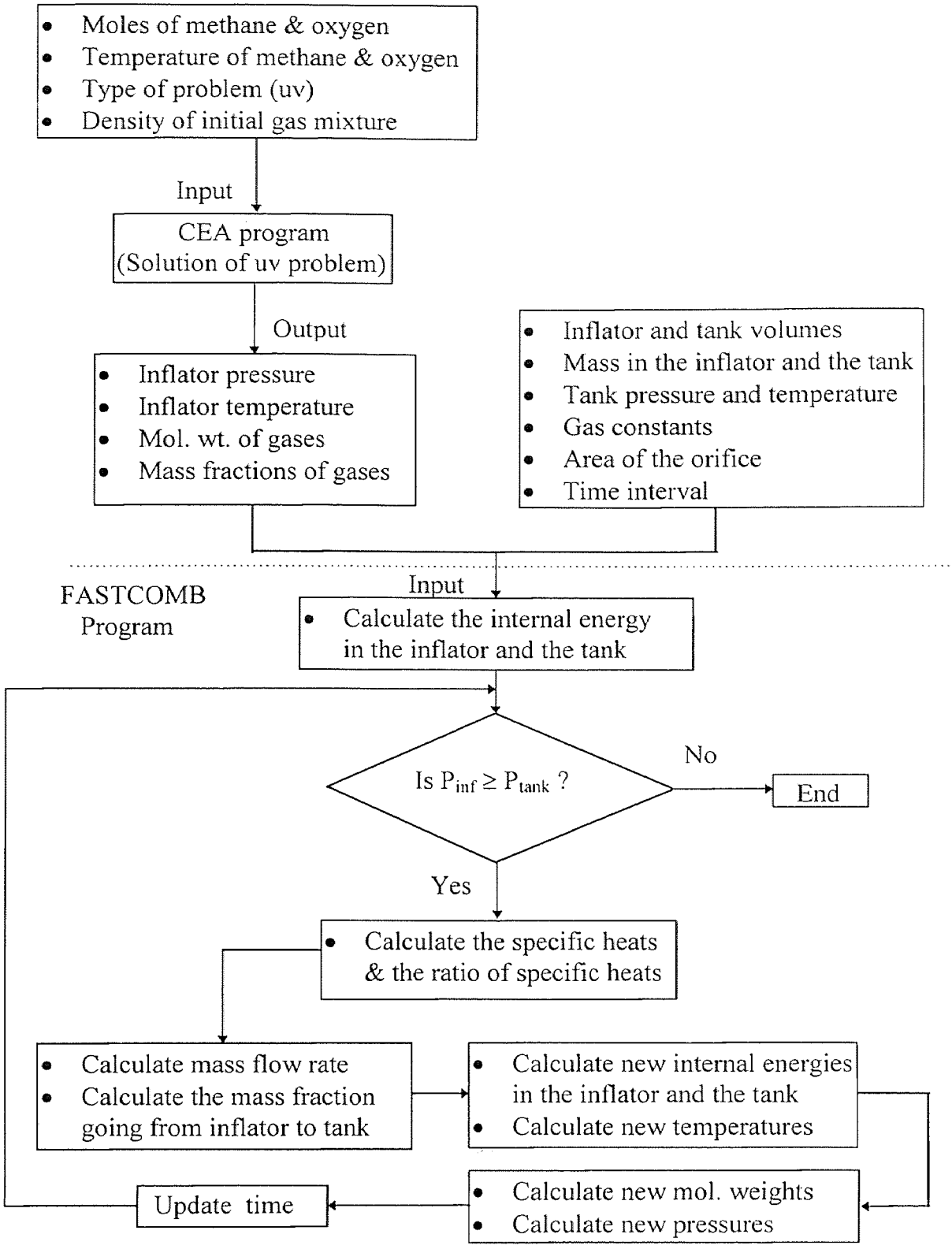

Figure 4.6 Flow chart of the Fast Combustion Model

Example 1 : Consider an experiment with stoichiometric mixture (methane = 30 psi and oxygen = 60 psi) inside a 0.250 liter inflator. The mixture is ignited with an electric match. The thickness of the burst disk used in the experiment is 0.004". The receiving tank in this experiment is not purged so it is in equilibrium with atmospheric air. The input parameters for the CEA program are shown in Table 4.7. The output from the CEA program is given in Appendix B.5.

Table 4.7 Input parameters for the CEA program (Example 1)

	Methane	Oxygen
Number of Moles	0.021	0.052
Temperature (K)	298.15	298.15
Density (g/cc)	0.008	

The equilibrium pressure and temperature of the inflator, the molecular weight and the mass fractions of product gases obtained as output from the CEA program are used as input to FASTCOMB program. The input data for FASTCOMB program is shown in Table 4.8.

Figure 4.7 compares the pressure and the temperature curves with the fast combustion model. Figure 4.7(a) shows that the pressure is maximum at about 10.8 msec and then it starts to drop until it is in equilibrium with the tank pressure at 15.8 msec.

Figure 4.7(b) shows that like the nitrogen experiments, the pressure trace in the tank is not smooth in the beginning. Again, this is due to the expansion of the product gases in the tank until the pressure is equal to the equilibrium pressure. In the tank, the pressure starts to increase at about 13.0 msec and it is maximum at about 17.8 msec.

Table 4.8 Input parameters for FASTCOMB program (Example 1)

Parameter	Value
Inflator Pressure (Pa)	10699701.52
Inflator Temperature (K)	3807.85
Inflator Volume (m^3)	0.000250
Mass inside the Inflator (kg)	0.001996
Mol. Wt. of Inflator Gases (kg/mole)	23.643
Tank Pressure (Pa)	101351.7
Tank Temperature (K)	298.15
Tank Volume (m^3)	0.07
Mass inside the Tank (kg)	0.082886
Mol. Wt. of Tank Gases (kg/mole)	28.96
Mass Fraction of CO_2	0.25207
Mass Fraction of H_2O	0.29529
Mass Fraction of H	0.00089
Mass Fraction of H_2	0.00313
Mass Fraction of O	0.02564
Mass Fraction of O_2	0.20502
Mass Fraction of CO	0.13216
Mass Fraction of OH	0.08469
Mass Fraction of HCO	0.00001
Mass Fraction of HO_2	0.00094
Mass Fraction of H_2O_2	0.00010
Mass Fraction of O_3	0.00001

Figure 4.7(c) compares the experimental temperature curve with the temperature curve obtained from the fast combustion model. The figure shows that the magnitude of the temperatures are in close agreement but the experimental curve is slower than the curve obtained from the model. This might be due to the slow response time of the thermocouple at this flow rate.

Example 2 : An experiment with 90/180 mixture (methane = 90 psi, oxygen = 180 psi) is considered. The mixture is ignited with an electric match. A 0.004" thick burst disk is used in the experiment. In this experiment the receiving tank is not purged. The input parameters for the CEA program are shown in Table 4.9. The output from the CEA

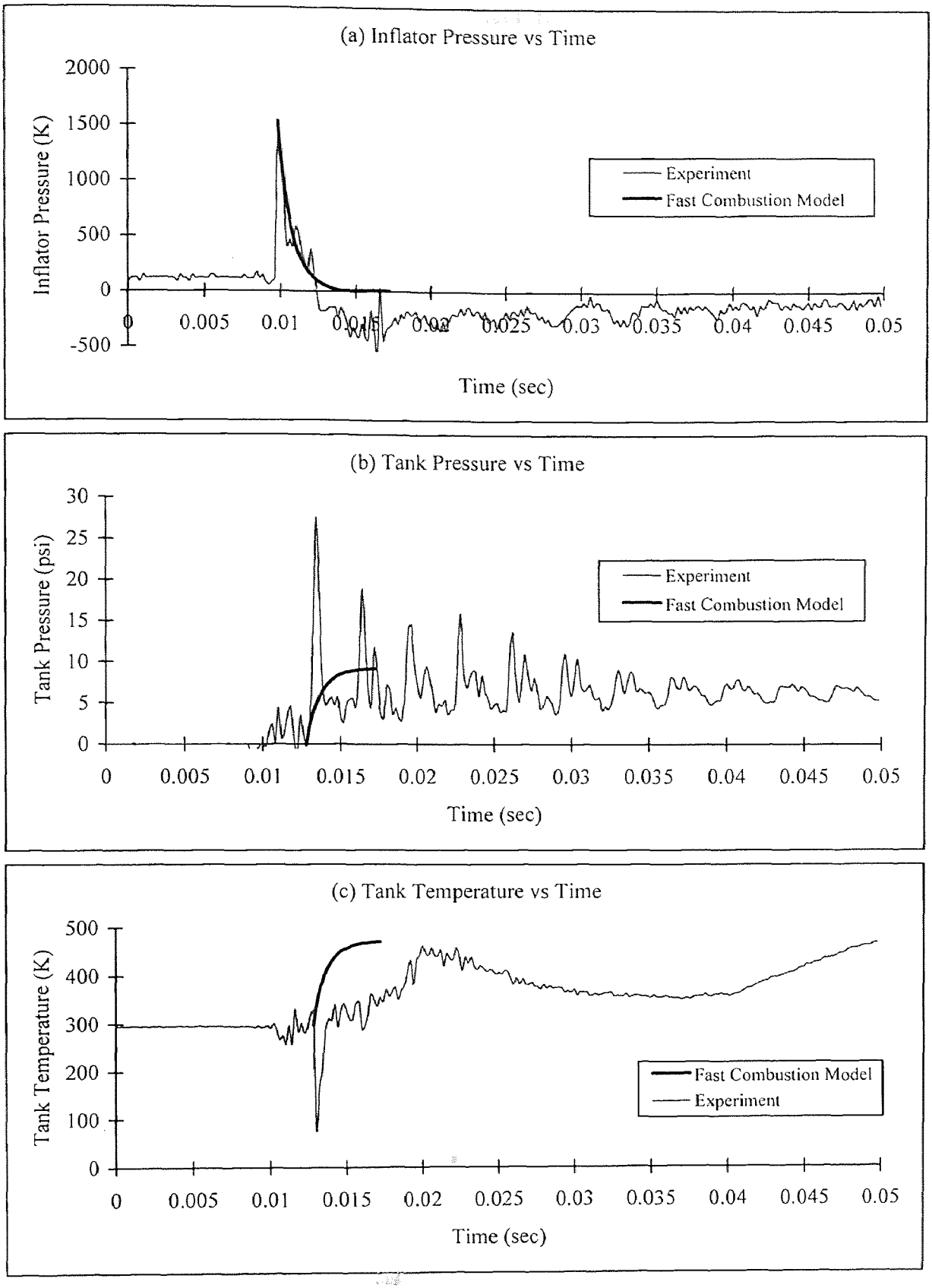

Figure 4.7 Comparison of pressure and temperature curves for a 30/60 mixture

program is given in Appendix B.6. The input data for FASTCOMB program is shown in Table 4.10.

Table 4.9 Input parameters for the CEA program (Example 2)

	Methane	Oxygen
Number of Moles	0.062	0.135
Temperature (K)	298.15	298.15
Density (g/cc)	0.021	

Table 4.10 Input parameters for FASTCOMB program (Example 2)

Parameter	Value
Inflator Pressure (Pa)	31311601.7
Inflator Temperature (K)	4046.39
Inflator Volume (m^3)	0.000250
Mass inside the Inflator (kg)	0.005335
Mol. Wt. of Inflator Gases (kg/mole)	22.945
Tank Pressure (Pa)	101351.7
Tank Temperature (K)	298.15
Tank Volume (m^3)	0.07
Mass inside the Tank (kg)	0.0802
Mol. Wt. of Tank Gases (kg/mole)	28.00
Mass Fraction of CO_2	0.26413
Mass Fraction of H_2O	0.34353
Mass Fraction of H	0.00087
Mass Fraction of H_2	0.00426
Mass Fraction of O	0.01741
Mass Fraction of O_2	0.11769
Mass Fraction of CO	0.16848
Mass Fraction of OH	0.08171
Mass Fraction of HCO	0.00006
Mass Fraction of HO_2	0.00141
Mass Fraction of H_2O_2	0.00027
Mass Fraction of O_3	0.00001

The pressure and the temperature curves are compared with the fast combustion model in Figure 4.8. The experimental results are in good agreement with the model. The

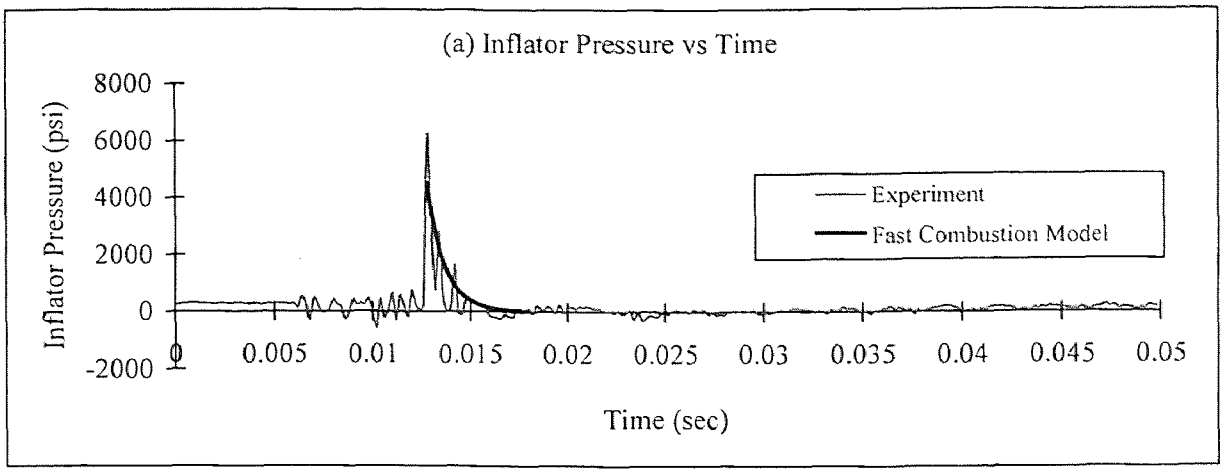

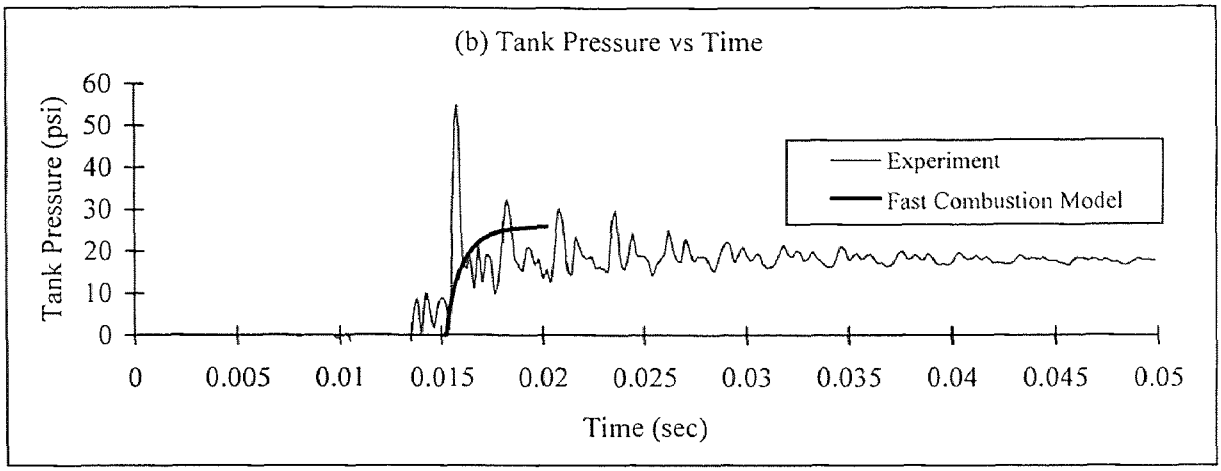

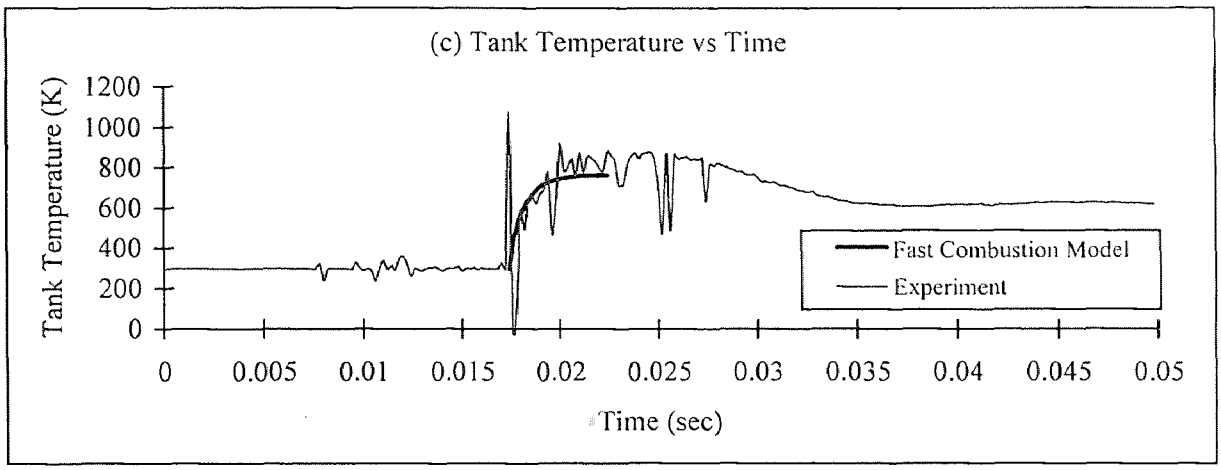

Figure 4.8 Comparison of pressure and temperature curves for a 90/180 mixture

inflator pressure is maximum at about 12.5 msec and then it starts to drop until it is in equilibrium with the tank pressure at 18 msec. Figure 4.8(b) shows that the tank pressure starts to increase at about 15.0 msec and it is maximum at about 20 msec. Figure 4.8(c) shows that the experimental temperature curve is in close agreement with the model.

Example 3 : Consider an experiment with 125/250 mixture (methane = 125 psi, oxygen = 250 psi) inside a 0.250 liter inflator. The mixture is ignited with an electric match. The thickness of the burst disk used in the experiment is 0.004". The receiving tank is not purged so it is in equilibrium with atmospheric air. The input parameters for the CEA program are shown in Table 4.11. The output from the CEA program is given in Appendix B.7. The input data for FASTCOMB program is shown in Table 4.12.

Table 4.11 Input parameters for the CEA program (Example 3)

	Methane	Oxygen
Number of Moles	0.087	0.184
Temperature (K)	298.15	298.15
Density (g/cc)	0.029	

The pressure and the temperature curves are compared with the fast combustion model in Figure 4.9. The figure shows that the experimental results for the inflator and the tank pressures are in close agreement with the model. Figure 4.9(b) shows that the maximum temperature obtained from the experiment is about 800 K whereas, from the model we are getting a value of about 913 K. This might be again due to slow response time of the thermocouple at the flow rate of this experiment.

Table 4.12 Input parameters for FASTCOMB program (Example 3)

Parameter	Value
Inflator Pressure (Pa)	43531579.0
Inflator Temperature (K)	4112.54
Inflator Volume (m^3)	0.000250
Mass inside the Inflator (kg)	0.007282
Mol. Wt. of Inflator Gases (kg/mole)	22.897
Tank Pressure (Pa)	101351.7
Tank Temperature (K)	298.15
Tank Volume (m^3)	0.07
Mass inside the Tank (kg)	0.082886
Mol. Wt. of Tank Gases (kg/mole)	28.96
Mass Fraction of CO_2	0.26201
Mass Fraction of H_2O	0.33984
Mass Fraction of H	0.00089
Mass Fraction of H_2	0.00423
Mass Fraction of O	0.01827
Mass Fraction of O_2	0.12303
Mass Fraction of CO	0.16734
Mass Fraction of OH	0.08259
Mass Fraction of HCO	0.00005
Mass Fraction of HO_2	0.00134
Mass Fraction of H_2O_2	0.00024
Mass Fraction of O_3	0.00001

Example 4 : An experiment with 150/300 mixture (methane = 150 psi, oxygen = 300 psi) is considered. The mixture is ignited with an electric match. In this experiment, a 0.015" thick burst disk is used and the receiving tank is purged with nitrogen. The input parameters for the CEA program are shown in Table 4.13. The output from the CEA program is given in Appendix B.8. The input data for FASTCOMB program is shown in Table 4.13.

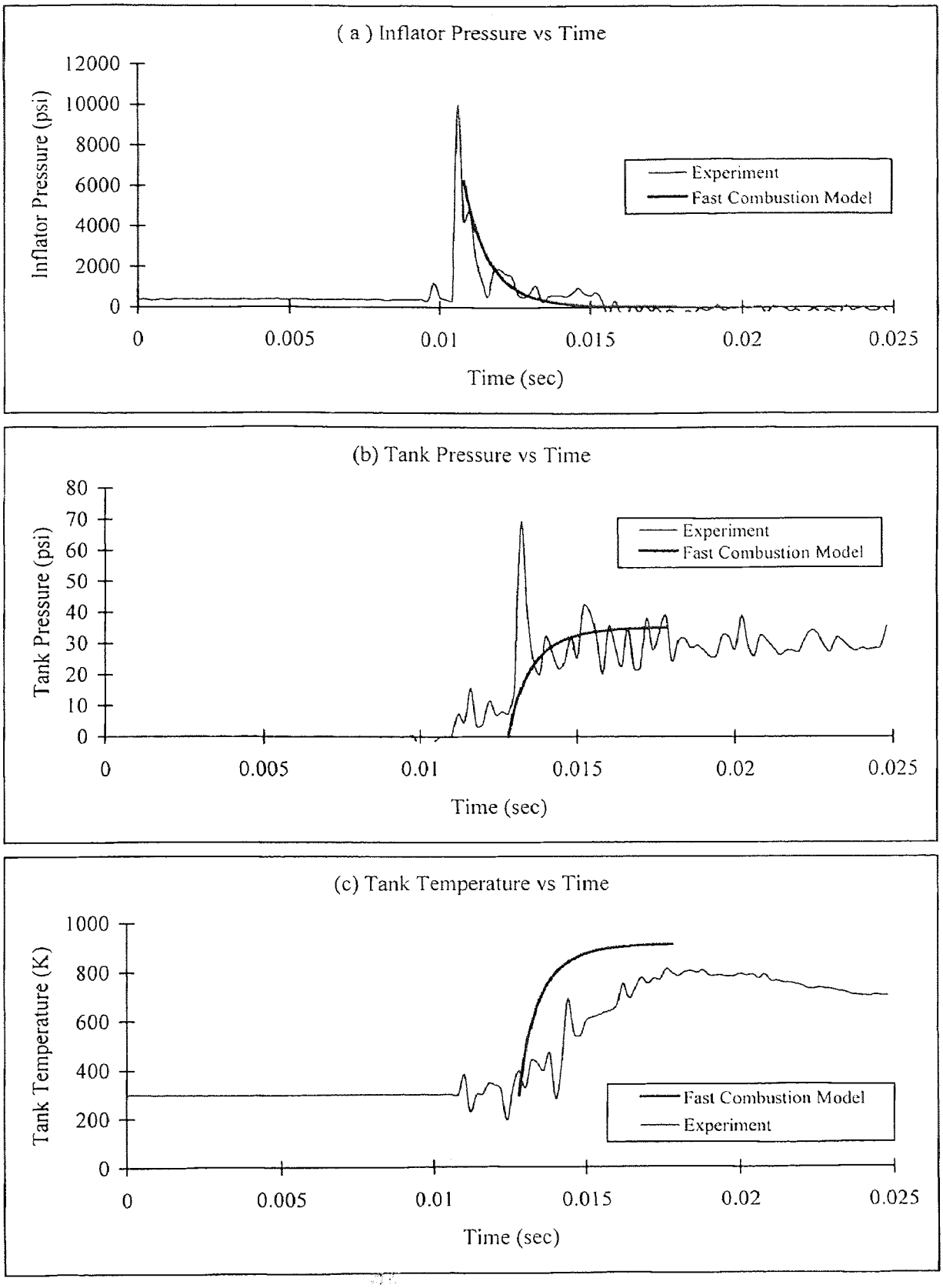

Figure 4.9 Comparison of pressure and temperature curves for a 125/250 mixture

Table 4.13 Input parameters for the CEA program (Example 4)

	Methane	Oxygen
Number of Moles	0.104	0.219
Temperature (K)	298.15	298.15
Density (g/cc)	0.035	

Table 4.14 Input parameters for FASTCOMB program

Parameter	Value
Inflator Pressure (Pa)	52316746.5
Inflator Temperature (K)	4148.77
Inflator Volume (m^3)	0.000250
Mass inside the Inflator (kg)	0.008673
Mol. Wt. of Inflator Gases (kg/mole)	22.891
Tank Pressure (Pa)	101351.7
Tank Temperature (K)	298.15
Tank Volume (m^3)	0.07
Mass inside the Tank (kg)	0.082886
Mol. Wt. of Tank Gases (kg/mole)	28.96
Mass Fraction of CO_2	0.25874
Mass Fraction of H_2O	0.33236
Mass Fraction of H	0.00093
Mass Fraction of H_2	0.00413
Mass Fraction of O	0.01991
Mass Fraction of O_2	0.13464
Mass Fraction of CO	0.16372
Mass Fraction of OH	0.08399
Mass Fraction of HCO	0.00004
Mass Fraction of HO_2	0.00122
Mass Fraction of H_2O_2	0.00020
Mass Fraction of O_3	0.00001

Figure 4.10 compares the pressure curves inside the inflator and the tank. The figure shows that the inflator and tank pressure curves obtained experimentally are in good agreement with the fast combustion model. Figure 4.10(c) shows that the magnitude of tank temperature is in agreement with the model but the experimental curve is slower than the one obtained from the model.

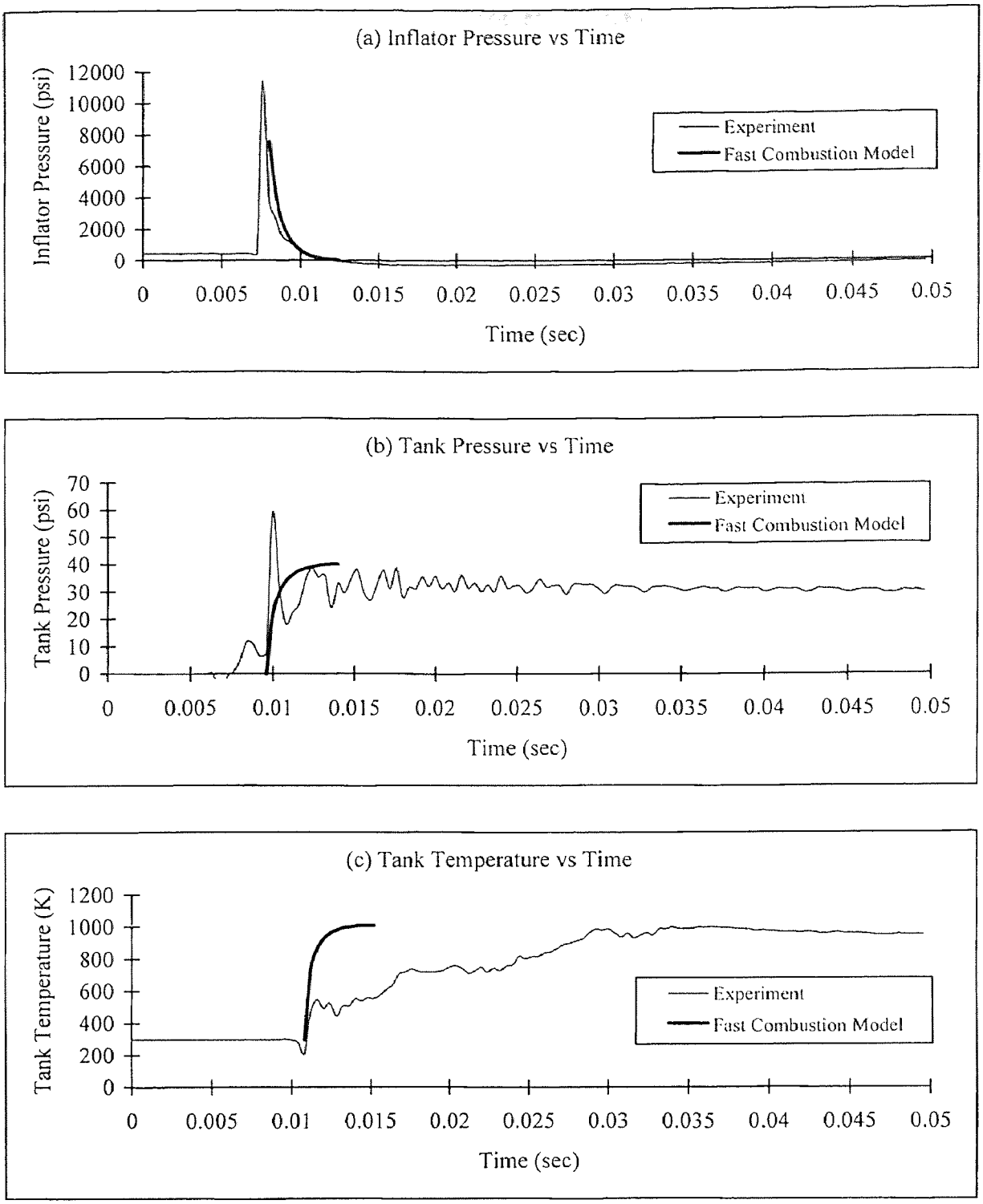

Figure 4.10 Comparison of pressure and temperature curves for a 150/300 mixture

Figure 4.11 shows the mass flow rate from the inflator to the tank and the percentage of mass inside the tank. The figure shows that the product gases start to come

out of the inflator at 8 msec and within another 4.4 msec, the entire mass is inside the tank. Also, about 80% mass of the mass is inside the tank within first 1.6 msec which is one of the design requirements of the inflators --- see section 3.2.

Figure 4.12 compares the tank pressure curves obtained from the model when the tank is not purged and when it is purged with nitrogen. The same trend for the tank pressure curve was obtained for the two purging gases experimentally --- see Chapter 3.

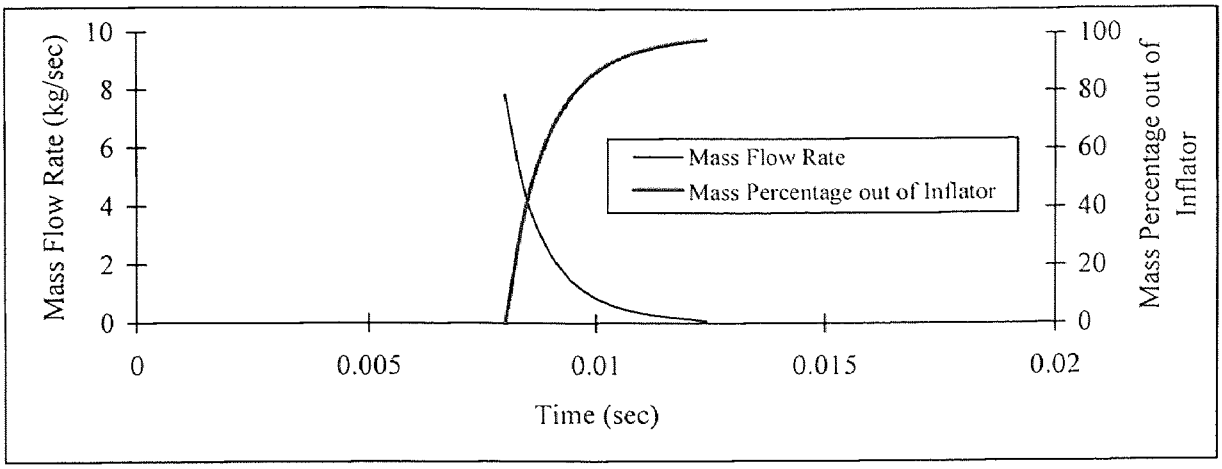

Figure 4.11 Mass flow rate and the mass percentage out of the inflator as a function of time

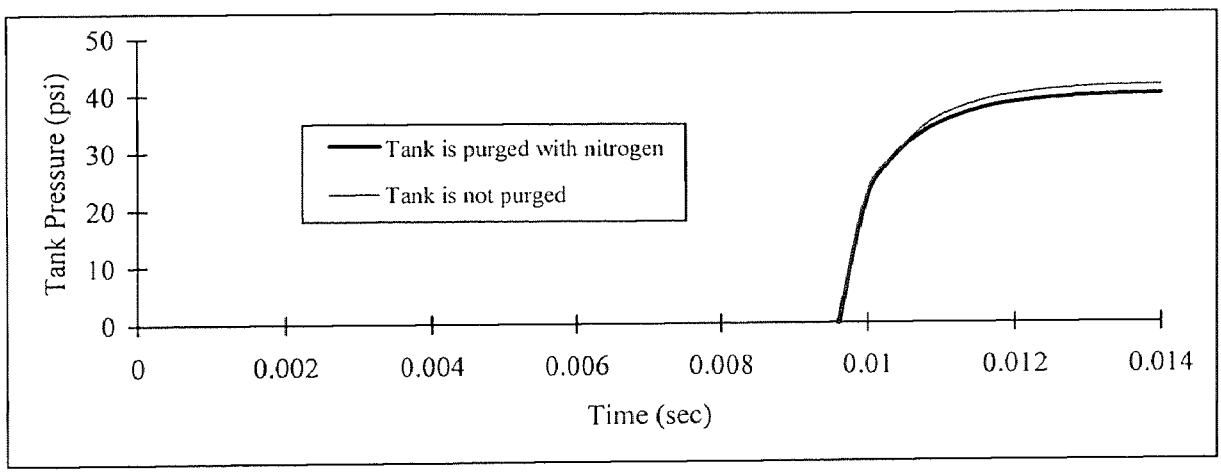

Figure 4.12 Comparison of tank pressure curves when the tank is not purged and when it is purged with nitrogen

4.4 Comparison of Maximum Tank Pressure and Temperature

The fast combustion model can be used to predict the maximum temperature and pressure in the tank for any initial pressure and for any size of inflator or tank. Figure 4.13 compares the predicted tank pressures and temperatures with the experimental values for different initial mixture pressures. The figure shows that the pressure and temperature in the tank increase linearly with the increase in the initial mixture pressure.

The fast combustion model is unique and different from other models since it shows the dynamics of the inflator based on the fast combustion of methane-oxygen mixtures. The model not only gives the maximum pressure and temperature but also predicts the dynamic conditions. These dynamic conditions are important in inflating an air bag. Figure 4.14 compares the tank pressure and temperature curves for different initial pressures obtained from the model. The figure shows that both the tank pressure and the tank temperature increase with the increase in the initial mixture pressure.

4.6 Conclusions

1. An integrated model, "Fast Combustion Model", based on equilibrium thermodynamics and mass flow rate has been developed and compared with the experimental results.
2. The experimental results for the transient pressure measurement in the inflator and the tank are in good agreement with the fast combustion model.
3. The experimental results for transient temperature measurement in the tank are in good agreement with the model in terms of the magnitudes of temperature but the experimental curves are slower in time than the ones obtained from the model. The

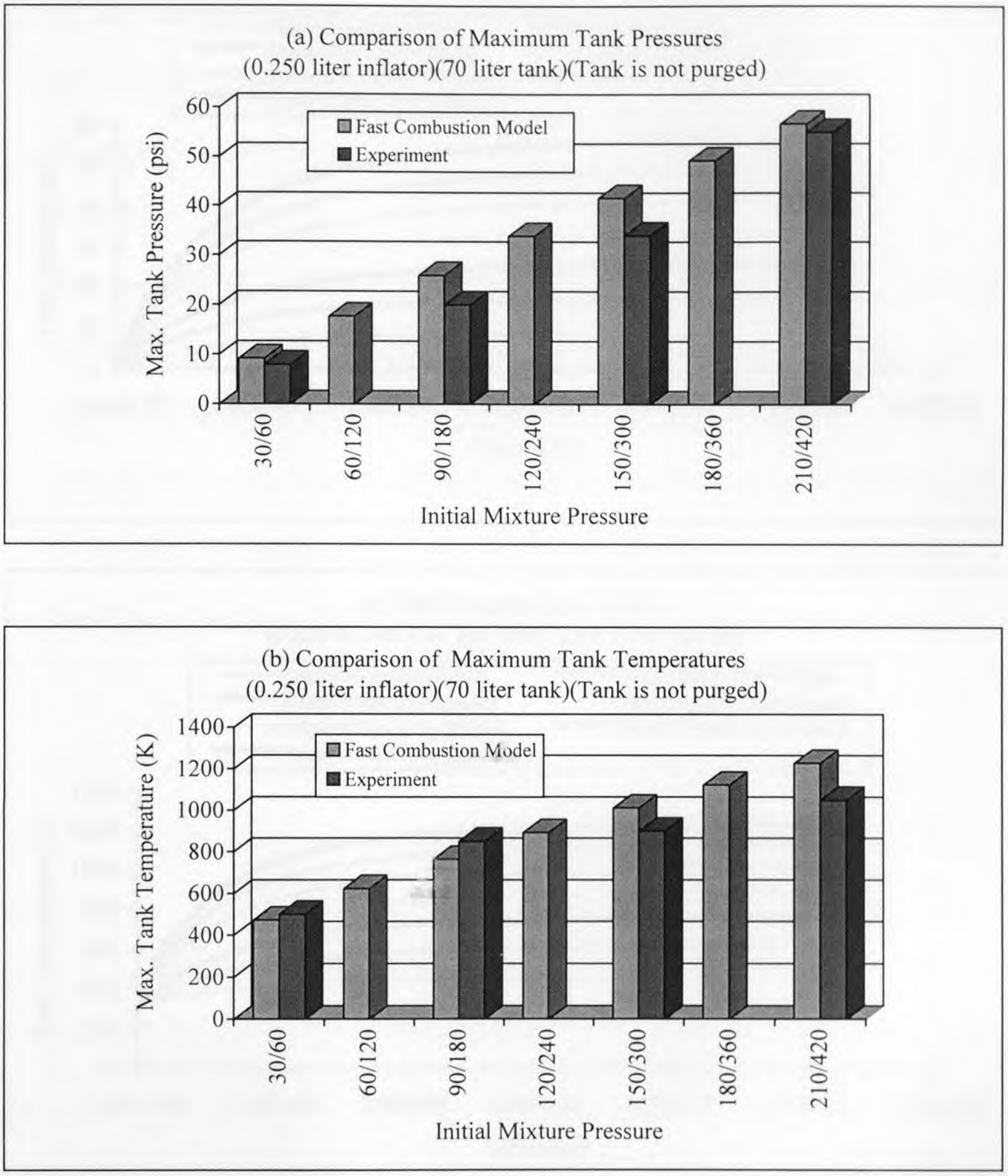

Figure 4.13 Comparison of maximum tank pressure and temperature for different initial mixture pressures.

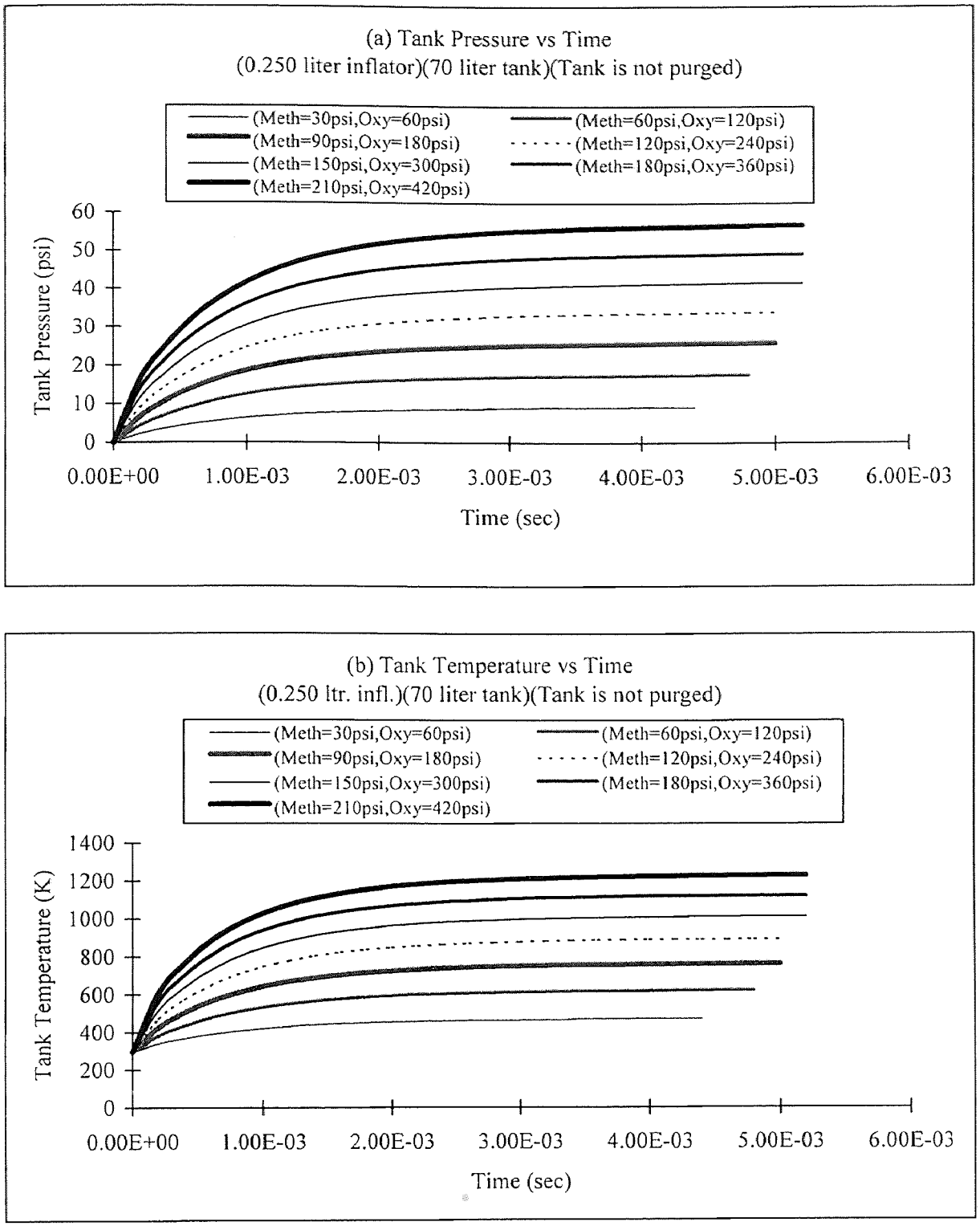

Figure 4.14 Comparison of tank pressure and temperature for different initial mixture pressures

reason for this might be the slow response time of the thermocouple at the flow rates of these experiments.

4. The fast combustion model is predictive for tank's pressure, temperature and mass flow rate and is sensitive to the nature of purging gas in the tank.
5. The model is applicable for different initial mixture pressures and is expected to apply for different inflator sizes.
6. Once the tank's temperature and pressure are predicted from the fast combustion model, we can find the composition of gas products in the tank, without experimentation using the Chemical Equilibrium and Applications (CEA) code.
7. Like all other models, the fast combustion model has some limitations. The model did not consider heat transfer and if we want to see the pressure and time behavior for longer period of time, we have to include the heat transfer effects in the model.

CHAPTER 5

COMPARISON OF THE FAST COMBUSTION INFLATOR WITH CURRENT TECHNOLOGY

5.1 Introduction

In this chapter, we have evaluated our fast combustion inflator with the sodium azide (NaN_3) inflator currently used in industry. Presently, the performance of the azide inflator sets the industry standards for a successful inflator. We will use these standards and criteria to assess the performance of our fast combustion inflator in terms of pressure-time, temperature-time, pressure impulse and the number of moles required for a successful air bag inflation system.

Currently, the sodium azide (NaN_3) based inflator is most commonly used in the U. S. air bag industry. Sodium azide-based system has been used in air bag applications because of its low combustion temperatures (about 1200 K) [10] and because its combustion products consist mostly of nitrogen gas (99.2%). However, along with nitrogen, this system produces considerable amounts of condensed-phase residues such as Na_2O, Na_2SiO_3 and FeO. The latter must be removed from the combustion products prior to entering the air bag. Furthermore, the design of the azide system is complex and expensive because it includes many dynamically-linked components, including : a squib igniter, an ignition enhancing sytem, the propellant grains assembly, filter system, controlled bursting foil and the exhaust nozzles. A major strict requirement of the azide inflator necessitates that all the elements in the inflator function optimally to minimize the delay time [24]. The delay time is the time between the supply of current and the instant of ignition.

In contrast, the fast combustion inflator does not produce particulate or objectionable gaseous emissions. There are no toxic compounds to complicate either the manufacturing or eventual disposal or recycling of the fast combustion inflator. This inflator has the advantage of simplicity of its basic process.

As discussed in Chapters 3 and 4, the fast combustion inflator developed during this research satisfies most of the design and performance requirements of a successful inflator, including the tank pressure and temperature as a function of time, extreme hot and cold operating conditions, concentration of toxic gases in the products of combustion. However, for this inflator to be used in industry, it must satisfy all of the strict requirements mandated by industry standards. In this chapter, the fast combustion system is compared with the sodium azide system, especially on the basis of the published works of Butler et al. [22] and Wang [21]. In addition, we will attempt to show what is needed for the fast combustion inflator to be implemented in an actual air bag system.

5.2 Review of the Sodium Azide Inflator Performance

Butler et al. [22] developed a mathematical model to simulate the transient, thermochemical events associated with ignition and combustion of a sodium azide inflator. The performance of this inflator was also evaluated in terms of pressure-time and temperature-time profiles in the inflator and the receiving tank as well as pressure-time integrals at specified times after ignition. The process of inflating a vehicle air bag from the generated combustion gases was modeled by applying basic energy and mass conservation principles to various sub-components of the inflator and the receiving tank.

Equally important, Wang [21] developed a semi-analytical procedure, called the dual pressure method, for computing the output from a pyrotechnic inflator (sodium

azide-based). In the dual pressure method, the pressures in the inflator and the tank are measured first. By using these pressures, the inflator output is computed in the form of the time histories of the gas temperature and mass flow rate.

Analogous to Butler's work, Chan [24] presented a mathematical model in which the propellant combustion , filter pressure drop, heat transfer due to filter, nozzle and tank behavior were all considered. Inflator pressure and temperature are predicted from energy balance and an ideal gas equation.

Materna [23] presented an analytical model which predicts the performance of a pyrotechnic (sodium azide-based) air bag inflator by accounting for the heat transfer, filtration, combustion, fluid flow and thermodynamic processes occurring during the inflation event. He considered all the essential aspects of the inflator.

In all inflator models, including ours, the pressure and temperature were predicted from the energy balance using the assumption of ideal gas equation.

5.3 Comparison of Fast Combustion System with the Sodium Azide System

In this section, a comparison of fast combustion system with the sodium azide system will be presented in terms of pressure and temperature as a function of time, pressure impulses and the mass flow rate and the number of moles.

5.3.1 Tank Pressure-Time Behavior

Figure 5.1 compares the tank pressure curve for standard sodium azide system with the experimental tank pressure curve for fast combustion inflator having an initial mixture pressure of 210/420 (methane = 210 psi, oxygen = 420 psi) in a 0.250 liter inflator. The figure shows that in the case of fast combustion system, the maximum pressure in the

tank is attained in less than 10 msec after ignition; whereas, in the case of sodium azide system, the tank pressure is maximum in about 75 msec. The reason for this is that in the sodium azide system, the solid propellant keeps on generating gases at a slower rate inside the inflator. In contrast, in the fast combustion system, the whole mass is transferred into the tank within 5 - 10 msec after the burst disk ruptures. Based on the above discussion, we can say that fast combustion inflator satisfies the pressure-time requirement for inflating an air bag.

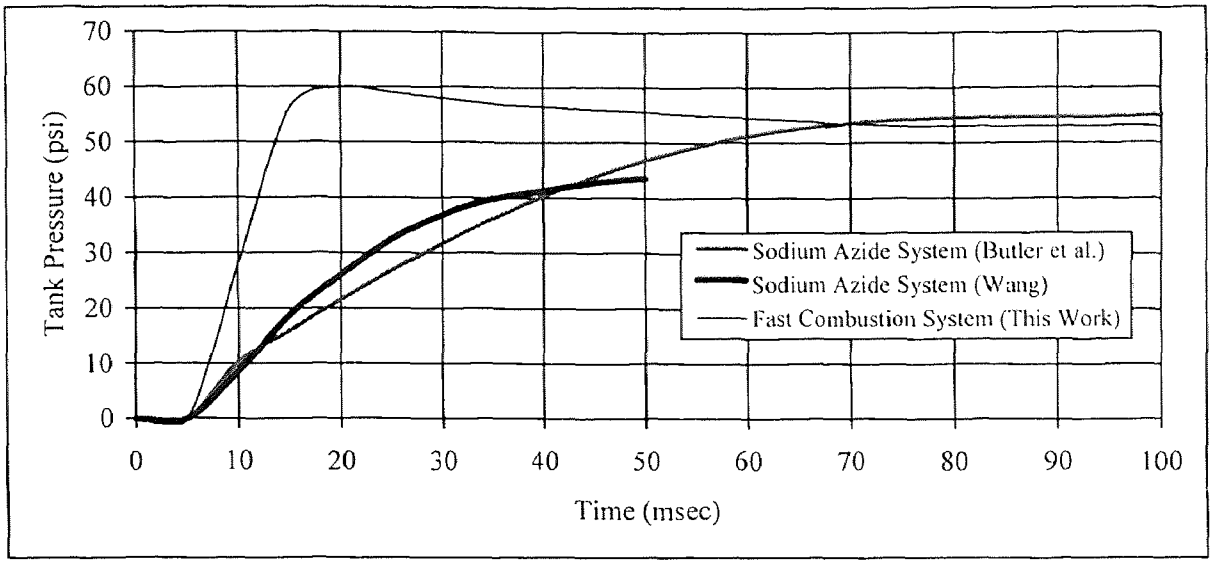

Figure 5.1 Comparison of tank pressure curves for the sodium azide and fast combustion inflators

5.3.2 Tank Temperature-Time Behavior

Figure 5.2 compares the tank temperature curves for the two systems. The figure shows that the maximum temperature for the fast combustion system is about 1000 K whereas for the sodium azide system, the maximum temperature is about 700 K. It should be noted that the temperature value given above for sodium azide is the value predicted from the model developed by Butler et al. [22], and not the actually measured value. The 1000

K tank temperature measured in the case of fast combustion inflator is not uncommon in combustion based air bag systems [35]. As shown in Figure 5.2, the temperature of the fast combustion inflator decreases rapidly as a function of time and the difference between the two inflators becomes less at about 100 msec.

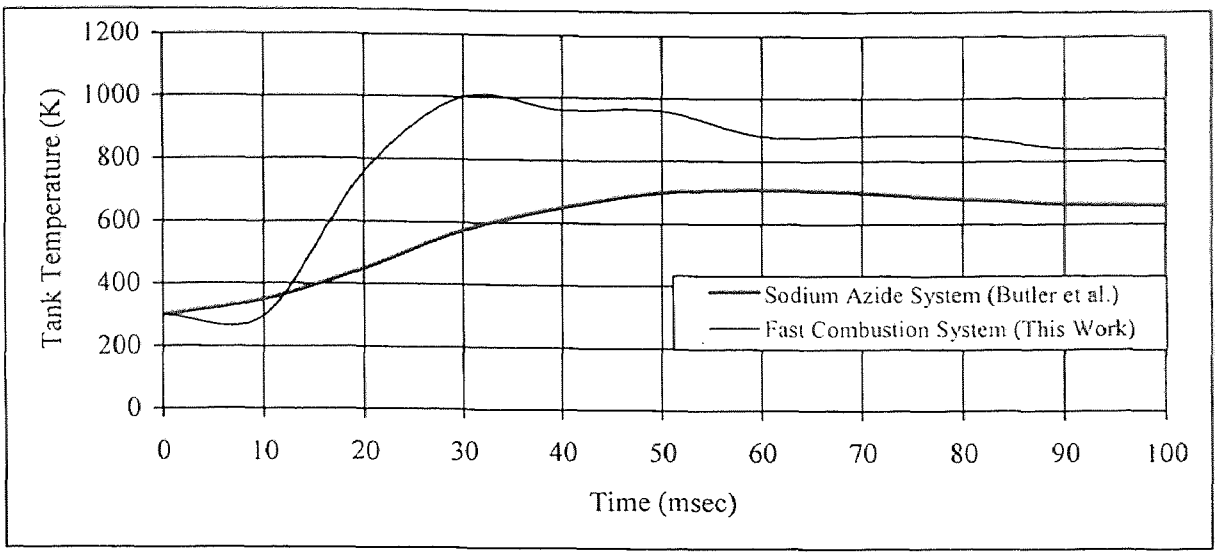

Figure 5.2 Comparison of tank temperatures for the sodium azide and fast combustion inflators

5.3.3 Inflator Pressure-Time Behavior

Figure 5.3 compares the inflator and tank pressure curves of the two systems. The figure shows that in the case of fast combustion system, inflator pressure rises and drops very quickly and reaches equilibrium with the tank pressure in about 5 msec after ignition, whereas, in the case of sodium azide system, the pressure keeps on increasing for up to about 30 msec after ignition. The reason for the latter is due to the continuous generation of gas from the solid propellant over time. Figure 5.3 also shows that in the case of sodium azide system, the maximum pressure in the inflator is about 2400 psi whereas, in

the case of fast combustion system, the inflator pressure ranges from 1,500 psi for a 30/60 mixture to about 12,000 psi for a 150/300 mixture in a 0.250 liter inflator.

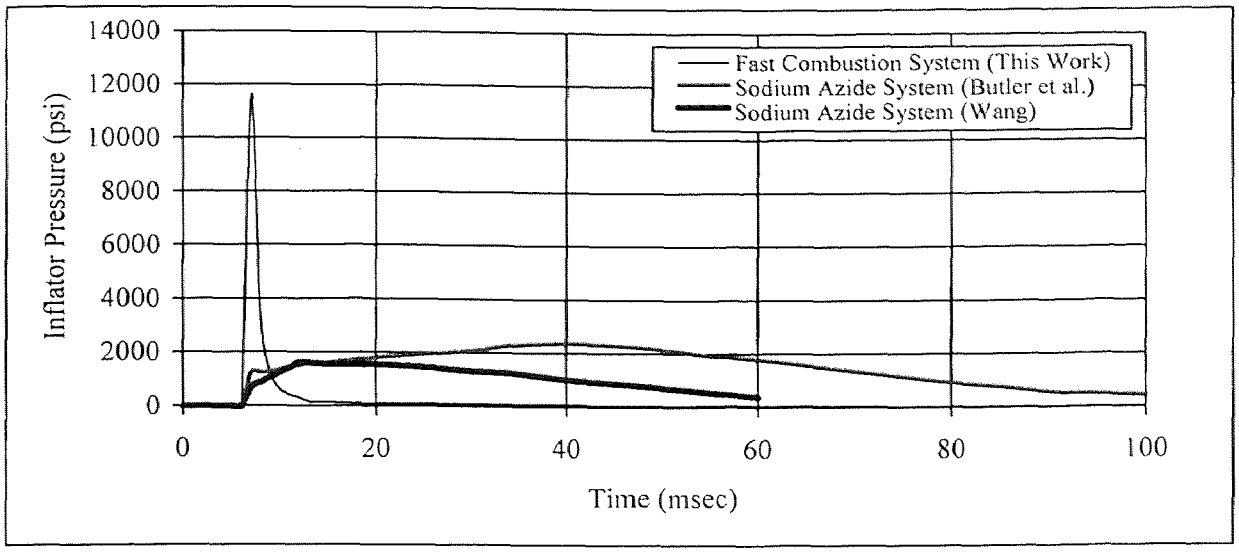

Figure 5.3 Comparison of inflator pressures for the sodium azide and fast combustion inflators

5.3.4 Pressure Impulse-Time Behavior

According to Butler et al. [22], pressure impulse or pressure integration over time in the receiving tank is an important parameter in evaluating the performance of an inflator. The tank pressure impulse represents the momentum transferred from the bag to the occupant which is ultimately transferred to the vehicle occupant. If two inflators have the same tank impulse, it is expected that they have similar inflating abilities. Figure 5.4 compares the tank pressure impulse of the two systems and shows that the tank pressure impulse curves for fast combustion system is initially higher than the sodium azide system. In actual implementation, the pressure impulse can be modulated by using pulse-shaping, if required. Pulse shaping is accomplished by varying an orifice area in a time-dependent manner. Pulse shaping is necessary to lessen the stresses on the housing, air bag and

related structures and is a common design consideration in the air bag industry. In all, the fast combustion inflator meet the pressure impulse required for a practical fast responding air bag system.

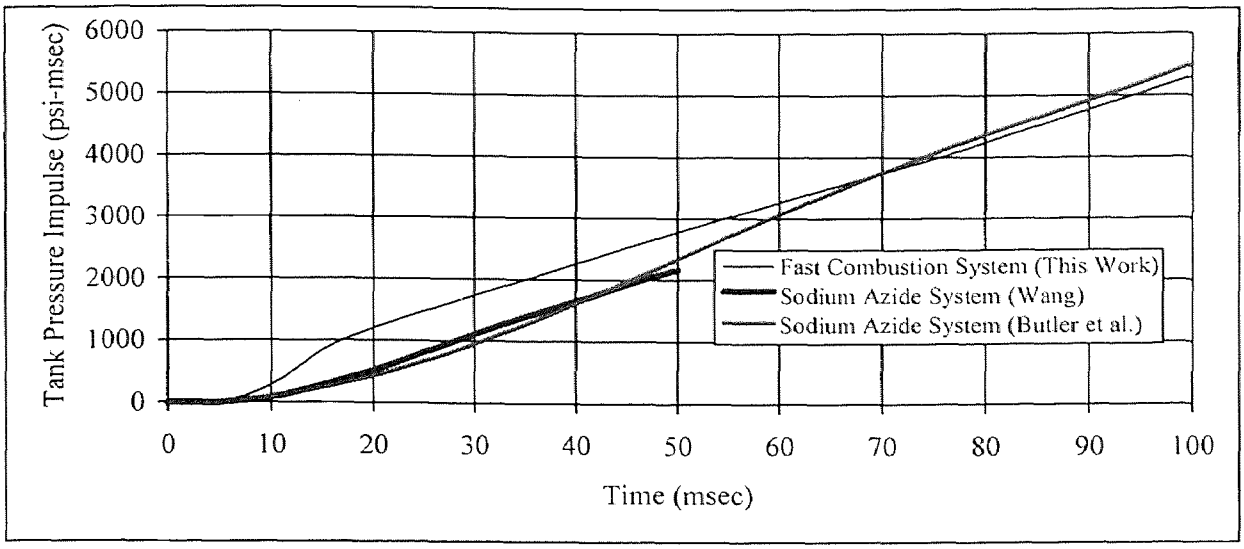

Figure 5.4 Comparison of pressure impulse vs time for the sodium azide and fast combusiton inflators

5.3.5 Mass Flow Behavior

Figure 5.5 compares the theoretical mass flow rates of the two inflator systems --- the standard sodium azide inflator and the fast combustion with an initial mixture pressure of 210/420 (methane = 210 psi, oxygen = 420 psi) in a 0.250 liter inflator. It can be seen that the mass flow rates of the two systems are quite different in behavior. In the case of fast combustion system, the total mass leaves the inflator in less than 5 msec after ignition. In contrast, for sodium azide system, the solid propellant keeps on generating gas for up to 75 msec. If we calculate the area under the curves for two cases, we see that the total mass in the case of sodium azide system is roughly 76 gm (3 moles) whereas, in the case of the fast combustion system, it is about 12 gm (0.52 moles). Although, the two inflators

have different volumes, the comparison is only in respect to mass flow trend from the inflator to the tank.

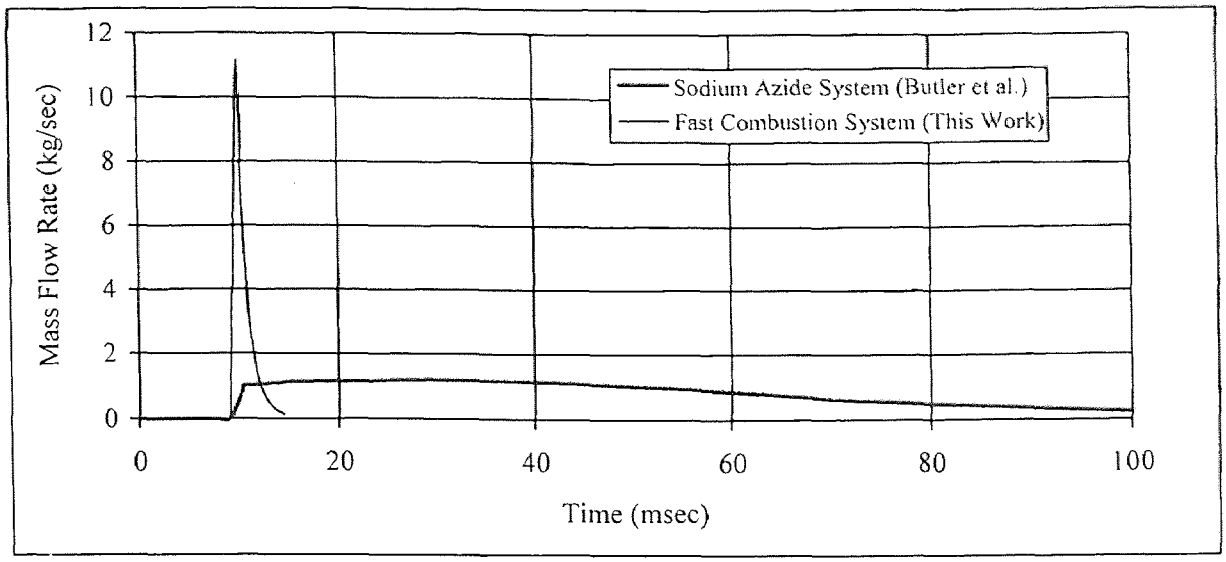

Figure 5.5 Comparison of mass flow rates for the sodium azide and fast combustion inflators

5.4 Discussion

In general, most of the requirements for a successful inflator such as pressure-time, and temperature-time behavior are satisfied by the fast combustion inflator. As described in section 5.3.4, to satisfy the pressure impulse requirement, a pulse shaping mechanism can be used to tailor the inflator requirement for various air bag types. Also, for the fast combustion inflator to satisfy the total mass (number of moles) requirement for an air bag system, we must adopt suitable strategies.

In the fast combustion system, the total mass of gases for an initial mixture pressure of 630 psi (methane = 210 psi, oxygen = 420 psi) in a 0.250 liter inflator is 12.01 gm (methane = 2.34 gm, oxygen = 9.67 gm) or 0.45 moles. This inflator size corresponds to a typical driver side air bag inflator. The number of moles of product gases formed

during the reaction is about 0.52. This is about half the number of moles required to inflate the driver side air bag and provide the required cushioning effects needed for full protection. The remaining challenge in our case is to satisfy the requirement of the total number of moles.

The number of moles in the fast combustion inflator can be increased by two means :

1. ***By increasing the initial mixture pressure :*** In order to satisfy the requirement of the number of moles, one possible solution is to increase the initial mixture pressure. Figure 5.6 shows the effect of increasing the initial mixture pressure from 210/420 (methane = 210 psi, oxygen = 420 psi) to 350/700 (methane = 350 psi, oxygen = 700 psi). The figure shows that if we increase the initial mixture pressure to 350/700, the number of moles of product gases will be approximately 0.86 but the maximum tank pressure and temperature will be 90 psi and 1650 K respectively. The high temperature in the tank might limit the use of higher initial pressure. In order to remedy this, the ideal option will be to use a hybrid system.
2. ***By using a hybrid system :*** In a hybrid system, the products of combustion are mixed with another inert gas at ambient temperature before being discharged into a tank or an air bag. Since the combustion temperature in the fast combustion inflator is higher (about 4000 K), mixing of the combustion products with the inert gas will lower the average gas temperature in the tank. To use our system as a hybrid system, our combustion chamber will be coupled with the stored gas chamber to cool the gases (Figure 5.7). With a slight modification in the fast combustion model, it can be used to predict the behavior of a hybrid system.

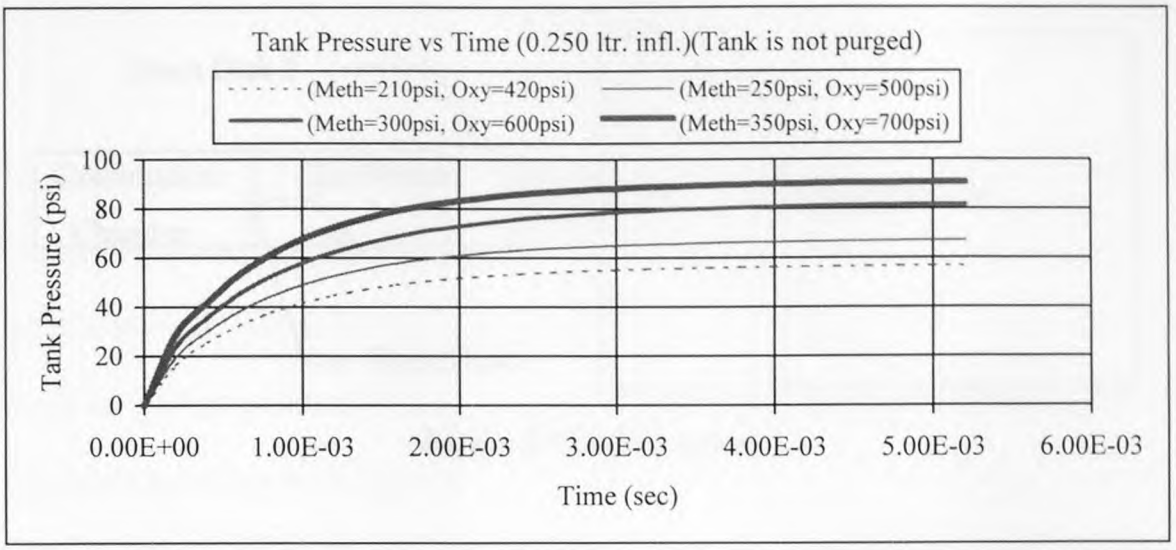

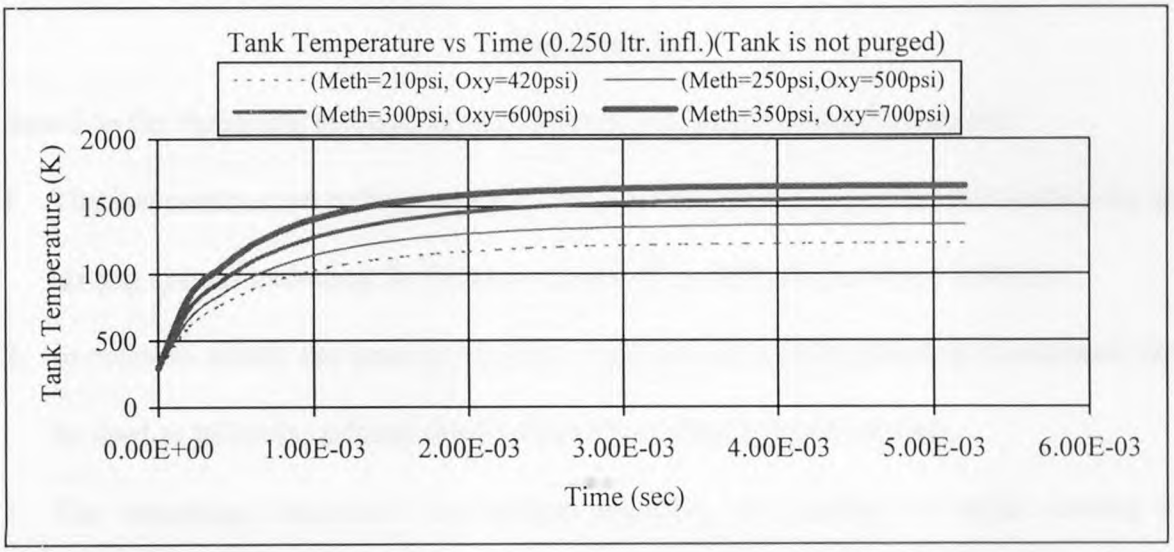

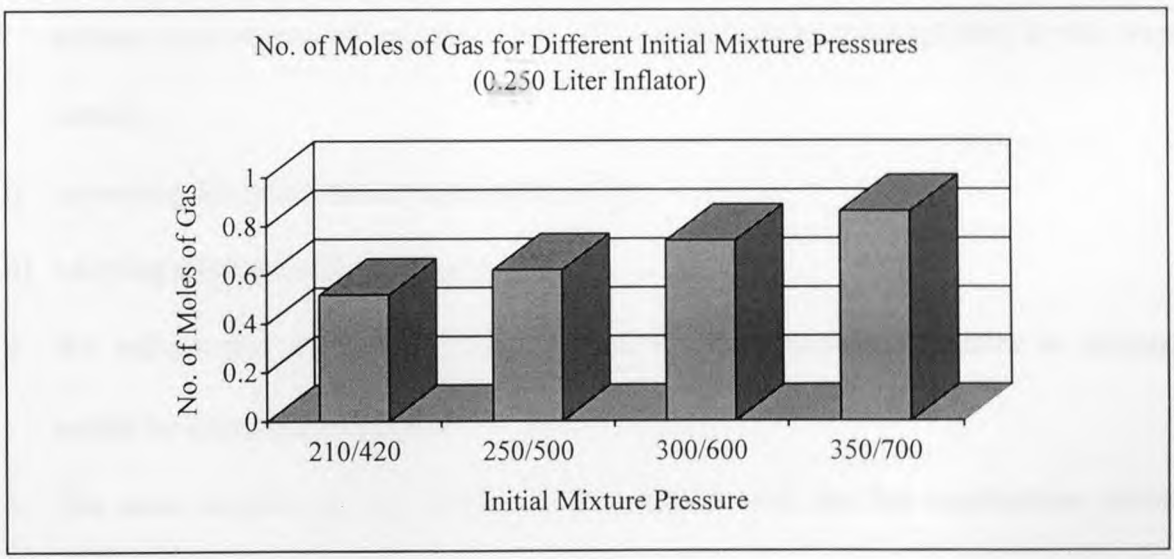

Figure 5.6 Effect of increasing the initial mixture pressure of methane-oxygen mixture

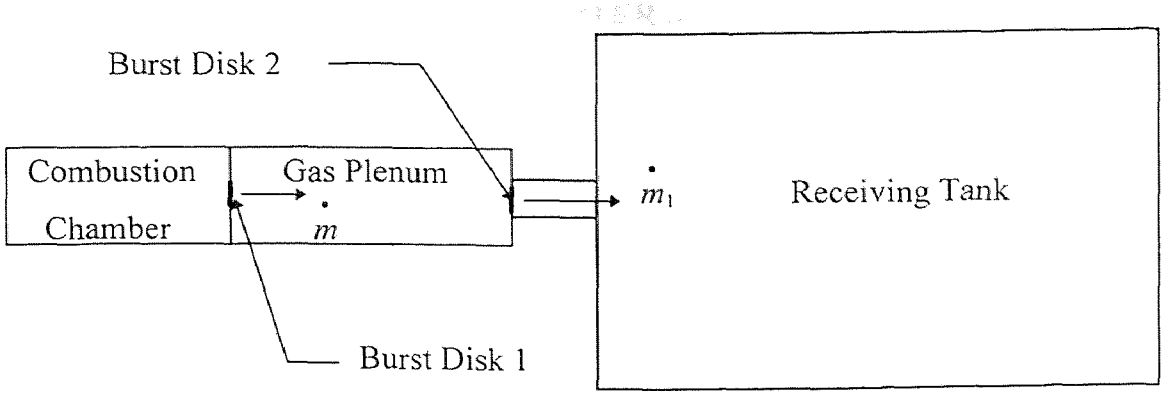

Figure 5.7 Hybrid system

Conclusions

Based on the foregoing discussion, the following conclusions are formulated :

1. The fast combustion inflator satisfies most of the dynamic requirements needed for an air bag system including the pressure-time and the temperature-time behavior.
2. In order to satisfy the pressure impulse requirement, a pulse shaping mechanism can be used to tailor the inflator requirement for various types of air bags.
3. The remaining important requirement regarding the number of moles needed to achieve equivalent performance to the azide system can be accomplished in two ways namely :

i) increasing the initial mixture pressure and/or

ii) adopting a hybrid inflator design.

4. We believe that the hybrid inflator, which is now a common practice in industry would be a preferred solution.
5. The most suitable air bag inflator to be satisfied with the fast combustion system without any modifications is the side impact type.

CHAPTER 6

GENERAL CONCLUSIONS

A new and novel air bag inflator based on fast combustion reactions of methane-oxygen mixtures has been developed and studied. The performance of the fast combustion inflator was evaluated in terms of pressure-time relationships inside the inflator and in a receiving tank as well as the temperature-time relationship in a tank. A theoretical and integrated model has been developed to simulate the transient pressure and temperature as well as the mass flow rate from the inflator to the tank. Conclusions drawn from this work are :

1. The dynamic condition with respect to pressure variation with time i.e. with respect to inflating a bag in the required time is satisfied.
2. The fast combustion system is a well behaved system, easy to activate and is applicable for different size inflators.
3. Most of the design requirements are satisfied such as hot and cold operating conditions, concentration of carbon monoxide produced and the effect of burst disk.
4. An integrated model, "Fast Combustion Model", based on equilibrium thermodynamics and mass flow rate has been developed to predict the dynamics and behavior of the new inflator.
5. The experimental results for transient pressure measurement in the inflator and the tank are in good agreement with the fast combustion model.
6. The experimental results for transient temperature measurement in the tank are in good agreement with the model in terms of the magnitudes of temperature but the experimental curves are slower in time than the ones obtained from the model.

7. The fast combustion model is predictive for tank's pressure, temperature, and mass flow rate.
8. The model is applicable for different initial mixture pressures, inflator sizes and tank purging gases.
9. The model can be used to predict results under hot and cold conditions.
10. With a slight modification in the model, it can be used to predict the behavior of a hybrid inflator.
11. In general, most of the requirements for a successful inflator are satisfied by the fast combustion inflator but we need to consider how to satisfy the pressure impulse and the total mass or the number of moles requirements in the case of fast combustion inflator.
12. The pressure impulse requirement can be satisfied by a pulse shaping mechanism to tailor the inflator requirement for various types of air bags.
13. The requirement for the number of moles needed to achieve equivalent performance to the azide system can be accomplished in two ways :

i) increasing the initial mixture pressure and/or

ii) adopting a hybrid inflator design.

We believe that the hybrid inflator, which is now a common practice in industry would be a preferred solution.

14. The most suitable air bag inflator to be satisfied with the fast combustion system without any modifications is the side impact type.

APPENDIX A

CALIBRATION PROCEDURES AND INSTRUMENTATION

A.1 Procedure for the Calibration of Pressure Transducers

1. Turn on the data acquisition box and start the software 'NJIT'. Attach the calibrated transducer and the transducer(s) to be calibrated to the inflator (or receiving tank). Zero all the channels by pressing the key 'Z' from the keyboard.
2. Fill the inflator (or receiving tank)with a measured quantity of gas (say 1500 psi of oxygen) by opening the inlet valve. Discharge the gas (oxygen) by opening the release valve and at the same time hit any key of the keyboard to take data.
3. Take data for about 4-5 minutes.

A.1.1 Calibration Results of the Pressure Transducers

Figure A.1 shows the calibration curves for Data Instrument XPRO (5000 psi) and Barksdale (10,000 psi) transducers.

A.2 Procedure for the Calibration of Thermocouples

1. Turn on the data acquisition box and start the software 'NJIT'. Zero all the channels of the software.
2. Take a beaker filled with ice and insert a thermometer and the thermocouple to be calibrated inside the beaker.
3. Read the temperature from the thermometer and the voltage from the thermocouple on the computer screen. Take readings from 0°C to 22°C (room temperature) at every 2°C interval.

4. Put the beaker on the hot plate and take readings up to 100°C at 2°C intervals.
5. Take a beaker filled with oil at -35°C and insert the thermometer and the thermocouple. Take readings at 2°C intervals up to room temperature.
6. Find a linear least squares polynomial to fit the data.

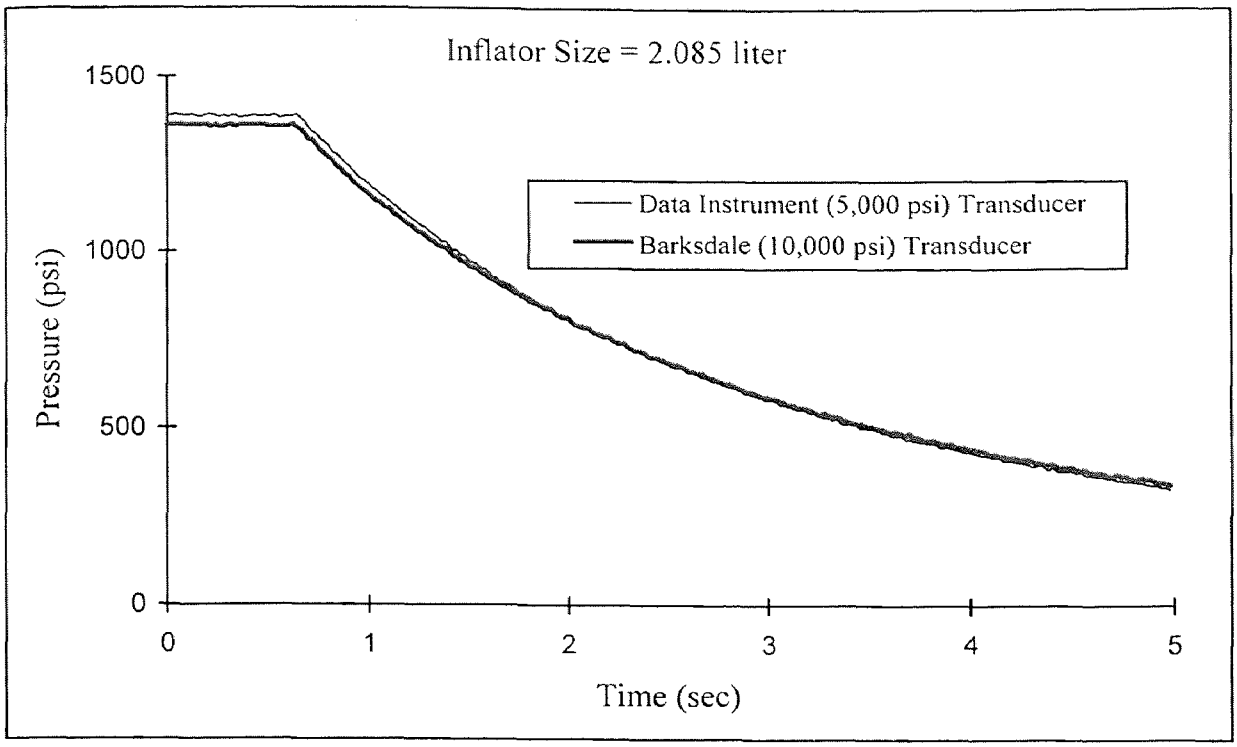

Figure A.1 Calibration curves for Data Instrument (5,000 psi) and Barksdale (10,000 psi) transducers

A.2.1 Calibration Results for Thermocouples

The calibration result for NANMAC E12-3-E-U thermocouple is shown in Figure A.2. A computer program 'THERM' is written to find the best linear least squares polynomial through the calibration data. The program is given in Appendix B.1. The best linear least squares polynomial for the above thermocouple is :

$$Y = 318.6907\ X - 0.1535053$$

where : Y = temperature (°C)

X = voltage (volt)

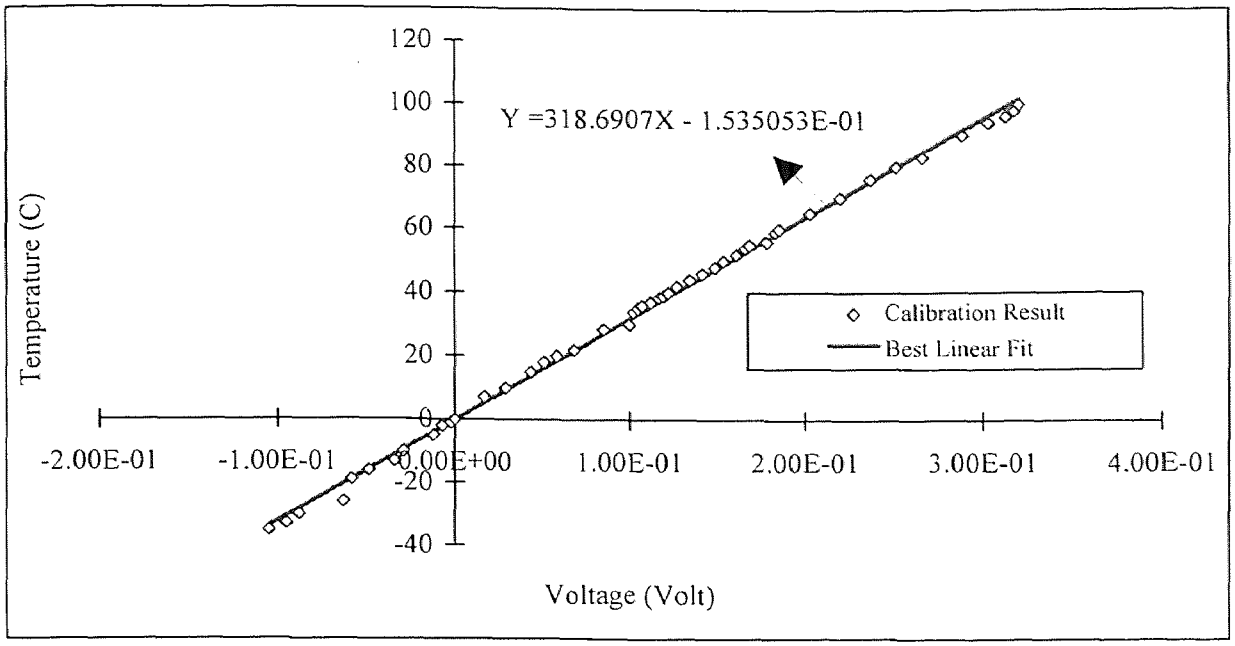

Figure A.2 Calibration result for NANMAC E12-3-E-U thermocouple

A.2.2 Testing the Response Time of Thermocouples

The response time of a thermocouple is defined as the time it takes for the thermocouple to produce 63.2% of its maximum output when subjected to a step-function of temperature [30]. The response time of thermocouple is tested by letting a drop of molten solder fall onto the surface of the thermocouple from a height of about 3 inches. The voltage change is measured using a memory oscilloscope. The summary of tests is given in Table A.1. Figure A.3 shows a typical output from the oscilloscope.

Table A.1 Summary of tests for response time of thermocouple

Resistance (ohm)	Volt. Inc. (ΔV) (mvolt)	Time Inc. (Δt) (msec)	ΔV/Δt (mvolt/msec) (°C/msec)	
5.1	350.00	4.0	87.50	27.73
5.9	321.87	7.0	45.98	14.51
6.1	84.37	19.0	4.44	1.25
6.3	184.37	9.0	20.48	6.38
6.1	84.37	8.0	10.55	3.35
6.0	140.62	6.0	23.44	7.30
Average :			32.06	10.37

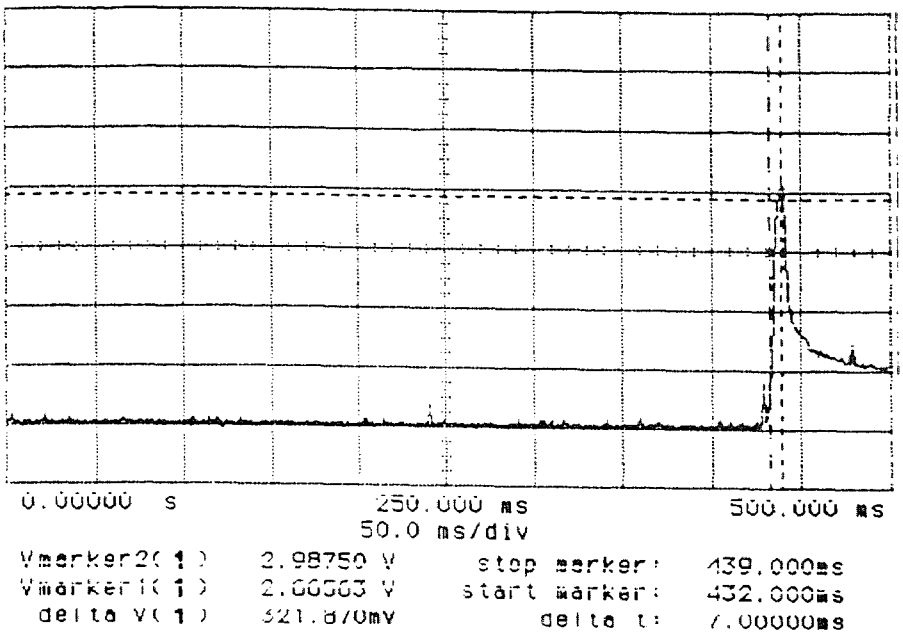

Figure A.3 Output from the oscilloscope for the response time of thermocouple

A.3 Testing the Burning Time of Electric Matches

The burning time of electric matches is calculated by putting a 0.2 ohm resistor in series with and measuring the voltage across the match. The circuit diagram is shown in Figure A.4. Both types of electric match are tested.

Type 1 : 18" (yellow wire)

Type 2 : 1.8 m (white wire)

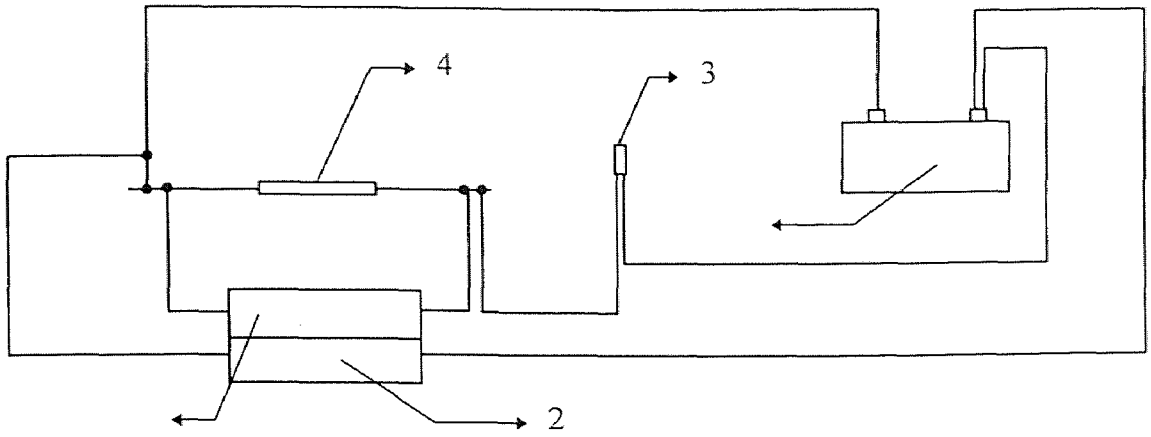

1 Oscilloscope (Channel 1)
2 Oscilloscope (Channel 2)
3 Electric match
4 Resistor (0.2 Ohm)
5 Battery

Figure A.4 Circuit diagram for testing the burning time of electric matches

The results for testing the burning time of electric matches are shown in Table A.2. A typical result from the oscilloscope is shown in Figure A.5.

Table A.2 Results for testing the burning time of electric matches

Match Type	Volt. Inc.(ΔV) (volt)	Time Inc.(Δt) (msec)	Current (I) (ampere)	(ΔV/Δt) (volt/msec)
2	1.39	310E-03	6.95	4.48
2	1.29	324E-03	6.47	3.99
1	1.50	246E-03	7.50	6.10
1	1.56	222E-03	7.78	7.01
1	1.49	358E-03	7.44	4.16
1	1.47	282E-03	7.37	5.23
1	1.46	246E-03	7.28	5.92
1	1.44	295E-03	7.22	4.89
Average :	1.45	285.4E-03	7.25	5.22

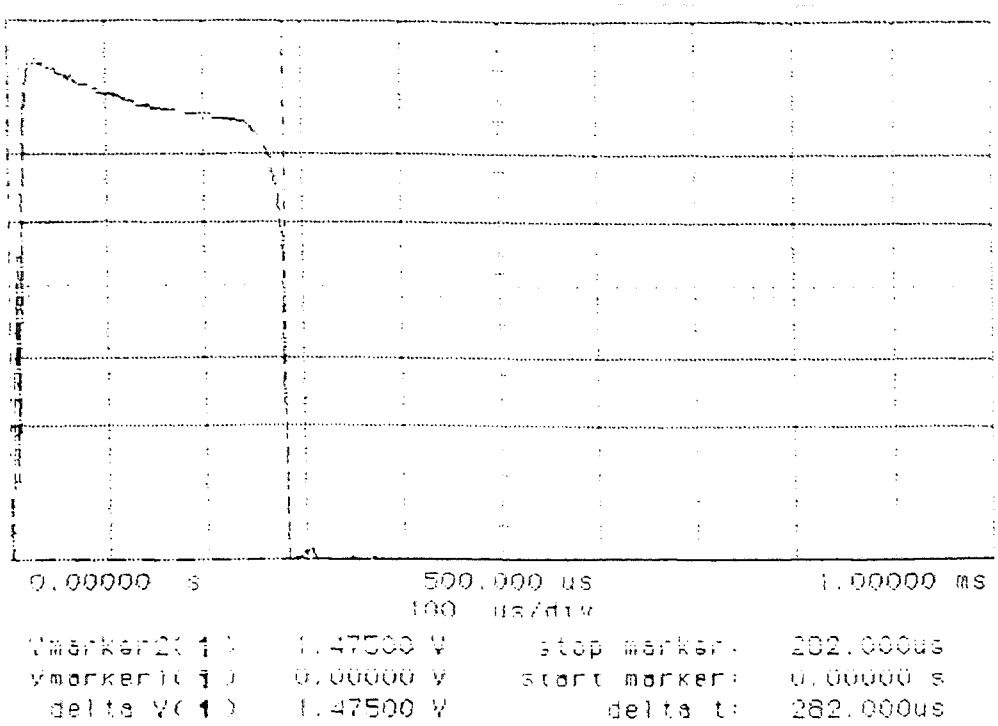

Figure A.5 Output from the oscilloscope for testing the burning time of electric match

A.4 Procedure for the Calibration of Carbon Monoxide

1. Take a 10 ml sample in a syringe from a CO standard (say 100 ppm CO) and inject it in the chromatograph. Note the area of CO peak by using the HP3396 Series II Integrator. Repeat this procedure four or five times and take the average value of area.
2. Repeat step 1 for other CO standards (1000 ppm and 1%).

A.4.1 Calibration Results for Carbon Monoxide

The calibration curves for carbon monoxide with two different flow rates used in the analysis are shown in Figure A.6. A typical output for a 10 ml sample of CO standard (1000 ppm) is shown in Figure A.7.

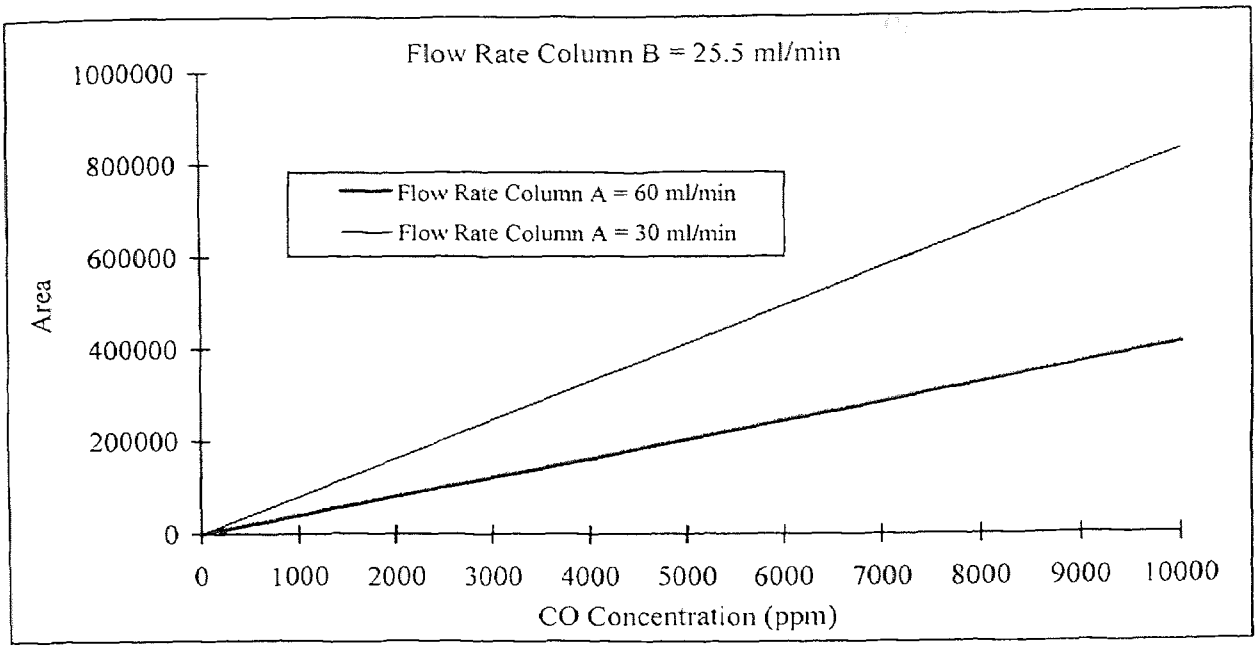

Figure A.6 Calibration curves for carbon monoxide

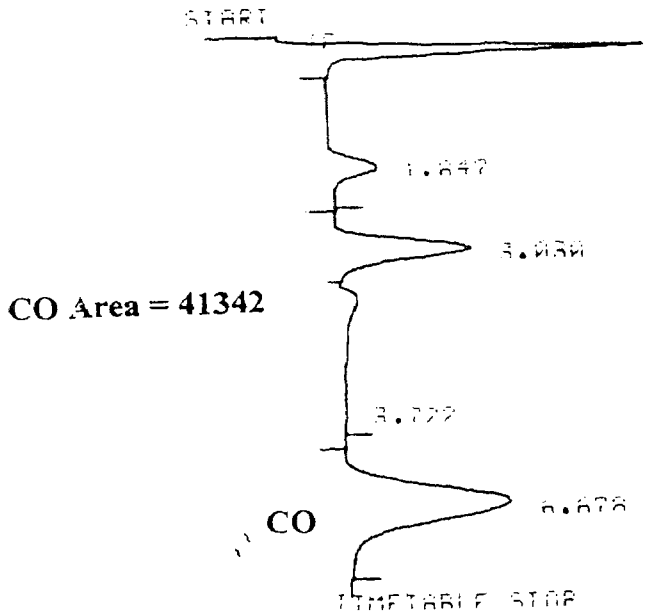

Figure A.7 Typical output of 10 ml sample of CO standard (1000 ppm)

A.5 Precautions, Handling of Electric Matches and Procedures for Safety

A.5.1 Precautions :

1. Check the voltage in the leads to be connected to the electric match adapter. Make sure that there is no voltage in the leads before connecting it to the adapter.

2. Make sure that all the leads from the pressure transducers, thermocouples and electric match are connected to the data acquisition box.
3. Make sure that there are no gas leaks in the inflator, receiving tank and the other fittings.
4. After the experiment, make sure that all the valves of gas cylinders are closed and the cylinders are chained all the times.
5. Make sure that the inlet valve to the inflator is closed and the release valve is open before firing the shot. Also, before firing the shot, make sure that the supply and discharge valves of the receiving tank are closed.

A.5.2 Handling of Electric Matches

1. The electric matches used in this study are classified as Class C explosives and require a Class H license from the New Jersey Department of Labor to handle them.
2. While handling the matches, avoid flame, temperatures over 71 °C, stray electrical currents, static electricity, and impact. To protect eyes, wear safety glasses with side shields.
3. Electric matches are stored in a ventilated, non-sparking cabinet and are brought into the laboratory in a metal box which has a wood lining inside. Not more than 50 matches are allowed in the work area.
4. The storage of electric matches requires permits from the Newark Fire Department and the New Jersey Department of Labor.

A.5.3 Procedures for Safety

1. Due to high pressures and high temperatures involved in the experiments, the experiments are performed in an explosion-proof laboratory with all the explosion-proof fittings.
2. The computer and the data acquisition system are kept outside the laboratory and the electric match is ignited by pressing any key of the computer keyboard.

APPENDIX B

COMPUTER PROGRAMS

B.1 Program THERM

```
*                                    PROGRAM  THERM
*                                         BY
*                                    YACOOB  TABANI

      PROGRAM THERM
      INTEGER DIM
      PARAMETER (DIM=100)
      INTEGER I,N
      REAL X(DIM), Y(DIM), XY(DIM), XX(DIM)
      REAL SUMX, SUMY, SUMXY, SUMXX

* Read in the no. of data points
      READ *, N
      PRINT *, 'N=',N
      PRINT *, '          X                Y'
      SUMX=0
      SUMY=0
      SUMXY=0
      SUMXX=0

* Read in the values of X and Y
      DO 50 I=1, N
      READ *, X(I), Y(I)
      PRINT *, X(I), Y(I)

* Calculate the sum of X,Y,XY and XX
      XY(I) = X(I) * Y(I)
      XX(I) = X(I) ** 2
      SUMX = SUMX + X(I)
      SUMY = SUMY + Y(I)
      SUMXY = SUMXY + XY(I)
      SUMXX = SUMXX + XX(I)
 50   CONTINUE

* Calculate the coefficients A and B of linear least
* squares polynomial
      A = ((N*SUMXY)-(SUMX*SUMY))/((N*SUMXX)-(SUMX**2))
      B = ((SUMXX*SUMY)-(SUMXY*SUMX))/((N*SUMXX)-(SUMX**2

* Print the best linear least squares polynomial
      PRINT *,'THE BEST LINEAR LEAST SQUARES POLYNOMIAL I
      PRINT *,'Y=',A,'X+',B
      END
```

N	=	48
X		Y
-1.050000E-01		-35.000000
-9.520000E-02		-33.000000
-8.790000E-02		-30.000000
-6.350000E-02		-26.000000
-5.860000E-02		-19.000000
-4.880000E-02		-16.000000
-3.420000E-02		-13.000000
-2.930000E-02		-10.000000
-1.220000E-02		-5.000000
-7.300000E-03		-2.000000
-2.400000E-03		-1.000000
0.000000E+00		0.000000
1.710000E-02		7.000000
2.930000E-02		10.000000
4.400000E-02		15.000000
5.130000E-02		18.000000
5.860000E-02		20.000000
6.840000E-02		22.000000
8.550000E-02		28.500000
1.001000E-01		30.000000
1.026000E-01		34.000000
1.050000E-01		35.000000
1.074000E-01		36.000000
1.123000E-01		37.000000
1.172000E-01		38.500000
1.197000E-01		39.000000
1.221000E-01		40.000000
1.270000E-01		42.000000
1.343000E-01		44.000000
1.416000E-01		46.000000
1.490000E-01		48.000000
1.538000E-01		50.000000
1.612000E-01		52.000000
1.661000E-01		54.000000
1.685000E-01		55.000000
1.783000E-01		56.000000
1.832000E-01		59.000000
1.856000E-01		60.000000
2.027000E-01		65.000000
2.198000E-01		70.000000
2.369000E-01		76.000000
2.515000E-01		80.000000
2.662000E-01		83.000000
2.882000E-01		90.000000
3.028000E-01		94.000000
3.126000E-01		96.000000
3.175000E-01		98.000000
3.199000E-01		100.000000

THE BEST LINEAR LEAST SQUARES POLYNOMIAL IS :

Y= 318.690700X+ -1.535053E-01

B.2 Program FASTN2

```
*                                PROGRAM FASTN2
*                                      BY
*                                YACOOB  TABANI

      PROGRAM FASTN2
      INTEGER DIM
      PARAMETER (DIM=800)
      REAL PI(DIM),TI(DIM),VI,MI(DIM),RI(DIM),PT(DIM),TT(DIM),VT
      REAL MT(DIM),RT(DIM),CP,R,CV,GAMMA,A,DELT,TIME(DIM),PCRIT
      REAL UI(DIM),UT(DIM),PRATIO(DIM),B(DIM),C(DIM),MFL(DIM)
      REAL MACH(DIM),D(DIM),M(DIM)
      INTEGER J,K,N,COUNT

* Initial Conditions
* Inflator
      PI(1) = 5960248.3
      TI(1) = 298.15
      VI    = 0.000250
      MI(1) = 0.01684
      RI(1) = 67.36
* Tank
      PT(1) = 101351.7
      TT(1) = 298.15
      VT    = 0.07
      MT(1) = 0.08020
      RT(1) = 1.1457

* Properties of Nitrogen
      CP    = 1040.04
      R     = 296.76
      CV    = 743.28
      GAMMA = 1.399

* Area of the orifice and time step
      A     = 0.0002280
      DELT  = 0.0004

* Other constants
      TIME(1) = 0.0000
      COUNT   = 0
      N       = 800

* Critical Pressure Ratio
      PCRIT = (2.0/(GAMMA+1))**(GAMMA/(GAMMA-1))

* Calculate the internal energy in the inflator and the tank
      UI(1) = MI(1)*CV*TI(1)
      UT(1) = MT(1)*CV*TT(1)
```

```
* If the tank pressure is greater than or equal to the inflator
* pressure then the program stops
      OPEN (UNIT=5, FILE='FASTN2F.OUT', STATUS='NEW')
      DO 200 J=1,N
      IF (PT(J) .GE. PI(J)) THEN
      GO TO 300
      ELSE
      GO TO 100
      END IF

* Calculate the tank to inflator pressure ratio
 100  PRATIO(J) = PT(J)/PI(J)
      IF (PRATIO(J) .LT. PCRIT) THEN
      B(J)=(PI(J)/(TI(J)**0.5))*((GAMMA/R)**0.5)
      C(J)=((2.0/(GAMMA+1))**((GAMMA+1)/(2.0*(GAMMA-1))))
      MFL(J) = A*B(J)*C(J)
      ELSE
      B(J)=(PI(J)/(TI(J)**0.5))*((GAMMA/R)**0.5)
      MACH(J)=((2.0/(GAMMA-1))*(((PT(J)/PI(J))**((1-GAMMA)
     +  /GAMMA))-1))**0.5
      D(J)=(1+(((GAMMA-1)/2.0)*(MACH(J)**2)))**
     +  ((GAMMA+1)/(2.0*(GAMMA-1)))
      MFL(J) = A*B(J)*(MACH(J)/D(J))
      END IF

* Calculate mass fraction and mass in the inflator and the tank
      M(J) = MFL(J)*DELT
      MI(J+1) = MI(J)-M(J)
      MT(J+1) = MT(J)+M(J)

* Calculate density in the inflator and the tank
      RI(J+1) = MI(J+1)/VI
      RT(J+1) = MT(J+1)/VT

* Calculate new internal energy
      UI(J+1) = UI(J)-(M(J)*CP*TI(J))
      UT(J+1) = UT(J)+(M(J)*CP*TI(J))

* Calculate new temperatures
      TI(J+1) = UI(J+1)/(MI(J+1)*CV)
      TT(J+1) = UT(J+1)/(MT(J+1)*CV)

* Calculate new pressures
      PI(J+1) = RI(J+1)*R*TI(J+1)
      PT(J+1) = RT(J+1)*R*TT(J+1)

* Update time
      COUNT = COUNT + 1
      TIME(J+1) = TIME(J)+DELT

 200  CONTINUE
```

```
*  Print the values of the variables
 300     WRITE (5,*) 'CRITICAL PRESSURE RATIO =',PCRIT
         WRITE (5,*) ' TIME          MFLOW                  MASS'
         DO 400 K=1,COUNT
         WRITE (5,*) TIME(K),MFL(K),M(K)
 400     CONTINUE
         WRITE (5,*) ' TIME          INFL MASS                TANK MASS'
         DO 500 L=1,COUNT
         WRITE (5,*) TIME(L),MI(L),MT(L)
 500     CONTINUE
         WRITE (5,*) ' TIME          INFL IE                  TANK IE'
         DO 600 L=1,COUNT
         WRITE (5,*) TIME(L),UI(L),UT(L)
 600     CONTINUE
         WRITE (5,*)  ' TI            TT            PI              PT'
         DO 700 L=1,COUNT
         WRITE (5,*) TI(L),TT(L),PI(L),PT(L)
 700     CONTINUE
         CLOSE (UNIT=5, STATUS='KEEP')
         END
```

CRITICAL PRESSURE RATIO = 5.284503E-01

TIME	MFLOW	MASS
0.000000E+00	3.127464	1.250985E-03
4.000000E-04	2.848233	1.139293E-03
8.000000E-04	2.598189	1.039275E-03
1.200000E-03	2.373720	9.494878E-04
1.600000E-03	2.171846	8.687383E-04
2.000000E-03	1.989976	7.959902E-04
2.400000E-03	1.825850	7.303401E-04
2.800000E-03	1.677497	6.709989E-04
3.200000E-03	1.543190	6.172758E-04
3.600000E-03	1.421412	5.685648E-04
4.000000E-03	1.310832	5.243328E-04
4.400000E-03	1.210276	4.841105E-04
4.799999E-03	1.118709	4.474837E-04
5.199999E-03	1.035215	4.140860E-04
5.599999E-03	9.589823E-01	3.835929E-04
5.999999E-03	8.892916E-01	3.557166E-04
6.399998E-03	8.255028E-01	3.302011E-04
6.799998E-03	7.670460E-01	3.068184E-04
7.199998E-03	7.134133E-01	2.853653E-04
7.599998E-03	6.641509E-01	2.656603E-04
7.999998E-03	6.188527E-01	2.475411E-04
8.399998E-03	5.771552E-01	2.308621E-04
8.799998E-03	5.387318E-01	2.154927E-04
9.199998E-03	5.032897E-01	2.013159E-04
9.599999E-03	4.705650E-01	1.882260E-04
9.999999E-03	4.403201E-01	1.761280E-04
1.040000E-02	4.123408E-01	1.649363E-04
1.080000E-02	3.864337E-01	1.545735E-04
1.120000E-02	3.624236E-01	1.449694E-04
1.160000E-02	3.401523E-01	1.360609E-04
1.200000E-02	3.194760E-01	1.277904E-04
1.240000E-02	3.002646E-01	1.201058E-04
1.280000E-02	2.823997E-01	1.129599E-04
1.320000E-02	2.657737E-01	1.063095E-04
1.360000E-02	2.502885E-01	1.001154E-04
1.400000E-02	2.358550E-01	9.434199E-05
1.440000E-02	2.223916E-01	8.895664E-05
1.480000E-02	2.098240E-01	8.392958E-05
1.520000E-02	1.980842E-01	7.923367E-05
1.560000E-02	1.868070E-01	7.472279E-05
1.600000E-02	1.751917E-01	7.007668E-05
1.640000E-02	1.631901E-01	6.527602E-05
1.680000E-02	1.507916E-01	6.031664E-05
1.720000E-02	1.379862E-01	5.519448E-05
1.760000E-02	1.247635E-01	4.990541E-05
1.800000E-02	1.111114E-01	4.444455E-05
1.840000E-02	9.701233E-02	3.880493E-05
1.880000E-02	8.243610E-02	3.297444E-05
1.920000E-02	6.732164E-02	2.692865E-05
1.960000E-02	5.152803E-02	2.061121E-05
2.000000E-02	3.465426E-02	1.386171E-05
2.040000E-02	1.464830E-02	5.859320E-06

TIME	INFL MASS	TANK MASS
0.000000E+00	1.684000E-02	8.020000E-02
4.000000E-04	1.558901E-02	8.145098E-02
8.000000E-04	1.444972E-02	8.259027E-02
1.200000E-03	1.341045E-02	8.362955E-02
1.600000E-03	1.246096E-02	8.457904E-02
2.000000E-03	1.159222E-02	8.544777E-02
2.400000E-03	1.079623E-02	8.624376E-02
2.800000E-03	1.006589E-02	8.697411E-02
3.200000E-03	9.394890E-03	8.764511E-02
3.600000E-03	8.777614E-03	8.826238E-02
4.000000E-03	8.209049E-03	8.883094E-02
4.400000E-03	7.684716E-03	8.935528E-02
4.799999E-03	7.200606E-03	8.983938E-02
5.199999E-03	6.753122E-03	9.028687E-02
5.599999E-03	6.339036E-03	9.070095E-02
5.999999E-03	5.955443E-03	9.108455E-02
6.399998E-03	5.599726E-03	9.144026E-02
6.799998E-03	5.269525E-03	9.177046E-02
7.199998E-03	4.962707E-03	9.207728E-02
7.599998E-03	4.677342E-03	9.236264E-02
7.999998E-03	4.411682E-03	9.262830E-02
8.399998E-03	4.164141E-03	9.287584E-02
8.799998E-03	3.933278E-03	9.310670E-02
9.199998E-03	3.717786E-03	9.332220E-02
9.599999E-03	3.516470E-03	9.352351E-02
9.999999E-03	3.328244E-03	9.371173E-02
1.040000E-02	3.152116E-03	9.388787E-02
1.080000E-02	2.987180E-03	9.405280E-02
1.120000E-02	2.832606E-03	9.420737E-02
1.160000E-02	2.687637E-03	9.435233E-02
1.200000E-02	2.551576E-03	9.448840E-02
1.240000E-02	2.423785E-03	9.461619E-02
1.280000E-02	2.303679E-03	9.473629E-02
1.320000E-02	2.190720E-03	9.484925E-02
1.360000E-02	2.084410E-03	9.495556E-02
1.400000E-02	1.984295E-03	9.505568E-02
1.440000E-02	1.889953E-03	9.515002E-02
1.480000E-02	1.800996E-03	9.523898E-02
1.520000E-02	1.717067E-03	9.532291E-02
1.560000E-02	1.637833E-03	9.540214E-02
1.600000E-02	1.563110E-03	9.547687E-02
1.640000E-02	1.493033E-03	9.554695E-02
1.680000E-02	1.427757E-03	9.561222E-02
1.720000E-02	1.367441E-03	9.567254E-02
1.760000E-02	1.312246E-03	9.572773E-02
1.800000E-02	1.262341E-03	9.577764E-02
1.840000E-02	1.217896E-03	9.582208E-02
1.880000E-02	1.179091E-03	9.586088E-02
1.920000E-02	1.146117E-03	9.589386E-02
1.960000E-02	1.119188E-03	9.592079E-02
2.000000E-02	1.098577E-03	9.594139E-02
2.040000E-02	1.084715E-03	9.595525E-02

TIME	INFL IE	TANK IE
0.000000E+00	3731.895000	17773.040000
4.000000E-04	3343.979000	18160.950000
8.000000E-04	3002.017000	18502.920000
1.200000E-03	2699.895000	18805.040000
1.600000E-03	2432.416000	19072.520000
2.000000E-03	2195.129000	19309.800000
2.400000E-03	1984.218000	19520.710000
2.800000E-03	1796.399000	19708.530000
3.200000E-03	1628.839000	19876.090000
3.600000E-03	1479.090000	20025.840000
4.000000E-03	1345.031000	20159.900000
4.400000E-03	1224.820000	20280.110000
4.799999E-03	1116.854000	20388.080000
5.199999E-03	1019.736000	20485.200000
5.599999E-03	932.243300	20572.690000
5.999999E-03	853.307400	20651.630000
6.399998E-03	781.990400	20722.940000
6.799998E-03	717.468000	20787.460000
7.199998E-03	659.014500	20845.920000
7.599998E-03	605.990200	20898.940000
7.999998E-03	557.829800	20947.100000
8.399998E-03	514.033000	20990.900000
8.799998E-03	474.156600	21030.770000
9.199998E-03	437.807200	21067.120000
9.599999E-03	404.635000	21100.290000
9.999999E-03	374.328600	21130.600000
1.040000E-02	346.610500	21158.320000
1.080000E-02	321.232700	21183.700000
1.120000E-02	297.973700	21206.960000
1.160000E-02	276.635100	21228.290000
1.200000E-02	257.039100	21247.890000
1.240000E-02	239.026100	21265.900000
1.280000E-02	222.452700	21282.480000
1.320000E-02	207.189700	21297.740000
1.360000E-02	193.121100	21311.810000
1.400000E-02	180.142000	21324.790000
1.440000E-02	168.157800	21336.770000
1.480000E-02	157.082800	21347.850000
1.520000E-02	146.839800	21358.090000
1.560000E-02	137.358600	21367.570000
1.600000E-02	128.589800	21376.340000
1.640000E-02	120.523300	21384.410000
1.680000E-02	113.150100	21391.780000
1.720000E-02	106.461500	21398.470000
1.760000E-02	100.448700	21404.480000
1.800000E-02	95.103380	21409.830000
1.840000E-02	90.418100	21414.510000
1.880000E-02	86.386940	21418.540000
1.920000E-02	83.006480	21421.930000
1.960000E-02	80.277530	21424.650000
2.000000E-02	78.208850	21426.720000
2.040000E-02	76.828030	21428.100000

TI	TT	PI	PT
298.150000	298.150000	5960249.000000	101351.700000
288.597400	299.978300	5340433.000000	103584.200000
279.512500	301.410800	4794309.000000	105534.600000
270.863900	302.525500	4311811.000000	107257.800000
262.623700	303.384100	3884639.000000	108783.500000
254.765700	304.035800	3505686.000000	110136.900000
247.266300	304.519800	3168855.000000	111339.800000
240.103400	304.868000	2868902.000000	112411.100000
233.256700	305.106100	2601304.000000	113366.800000
226.707500	305.254900	2362151.000000	114220.900000
220.438400	305.331500	2148055.000000	114985.500000
214.433300	305.349800	1956074.000000	115671.200000
208.677200	305.321300	1783649.000000	116287.000000
203.156500	305.255200	1628548.000000	116840.900000
197.858000	305.159400	1488820.000000	117340.000000
192.769800	305.040200	1362757.000000	117790.200000
187.880700	304.902900	1248862.000000	118197.000000
183.180200	304.751700	1145817.000000	118565.000000
178.658600	304.590300	1052466.000000	118898.400000
174.306700	304.421600	967784.100000	119200.800000
170.116000	304.248000	890870.500000	119475.500000
166.078400	304.071500	820925.800000	119725.300000
162.186500	303.893800	757241.900000	119952.700000
158.433200	303.716100	699190.900000	120160.000000
154.811800	303.539500	646214.000000	120349.300000
151.316200	303.365000	597813.800000	120522.100000
147.940500	303.193100	553547.100000	120680.200000
144.679200	303.024400	513018.100000	120824.900000
141.527000	302.859400	475872.800000	120957.600000
138.479100	302.698300	441794.400000	121079.300000
135.530900	302.541400	410499.000000	121191.100000
132.677900	302.389000	381731.700000	121293.800000
129.916100	302.241000	355263.400000	121388.400000
127.241600	302.097500	330888.100000	121475.400000
124.650600	301.958600	308420.100000	121555.700000
122.139600	301.824300	287692.100000	121629.700000
119.705300	301.694500	268552.900000	121698.100000
117.344700	301.569200	250865.800000	121761.200000
115.054600	301.448200	234507.400000	121819.600000
112.832400	301.331500	219365.700000	121873.700000
110.678800	301.219200	205361.700000	121923.700000
108.604800	301.111900	192479.200000	121969.700000
106.622300	301.010100	180704.100000	122011.800000
104.744600	300.914400	170022.200000	122049.900000
102.985600	300.825400	160419.500000	122084.200000
101.360100	300.743700	151882.900000	122114.700000
99.883240	300.670000	144400.400000	122141.500000
98.570780	300.604900	137962.500000	122164.400000
97.438510	300.549000	132563.800000	122183.700000
96.502460	300.502900	128205.600000	122199.300000
95.779580	300.467300	124901.800000	122211.100000
95.290900	300.443300	122696.600000	122219.000000

B.3 Program MFLOW

```
*                              PROGRAM  MFLOW
*                                    BY
*                              YACOOB  TABANI

      PROGRAM MFLOW
      INTEGER DIM
      PARAMETER (DIM=800)
      REAL PI(DIM),TI(DIM),VI,MI(DIM),RI(DIM),PT(DIM),TT(DIM),VT
      REAL MT(DIM),RT(DIM),R,GAMMA,A,DELT,TIME(DIM),PCRIT
      REAL PRATIO(DIM),B(DIM),C(DIM),MFL(DIM)
      REAL MACH(DIM),D(DIM),M(DIM)
      INTEGER J,K,N,COUNT

      OPEN (UNIT=5, FILE='MFLOWB.INP', STATUS='OLD')

* Read the input parameters
      READ (5,*) TI(1), TT(1), VI, VT
      READ (5,*) MI(1), MT(1), RI(1), RT(1)
      READ (5,*) R, GAMMA

* Read the transient values of inflator and tank pressures
      DO 50 J=1,200
      READ (5,*) TIME(J), PI(J), PT(J)
 50   CONTINUE

      CLOSE (UNIT=5, STATUS='KEEP')

* Other variables and constants
      A     = 0.0002850
      DELT  = 0.0004
      COUNT = 0
      N     = 43

* Calculate the  critical pressure ratio
      PCRIT = (2.0/(GAMMA+1))**(GAMMA/(GAMMA-1))

* If the tank pressure is greater than or equal to the inflator
* pressure then the program stops

      OPEN (UNIT=5, FILE='MFLOWB.OUT', STATUS='NEW')
      DO 200 J=1,N
      IF (PT(J) .GE. PI(J)) THEN
      GO TO 300
      ELSE
      GO TO 100
      END IF
```

```
* Calculate the tank to inflator pressure ratio
 100    PRATIO(J) = ABS(PT(J)/PI(J))

* Calculate the mass flow rate
        IF (PRATIO(J) .LT. PCRIT) THEN
        B(J)=(PI(J)/(TI(J)**0.5))*((GAMMA/R)**0.5)
        C(J)=((2.0/(GAMMA+1))**((GAMMA+1)/(2.0*(GAMMA-1))))
        MFL(J) = A*B(J)*C(J)
        ELSE
        B(J)=(PI(J)/(TI(J)**0.5))*((GAMMA/R)**0.5)
        MACH(J)=((2.0/(GAMMA-1))*(((PT(J)/PI(J))**((1-GAMMA)
     +  /GAMMA))-1))**0.5
        D(J)=(1+(((GAMMA-1)/2.0)*(MACH(J)**2)))**
     +  ((GAMMA+1)/(2.0*(GAMMA-1)))
        MFL(J) = A*B(J)*(MACH(J)/D(J))
        PRINT *, MFL(J)
        END IF

* Calculate mass fraction and mass in the inflator and the tank
        M(J) = MFL(J)*DELT
        MI(J+1) = MI(J)-M(J)
        MT(J+1) = MT(J)+M(J)

* Calculate density in the inflator and the tank
        RI(J+1) = MI(J+1)/VI
        RT(J+1) = MT(J+1)/VT

* Calculate new temperatures
        TI(J+1) = PI(J+1)/(RI(J+1)*R)
        TT(J+1) = PT(J+1)/(RT(J+1)*R)

* Update the counter
        COUNT = COUNT + 1

 200    CONTINUE

* Print the values of the variables
 300    PRINT *,'CRITICAL PRESSURE RATIO =',PCRIT
        WRITE (5,*)' TIME          MFLOW              MASS'
        DO 400 K=1,COUNT
        WRITE (5,*) TIME(K),MFL(K),M(K)
 400    CONTINUE
        WRITE (5,*)' TIME          INFL MASS              TANK MASS'
        DO 500 L=1,COUNT
        WRITE (5,*) TIME(L),MI(L),MT(L)
 500    CONTINUE
        WRITE (5,*)' PI            TI            PT             TT'
        DO 600 L=1,COUNT
        WRITE (5,*) PI(L),TI(L),PT(L),TT(L)
 600    CONTINUE
        CLOSE (UNIT=5, STATUS='KEEP')
        END
```

TIME	MFLOW	MASS
1.800000E-02	3.910578	1.564231E-03
1.840000E-02	3.692148	1.476859E-03
1.880000E-02	3.322684	1.329073E-03
1.920000E-02	2.938350	1.175340E-03
1.960000E-02	2.669277	1.067711E-03
2.000000E-02	2.477256	9.909025E-04
2.040000E-02	2.323810	9.295239E-04
2.080000E-02	2.084569	8.338278E-04
2.120000E-02	1.887940	7.551758E-04
2.160000E-02	1.701194	6.804775E-04
2.200000E-02	1.523894	6.095574E-04
2.240000E-02	1.385917	5.543670E-04
2.280000E-02	1.254842	5.019369E-04
2.320000E-02	1.100312	4.401249E-04
2.360000E-02	1.014053	4.056212E-04
2.400000E-02	9.316426E-01	3.726570E-04
2.440000E-02	8.530546E-01	3.412218E-04
2.480000E-02	7.782580E-01	3.113032E-04
2.520000E-02	6.794774E-01	2.717910E-04
2.560000E-02	6.414812E-01	2.565925E-04
2.600000E-02	5.777352E-01	2.310941E-04
2.640000E-02	5.175691E-01	2.070276E-04
2.680000E-02	4.858152E-01	1.943261E-04
2.720000E-02	4.307030E-01	1.722812E-04
2.760000E-02	3.790615E-01	1.516246E-04
2.800000E-02	3.535794E-01	1.414318E-04
2.840000E-02	3.280306E-01	1.312123E-04
2.880000E-02	2.619059E-01	1.047624E-04
2.920000E-02	2.427326E-01	9.709302E-05
2.960000E-02	2.234990E-01	8.939960E-05
3.000000E-02	2.041937E-01	8.167747E-05
3.040000E-02	1.687081E-01	6.748325E-05
3.080000E-02	1.525388E-01	6.101551E-05
3.120000E-02	1.362775E-01	5.451101E-05
3.160000E-02	1.072488E-01	4.289951E-05
3.200000E-02	9.412884E-02	3.765153E-05
3.240000E-02	7.005187E-02	2.802075E-05
3.280000E-02	6.010533E-02	2.404213E-05
3.320000E-02	5.001856E-02	2.000742E-05
3.360000E-02	3.971743E-02	1.588697E-05
3.400000E-02	2.904246E-02	1.161698E-05
3.440000E-02	1.411643E-02	5.646574E-06
3.480000E-02	6.771553E-03	2.708621E-06

B.4 Program FASTCOMB

```
*                                PROGRAM FASTCOMB
*                                      BY
*                                 YACOOB  TABANI

      PROGRAM FASTCOMB
      INTEGER DIM
      PARAMETER (DIM=100)
      REAL PI(DIM),TI(DIM),VI,MI(DIM),RI(DIM),PT(DIM),TT(DIM),VT
      REAL MT(DIM),RT(DIM),GAMMA(DIM),A,DELT,TIME(DIM)
      REAL UI(DIM),UT(DIM),PRATIO(DIM),B(DIM),C(DIM),MFL(DIM)
      REAL MACH(DIM),D(DIM),M(DIM),PCRIT(DIM)
      REAL CPCI(DIM),CPHI(DIM),CPCT(DIM),CPHT(DIM),CPPT(DIM)
      REAL CVCI(DIM),CVHI(DIM),CVCT(DIM),CVHT(DIM),CVPT(DIM)
      REAL R,RC,RH,RP,CI(DIM),CT(DIM)
      REAL CPH1I(DIM),CPH2I(DIM),CPO1I(DIM),CPO2I(DIM)
      REAL CPCOI(DIM),CPOHI(DIM)
      REAL CPHOI(DIM),CPI1I(DIM),CPI2I(DIM),CPO3I(DIM)
      REAL CPH1T(DIM),CPH2T(DIM),CPO1T(DIM),CPO2T(DIM)
      REAL CPCOT(DIM),CPOHT(DIM)
      REAL CPHOT(DIM),CPI1T(DIM),CPI2T(DIM),CPO3T(DIM)
      REAL CVH1I(DIM),CVH2I(DIM),CVO1I(DIM),CVO2I(DIM)
      REAL CVCOI(DIM),CVOHI(DIM)
      REAL CVHOI(DIM),CVI1I(DIM),CVI2I(DIM),CVO3I(DIM)
      REAL CVH1T(DIM),CVH2T(DIM),CVO1T(DIM),CVO2T(DIM)
      REAL CVCOT(DIM),CVOHT(DIM)
      REAL CVHOT(DIM),CVI1T(DIM),CVI2T(DIM),CVO3T(DIM)
      REAL RH1,RH2,RO1,RO2,RCO,ROH
      REAL RHO,RI1,RI2,RO3
      REAL MCP(DIM),MOLCP(DIM),MOLP,MWI(DIM),MWT(DIM)
      REAL MFC,MFH,MFH1,MFH2,MFO1,MFO2,MFCO,MFOH
      REAL MFHO,MFI1,MFI2,MFO3
      INTEGER J,K,N,COUNT

* Initial Conditions
* Inflator
      PI(1) = 52316746.5
      TI(1) = 4148.77
      VI    = 0.000250
      MI(1) = 0.008673
      RI(1) = 34.69
      MWI(1)= 22.891
* Tank
      PT(1) = 101351.7
      TT(1) = 298.15
      VT    = 0.07
      MT(1) = 0.0802
      RT(1) = 1.1457
      MWT(1)= 28.00
```

```
* Mass Fractions
        MFC    = 0.26413
        MFH    = 0.34353
        MFH1   = 0.00087
        MFH2   = 0.00426
        MFO1   = 0.01741
        MFO2   = 0.11769
        MFCO   = 0.16848
        MFOH   = 0.08171
        MFHO   = 0.00006
        MFI1   = 0.00141
        MFI2   = 0.00027
        MFO3   = 0.00001

* Gas Constants
        R      = 8314
        RC     = 188.9
        RH     = 461.9
        RH1    = 8248.0
        RH2    = 4124.0
        RO1    = 519.8
        RO2    = 259.8
        RCO    = 296.8
        ROH    = 488.8
        RHO    = 286.5
        RI1    = 251.9
        RI2    = 244.4
        RO3    = 173.2
        RP     = 296.9

* Area of the orifice and time step
        A        = 0.0002850
        DELT     = 0.0004

* Other constants
        TIME(1) = 0.0000
        COUNT   = 0
        N       = 100

* If the tank pressure is greater than or equal to the inflator
* pressure then the program stops
        OPEN (UNIT=5, FILE='F63N.OUT', STATUS='NEW')
        DO 200 J=1,N
        IF (PT(J) .GE. PI(J)) THEN
        GO TO 300
        ELSE
        GO TO 100
        END IF
```

```
* Calculate the temperatures in Centigrade
 100     CI(J) = TI(J) - 273.15
         CT(J) = TT(J) - 273.15

* Calculate the specific heats
         CPCI(J)=(0.04453623E+02+0.03140168E-01*(TI(J))-
      +  0.12784105E-05*(TI(J)**2)+0.02393996E-08*(TI(J)**3)-
      +  0.16690333E-13*(TI(J)**4))*RC
         CPHI(J)=(0.02672145E+02+0.03056293E-01*(TI(J))-
      +  0.08730260E-05*(TI(J)**2)+0.12009964E-09*(TI(J)**3)-
      +  0.06391618E-13*(TI(J)**4))*RH
         CPH1I(J)=(0.02500000E+02)*RH1
         CPH2I(J)=(0.02991423E+02+0.07000644E-02*(TI(J))-
      +  0.05633828E-06*(TI(J)**2)-0.09231578E-10*(TI(J)**3)+
      +  0.15827519E-14*(TI(J)**4))*RH2
         CPO1I(J)=(0.02542059E+02-0.02755061E-03*(TI(J))-
      +  0.03102803E-07*(TI(J)**2)+0.04551067E-10*(TI(J)**3)-
      +  0.04368051E-14*(TI(J)**4))*RO1
         CPO2I(J)=(0.03697578E+02+0.06135197E-02*(TI(J))-
      +  0.12588420E-06*(TI(J)**2)+0.01775281E-09*(TI(J)**3)-
      +  0.11364354E-14*(TI(J)**4))*RO2
         CPCOI(J)=(0.03025078E+02+0.14426885E-02*(TI(J))-
      +  0.05630827E-05*(TI(J)**2)+0.10185813E-09*(TI(J)**3)-
      +  0.06910951E-13*(TI(J)**4))*RCO
         CPOHI(J)=(0.02882730E+02+0.10139743E-02*(TI(J))-
      +  0.02276877E-05*(TI(J)**2)+0.02174683E-09*(TI(J)**3)-
      +  0.05126305E-14*(TI(J)**4))*ROH
         CPHOI(J)=(0.03557271E+02+0.03345572E-01*(TI(J))-
      +  0.13350060E-05*(TI(J)**2)+0.02470572E-08*(TI(J)**3)-
      +  0.01713850E-12*(TI(J)**4))*RHO
         CPI1I(J)=(0.04072191E+02+0.02131296E-01*(TI(J))-
      +  0.05308145E-05*(TI(J)**2)+0.06112269E-09*(TI(J)**3)-
      +  0.02841164E-13*(TI(J)**4))*RI1
         CPI2I(J)=(0.04573167E+02+0.04336136E-01*(TI(J))-
      +  0.14746888E-05*(TI(J)**2)+0.02348903E-08*(TI(J)**3)-
      +  0.14316536E-13*(TI(J)**4))*RI2
         CPO3I(J)=(0.05429371E+02+0.01820380E-01*(TI(J))-
      +  0.07705607E-05*(TI(J)**2)+0.14992929E-09*(TI(J)**3)-
      +  0.10755629E-13*(TI(J)**4))*RO3
         CPCT(J)=(0.02275724E+02+0.09922072E-01*(TT(J))-
      +  0.10409113E-04*(TT(J)**2)+0.06866686E-07*(TT(J)**3)-
      +  0.02117280E-10*(TT(J)**4))*RC
         CPHT(J)=(0.03386842E+02+0.03474982E-01*(TT(J))-
      +  0.06354696E-04*(TT(J)**2)+0.06968581E-07*(TT(J)**3)-
      +  0.02506588E-10*(TT(J)**4))*RH
         CPH1T(J)=(0.02500000E+02)*RH1
         CPH2T(J)=(0.03298124E+02+0.08249441E-02*(TT(J))-
      +  0.08143015E-05*(TT(J)**2)-0.09475434E-09*(TT(J)**3)+
      +  0.04134872E-11*(TT(J)**4))*RH2
```

```
      CPO1T(J)=(0.02946428E+02-0.16381665E-02*(TT(J))+
     +  0.02421031E-04*(TT(J)**2)-0.16028431E-08*(TT(J)**3)+
     +  0.03890696E-11*(TT(J)**4))*RO1
      CPO2T(J)=(0.03212936E+02+0.11274864E-02*(TT(J))-
     +  0.05756150E-05*(TT(J)**2)+0.13138773E-08*(TT(J)**3)-
     +  0.08768554E-11*(TT(J)**4))*RO2
      CPCOT(J)=(0.03262451E+02+0.15119409E-02*(TT(J))-
     +  0.03881755E-04*(TT(J)**2)+0.05581944E-07*(TT(J)**3)-
     +  0.02474951E-10*(TT(J)**4))*RCO
      CPOHT(J)=(0.03637266E+02+0.01850910E-02*(TT(J))-
     +  0.16761646E-05*(TT(J)**2)+0.02387202E-07*(TT(J)**3)-
     -  0.08431442E-11*(TT(J)**4))*ROH
      CPHOT(J)=(0.02898329E+02+0.06199146E-01*(TT(J))-
     +  0.09623084E-04*(TT(J)**2)+0.10898249E-07*(TT(J)**3)-
     +  0.04574885E-10*(TT(J)**4))*RHO
      CPI1T(J)=(0.02979963E+02+0.04996697E-01*(TT(J))-
     +  0.03790997E-04*(TT(J)**2)+0.02354192E-07*(TT(J)**3)-
     +  0.08089024E-11*(TT(J)**4))*RI1
      CPI2T(J)=(0.03388753E+02+0.06569226E-01*(TT(J))-
     +  0.14850125E-06*(TT(J)**2)-0.04625805E-07*(TT(J)**3)+
     +  0.02471514E-10*(TT(J)**4))*RI2
      CPO3T(J)=(0.02462608E+02+0.09582781E-01*(TT(J))-
     +  0.07087359E-04*(TT(J)**2)+0.13633683E-08*(TT(J)**3)+
     +  0.02969647E-11*(TT(J)**4))*RO3
      CPPT(J)=(0.03298677E+02+0.14082404E-02*(TT(J))-
     +  0.03963222E-04*(TT(J)**2)+0.05641515E-07*(TT(J)**3)-
     +  0.02444854E-10*(TT(J)**4))*RP
      CVCI(J)=CPCI(J)-RC
      CVHI(J)=CPHI(J)-RH
      CVH1I(J)=CPH1I(J)-RH1
      CVH2I(J)=CPH2I(J)-RH2
      CVO1I(J)=CPO1I(J)-RO1
      CVO2I(J)=CPO2I(J)-RO2
      CVCOI(J)=CPCOI(J)-RCO
      CVOHI(J)=CPOHI(J)-ROH
      CVHOI(J)=CPHOI(J)-RHO
      CVI1I(J)=CPI1I(J)-RI1
      CVI2I(J)=CPI2I(J)-RI2
      CVO3I(J)=CPO3I(J)-RO3
      CVCT(J)=CPCT(J)-RC
      CVHT(J)=CPHT(J)-RH
      CVH1T(J)=CPH1T(J)-RH1
      CVH2T(J)=CPH2T(J)-RH2
      CVO1T(J)=CPO1T(J)-RO1
      CVO2T(J)=CPO2T(J)-RO2
      CVCOT(J)=CPCOT(J)-RCO
      CVOHT(J)=CPOHT(J)-ROH
      CVHOT(J)=CPHOT(J)-RHO
      CVI1T(J)=CPI1T(J)-RI1
      CVI2T(J)=CPI2T(J)-RI2
      CVO3T(J)=CPO3T(J)-RO3
      CVPT(J)=CPPT(J)-RP
```

```
      GAMMA(J) = ((MFC*CPCI(J))+(MFH*CPHI(J))+
     +  (MFH1*CPH1I(J))+(MFH2*CPH2I(J))+(MFO1*CPO1I(J))+
     +  (MFO2*CPO2I(J))+(MFCO*CPCOI(J))+(MFOH*CPOHI(J))+
     +  (MFHO*CPHOI(J))+(MFI1*CPI1I(J))+
     +  (MFI2*CPI2I(J))+(MFO3*CPO3I(J)))/((MFC*CVCI(J))+
     +  (MFH*CVHI(J))+
     +  (MFH1*CVH1I(J))+(MFH2*CVH2I(J))+(MFO1*CVO1I(J))+
     +  (MFO2*CVO2I(J))+(MFCO*CVCOI(J))+(MFOH*CVOHI(J))+
     +  (MFHO*CVHOI(J))+(MFI1*CVI1I(J))+
     +  (MFI2*CVI2I(J))+(MFO3*CVO3I(J)))

* Calculate the initial internal energy in the inflator and the tank
      IF (J .EQ. 1) THEN
      UI(1) = MI(1)*((MFC*CVCI(1))+(MFH*CVHI(1))+
     +  (MFH1*CVH1I(1))+(MFH2*CVH2I(1))+(MFO1*CVO1I(1))+
     +  (MFO2*CVO2I(1))+(MFCO*CVCOI(1))+(MFOH*CVOHI(1))+
     +  (MFHO*CVHOI(1))+(MFI1*CVI1I(1))+
     +  (MFI2*CVI2I(1))+(MFO3*CVO3I(1)))*TI(1)
      UT(1) = MT(1)*CVPT(1)*TT(1)
      END IF

* Calculate the mass flow from the inflator to the tank
      PRATIO(J) = PT(J)/PI(J)
      PCRIT(J)  = (2.0/(GAMMA(J)+1))**(GAMMA(J)/(GAMMA(J)-1))
      IF (PRATIO(J) .LT. PCRIT(J)) THEN
      B(J)=(PI(J)/(TI(J)**0.5))*((GAMMA(J)/(R/MWI(J)))**0.5)
      C(J)=((2.0/(GAMMA(J)+1))**((GAMMA(J)+1)/(2.0*(GAMMA(J)-1))))
      MFL(J) = A*B(J)*C(J)
      ELSE
      B(J)=(PI(J)/(TI(J)**0.5))*((GAMMA(J)/(R/MWI(J)))**0.5)
      MACH(J)=((2.0/(GAMMA(J)-1))*(((PT(J)/PI(J))**((1-GAMMA(J))
     +  /GAMMA(J)))-1))**0.5
      D(J)=(1+(((GAMMA(J)-1)/2.0)*(MACH(J)**2)))**
     +  ((GAMMA(J)+1)/(2.0*(GAMMA(J)-1)))
      MFL(J) = A*B(J)*(MACH(J)/D(J))
      END IF

* Calculate mass fraction and mass in the inflator and the tank
      M(J) = MFL(J)*DELT
      MI(J+1) = MI(J)-M(J)
      MT(J+1) = MT(J)+M(J)

* Calculate density in the inflator and the tank
      RI(J+1) = MI(J+1)/VI
      RT(J+1) = MT(J+1)/VT

* Calculate new internal energy
      UI(J+1) = UI(J)-(M(J)*((MFC*CPCI(J))+(MFH*CPHI(J))+
     +  (MFH1*CPH1I(J))+(MFH2*CPH2I(J))+(MFO1*CPO1I(J))+
     +  (MFO2*CPO2I(J))+(MFCO*CPCOI(J))+(MFOH*CPOHI(J))+
     +  (MFHO*CPHOI(J))+(MFI1*CPI1I(J))+
     +  (MFI2*CPI2I(J))+(MFO3*CPO3I(J)))*TI(J))
```

```
      UT(J+1) = UT(J)+(M(J)*((MFC*CPCI(J))+(MFH*CPHI(J))+
     +  (MFH1*CPH1I(J))+(MFH2*CPH2I(J))+(MFO1*CPO1I(J))+
     +  (MFO2*CPO2I(J))+(MFCO*CPCOI(J))+(MFOH*CPOHI(J))+
     +  (MFHO*CPHOI(J))+(MFI1*CPI1I(J))+
     +  (MFI2*CPI2I(J))+(MFO3*CPO3I(J)))*TI(J))

* Calculate new temperatures
      TI(J+1) = UI(J+1)/(MI(J+1)*((MFC*CVCI(J))+
     -  (MFH*CVHI(J))+
     +  (MFH1*CVH1I(J))+(MFH2*CVH2I(J))+(MFO1*CVO1I(J))+
     +  (MFO2*CVO2I(J))+(MFCO*CVCOI(J))+(MFOH*CVOHI(J))+
     +  (MFHO*CVHOI(J))+(MFI1*CVI1I(J))+
     +  (MFI2*CVI2I(J))+(MFO3*CVO3I(J))))
      TT(J+1) = UT(J+1)/((MT(1)*CVPT(J))+((MT(J+1)-MT(1))*
     +  ((MFC*CVCT(J))+(MFH*CVHT(J))+
     +  (MFH1*CVH1T(J))+(MFH2*CVH2T(J))+(MFO1*CVO1T(J))+
     +  (MFO2*CVO2T(J))+(MFCO*CVCOT(J))+(MFOH*CVOHT(J))+
     +  (MFHO*CVHOT(J))+(MFI1*CVI1T(J))+
     +  (MFI2*CVI2T(J))+(MFO3*CVO3T(J))))))

* Calculate the molecular weight
      MCP(J+1)    = MT(J+1)-MT(1)
      MOLCP(J+1)=(MCP(J+1)*1000)/MWI(1)
      MOLP = (MT(1)*1000)/MWT(1)
      MWI(J+1)=MWI(1)
      MWT(J+1)=(MT(J+1)/(MOLCP(J+1)+MOLP))*1000

* Calculate new pressures
      PI(J+1) = (RI(J+1)*R*TI(J+1))/MWI(J+1)
      PT(J+1) = (RT(J+1)*R*TT(J+1))/MWT(J+1)

* Update time
      COUNT = COUNT + 1
      TIME(J+1) = TIME(J)+DELT
 200  CONTINUE

* Print the values of the variables
 300  WRITE (5,*)'COUNT=',COUNT,N
      WRITE (5,*)'TIME    PRES RATIO    CRIT PRES RATIO'
      DO 350 K=1,COUNT
      WRITE (5,*) TIME(K),PRATIO(K),PCRIT(K)
 350  CONTINUE
      WRITE (5,*)' TIME          MFLOW                MASS'
      DO 400 K=1,COUNT
      WRITE (5,*) TIME(K),MFL(K),M(K)
 400  CONTINUE
      WRITE (5,*)' TIME          INFL MASS              TANK MASS'
      DO 500 L=1,COUNT
      WRITE (5,*) TIME(L),MI(L),MT(L)
```

```
500     CONTINUE
        WRITE (5,*)' TIME          INFL IE                TANK IE'
        DO 600 L=1,COUNT
        WRITE (5,*) TIME(L),UI(L),UT(L)
600     CONTINUE
        WRITE (5,*)' TI            TT          PI             PT'
        DO 700 L=1,COUNT
        WRITE (5,*) TI(L),TT(L),PI(L),PT(L)
700     CONTINUE
        CLOSE (UNIT=5, STATUS='KEEP')
        END
```

COUNT = 12 100

TIME	PRES RATIO	CRIT PRES RATIO
0.000000E+00	1.937271E-03	5.645452E-01
4.000000E-04	8.638904E-03	5.639658E-01
8.000000E-04	1.721008E-02	5.635213E-01
1.200000E-03	3.048640E-02	5.630354E-01
1.600000E-03	5.054171E-02	5.625408E-01
2.000000E-03	8.038997E-02	5.620250E-01
2.400000E-03	1.239736E-01	5.614901E-01
2.800000E-03	1.866390E-01	5.609360E-01
3.200000E-03	2.754803E-01	5.603642E-01
3.600000E-03	3.998631E-01	5.597764E-01
4.000000E-03	5.720295E-01	5.591742E-01
4.400000E-03	8.077232E-01	5.585596E-01

TIME	MFLOW	MASS
0.000000E+00	7.876558	3.150623E-03
4.000000E-04	4.721460	1.888584E-03
8.000000E-04	2.977732	1.191093E-03
1.200000E-03	1.918157	7.672629E-04
1.600000E-03	1.264861	5.059446E-04
2.000000E-03	8.506652E-01	3.402661E-04
2.400000E-03	5.823665E-01	2.329466E-04
2.800000E-03	4.050603E-01	1.620241E-04
3.200000E-03	2.857921E-01	1.143168E-04
3.600000E-03	2.042704E-01	8.170816E-05
4.000000E-03	1.476802E-01	5.907209E-05
4.400000E-03	8.979551E-02	3.591820E-05

TIME	INFL MASS	TANK MASS
0.000000E+00	8.673000E-03	8.020000E-02
4.000000E-04	5.522377E-03	8.335062E-02
8.000000E-04	3.633793E-03	8.523920E-02
1.200000E-03	2.442700E-03	8.643030E-02
1.600000E-03	1.675437E-03	8.719756E-02
2.000000E-03	1.169493E-03	8.770350E-02
2.400000E-03	8.292268E-04	8.804377E-02
2.800000E-03	5.962802E-04	8.827672E-02
3.200000E-03	4.342561E-04	8.843875E-02
3.600000E-03	3.199393E-04	8.855306E-02
4.000000E-03	2.382311E-04	8.863477E-02
4.400000E-03	1.791590E-04	8.869385E-02

TIME	INFL IE	TANK IE
0.000000E+00	65486.290000	17723.130000
4.000000E-04	36948.120000	46261.300000
8.000000E-04	21975.760000	61233.670000
1.200000E-03	13393.580000	69815.840000
1.600000E-03	8375.466000	74833.960000
2.000000E-03	5352.496000	77856.930000
2.400000E-03	3487.762000	79721.660000
2.800000E-03	2312.269000	80897.160000
3.200000E-03	1556.916000	81652.510000
3.600000E-03	1063.109000	82146.310000
4.000000E-03	735.241600	82474.180000
4.400000E-03	514.553500	82694.870000

TI	TT	PI	PT
4148.770000	298.150000	5.231675E+07	101351.700000
3676.247000	737.974900	2.949415E+07	254797.100000
3372.571000	862.983300	1.780437E+07	306414.600000
3092.358000	926.126200	1.097401E+07	334557.900000
2853.851000	961.288500	6946480.000000	351087.000000
2645.067000	982.132000	4494066.000000	361277.800000
2461.773000	994.729500	2965696.000000	367668.000000
2299.338000	1002.518000	1991858.000000	371758.400000
2154.332000	1007.401000	1359139.000000	374416.000000
2023.946000	1010.505000	940744.500000	376169.000000
1905.952000	1012.500000	659653.300000	377341.200000
1798.624000	1013.796000	468149.200000	378134.900000

B.5 CEA Program Output for a 30/60 Mixture (Example 1)

```
*******************************************************************************
      NASA-LEWIS CHEMICAL EQUILIBRIUM PROGRAM CEA, DEC. 12, 1996
            BY BONNIE MCBRIDE AND SANFORD GORDON
    REFS: NASA RP-1311, PART I, 1994 AND NASA RP-1311, PART II, 1996
*******************************************************************************
reac  fuel=CH4 mole=0.02086448 t=298
      oxid=O2  mole=0.05195256 t=298
prob  uv  rho(g/cc)=0.007988575
output cal massf
end
```

THERMODYNAMIC PROPERTIES	
P, ATM	105.57
T, K	3807.85
RHO, G/CC	7.9886-3
H, CAL/G	112.14
U, CAL/G	-207.90
G, CAL/G	-10152.4
S, CAL/(G)(K)	2.6956
M, (1/n)	23.643
(dLV/dLP)t	-1.05134
(dLV/dLT)p	1.8547
Cp, CAL/(G)(K)	1.7079
GAMMAs	1.1337
SON VEL,M/SEC	1232.1

MASS FRACTIONS	
*CO	0.13216
*CO2	0.25207
COOH	0.00004
*H	0.00089
HCO	0.00001
HO2	0.00094
*H2	0.00313
H2O	0.29529
H2O2	0.00010
*O	0.02564
*OH	0.08469
*O2	0.20502
O3	0.00001

* THERMODYNAMIC PROPERTIES FITTED TO 20000.K

B.6 CEA Program Output for a 90/180 Mixture (Example 2)

```
*****************************************************************************
      NASA-LEWIS CHEMICAL EQUILIBRIUM PROGRAM CEA,  DEC. 12, 1996
            BY  BONNIE MCBRIDE AND SANFORD GORDON
       REFS: NASA RP-1311, PART I, 1994 AND NASA RP-1311, PART II, 1996
*****************************************************************************
reac  fuel=CH4 mole=0.0625934 t=298
      oxid=O2   mole=0.1354105 t=298
prob  uv  rho(g/cc)=0.02134858
output cal massf
end

THERMODYNAMIC PROPERTIES
P, ATM                    308.94
T, K                     4046.39
RHO, G/CC               2.1349-2
H, CAL/G                  119.34
U, CAL/G                  -231.12
G, CAL/G                 -10855.1
S, CAL/(G)(K)              2.7121
M, (1/n)                  22.945
(dLV/dLP)t              -1.05103
(dLV/dLT)p                1.7987
Cp, CAL/(G)(K)            1.6212
GAMMAs                    1.1387
SON VEL,M/SEC             1292.2

MASS FRACTIONS
*CO                     0.16372
*CO2                    0.25874
COOH                    0.00010
*H                      0.00093
HCO                     0.00004
HO2                     0.00122
*H2                     0.00413
HCOOH                   0.00001
H2O                     0.33236
H2O2                    0.00020
*O                      0.01991
*OH                     0.08399
*O2                     0.13464
O3                      0.00001
*  THERMODYNAMIC PROPERTIES FITTED TO 20000.K
```

B.7 CEA Program Output for a 125/250 Mixture (Example 3)

```
*****************************************************************************
      NASA-LEWIS CHEMICAL EQUILIBRIUM PROGRAM CEA,  DEC. 12, 1996
            BY  BONNIE MCBRIDE AND SANFORD GORDON
     REFS: NASA RP-1311, PART I, 1994 AND NASA RP-1311, PART II, 1996
*****************************************************************************
reac  fuel=CH4 mole=0.08693535 t=298
      oxid=O2   mole=0.18409430 t=298
prob  uv  rho(g/cc)=0.02914192
output cal massf
end

THERMODYNAMIC PROPERTIES
P, ATM                    429.51
T, K                     4112.54
RHO, G/CC                2.9142-2
H, CAL/G                  122.10
U, CAL/G                 -234.83
G, CAL/G                -10983.7
S, CAL/(G)(K)             2.7005
M, (1/n)                  22.897
(dLV/dLP)t              -1.04988
(dLV/dLT)p                1.7685
Cp, CAL/(G)(K)            1.5710
GAMMAs                    1.1401
SON VEL,M/SEC             1304.9

MASS FRACTIONS
*CO                     0.16734
*CO2                    0.26201
COOH                    0.00013
*H                      0.00089
HCO                     0.00005
HO2                     0.00134
*H2                     0.00423
HCOOH                   0.00002
H2O                     0.33984
H2O2                    0.00024
*O                      0.01827
*OH                     0.08259
*O2                     0.12303
O3                      0.00001
*  THERMODYNAMIC PROPERTIES FITTED TO 20000.K
```

B.8 CEA Program Output for a 150/300 Mixture (Example 4)

```
*****************************************************************************
      NASA-LEWIS CHEMICAL EQUILIBRIUM PROGRAM CEA,  DEC. 12, 1996
            BY  BONNIE MCBRIDE AND SANFORD GORDON
     REFS: NASA RP-1311, PART I, 1994 AND NASA RP-1311, PART II, 1996
*****************************************************************************
reac  fuel=CH4 mole=0.1043224 t=298
      oxid=O2   mole=0.2188684 t=298
prob  uv  rho(g/cc)=0.03470858
output cal massf
end

THERMODYNAMIC PROPERTIES
P, ATM                    516.19
T, K                     4148.77
RHO, G/CC              3.4709-2
H, CAL/G                  123.70
U, CAL/G                 -236.46
G, CAL/G                -11044.6
S, CAL/(G)(K)             2.6919
M, (1/n)                  22.891
(dLV/dLP)t              -1.04915
(dLV/dLT)p                1.7509
Cp, CAL/(G)(K)            1.5415
GAMMAs                    1.1409
SON VEL,M/SEC             1311.2

MASS FRACTIONS
*CO                     0.16848
*CO2                    0.26413
COOH                    0.00015
*H                      0.00087
HCO                     0.00006
HO2                     0.00141
*H2                     0.00426
HCOOH                   0.00003
H2O                     0.34353
H2O2                    0.00027
*O                      0.01741
*OH                     0.08171
*O2                     0.11769
O3                      0.00001
*  THERMODYNAMIC PROPERTIES FITTED TO 20000.K
```

REFERENCES

1. "Air Bags," Insurance Institute of Highway Safety, Arlington, VA, (Apr. 1992).

2. "Q & A : Airbags," Insurance Institute for Highway Safety, Arlington, VA, (Jan. 1997).

3. "Federal Motor Vehicle Safety Standards ; Occupant Crash Protection," Docket No. 74-14, National Highway Traffic Safety Administration, Washington, D. C.

4. "Airbag Statistics," Insurance Institute for Highway Safety, Arlington, VA, (Jun. 9, 1997).

5. "Slower Airbags Safer for Kids," The Courier-News, (Mar. 15, 1997).

6. "Air Bags Reduce Driver Fatalities by 11 Percent," NHTSA 74-96, U. S. Department of Transportation, Washington, D. C., (Oct. 3, 1996).

7. Crouch, E. T., "Evolution of Airbag Components and Materials," (SAE Paper No. 932912), Worldwide Passenger Car Conference and Exposition, Dearborn, MI, (Oct. 25-27, 1993).

8. Sherman, D., "The Rough Road to Air Bags," Invention & Technology, Vol. 11, No. 1, (Sept. 1995).

9. Private Communication with Jim Simmons, Department of Transportation, Washington, D. C., (Aug. 15, 1997).

10. Berger, J. M. and Butler, P.B., "Equilibrium Analysis of Three Classes of Automotive Airbag Inflator Propellants," Combustion Science and Technology, Vol. 104, (1995).

11. Vos, T. H., and Goetz, G.W., "Inflatable Restraint Systems : Helping Save Lives on the Road," TRW Space & Defense Quest (Winter 1989/1990).

12. "Side-Impact Air Bags New on Safety Marquee," Insurance Institute for Highway Safety Status Report, Vol. 31, No. 4, (May 1996).

13. Ashley, S., "Automotive Safety is in the Bag," Mechanical Engineering, (Jan. 1994).

14. Karlow, J. P. et al., "Development of a New Downsized Airbag System for Use in Passenger Vehicles," (SAE Paper No. 940804), Safety Technology (SP-1041), International Congress & Exposition, Detroit, MI, (Feb.28-Mar.3, 1994).

15. McBride, B.J. and Gordon, S., "Computer Program for Calculation of Complex Chemical Equilibrium Compositions and Applications, Vol. I : Analysis," NASA Reference Publication 1311, (Oct. 1994).

16. McBride, B.J. and Gordon, S., "Computer Program for Calculation of Complex Chemical Equilibrium Compositions and Applications, Vol. II : Users Manual and Program Description," NASA Reference Publication 1311, (June 1996).

17. Steinle, J. U. and Franck, E. U., "High Pressure Combustion-Ignition Temperatures to 1000 bar," Ber. Bunsen-Ges., Vol. 99, No. 1, (1995).

18. Dryer, F. L. and Glassman, I., 14th International Symposium on Combustion, Combustion Institute, Pittsburgh, Pennsylvania, page 987, (1972).

19. Westbrook, C. K., et al., Journal of Physical Chemistry, Vol. 81, page 2452, (1977).

20. Stevens, H.O., et al., "Computer Simulation of the Pyrotechnic Inflator for Automobile Inflatable Restraint Systems," DOT-806 267, (1982).

21. Wang, J. T. "Recent Advances in Modeling of Pyrotechnic Inflators for Inflatable Restraint Systems," ASME Publication AMD-Vol. 106 and BED-Vol. 13, (Dec. 1989).

22. Butler, P. B. et al., " Modeling and Numerical Simulation of the Internal Thermochemistry of Automotive Airbag Inflators," Prog. Energy Combust. Sci, Vol. 19, (1993).

23. Materna, P., "Advances in Analytical Modeling of Airbag Inflators," (SAE Paper No. 920120), Analytical Modeling and Occupant Protection Technologies (SP-906), International Congress & Exposition, Detroit, MI, (Feb. 24-28, 1992).

24. Chan, S.K., "A Lumped-Parameter Air Bag Gas Generator Model," Proceedings Int. Pyrotechnic Seminar, 20th , (1994).

25. "Rupture Disc Selection Guide," No. 1-1100, Continental Disc Corporation, (1991).

26. "Standard-Type Rupture Disc Catalog," No. STD-1184, Continental Disc Corporation, (1984).

27. "M-100 Series Electric Matches," Specification Sheet, ICI Aerospace, Valley Forge, PA, (1987).

28. "Specification Sheet for Pyrofuze Wire," Sigmund Cohn Corp., Mount Vernon, NY, (1993).

29. "NJIT – Data Acquisition Software," Breed Technologies, Inc., Boonton, NJ, (1994).

30. "Temperature Measurement Handbook," Vol. VIII, NANMAC Corporation, Framingham, MA.

31. "Series 550P Gas Chromatograph," Gow-Mac Instrument Co., Bound Brook, NJ, (Feb. 1986).

32. "Alltech Catalog 400," Alltech Associates, Inc., Deerfield, IL, (1997).

33. "HP3396 Series II Integrator Manual", Hewlett-Packard Co., (Jun. 1990).

34. Private Communication with Bill MaCloud, Breed Technologies, Inc., Lakeland, FL, (Jul. 1997).

35. Private Communication with Breed Technologies, Inc., Lakeland, FL, (Mar. 20, 1997).

36. "Specification Sheet on Hot and Cold Condition Experiments," Breed Technologies, Inc., Boonton, NJ.

37. "Carbon Monoxide Emission Limits for Airbags," Inter-Office Memo., Breed Technologies, Inc., Boonton, NJ, (Jan. 24, 1996).

38. Weast, R.C., *Handbook of Chemistry and Physics (49th Ed.)*, The Chemical Rubber Company, Cleveland, OH, (1968-69).

39. Perry, R. H. and Green, D. W., *Perry's Chemical Engineers' Handbook (6th Ed.)*, McGraw-Hill Book Company, New York, NY, (1984).

40. Bejan, A., *Advanced Engineering Thermodynamics*, John Wiley & Sons, Inc., New York, NY, (1988).

41. Shapiro, A.H., *The Dynamics and Thermodynamics of Compressible Fluid Flow (Vol. I)*, The Ronald Press Company, New York, NY, (1953).

42. Wang, J. T., "Are Tank Pressure Curves Sufficient to Discriminate Air Bag Inflators?," SAE Transactions, Vol. 100, (Paper No. 910808), (1991).

43. Butler, P. B. et al., "Numerical Simulation of Passenger-Side Automotive Airbag Inflators," (SAE Paper No.), (1992).

44. Materna, P. "Analytical Modeling of Pyrotechnic Airbag Inflators," Proceedings of International Symposium on Sophisticated Car Occupant Safety Systems, AIRBAG 2000, Karlsruhe, Germany, (Nov.2-3, 1992).

45. Schmitt, R. G. et al., "Performance and CO Production of a Non-azide Airbag Propellant in a Pre-pressurized Gas Generator," Combustion Science and Technology, Vol. 122, No. 1-6, (1997).

46. Yoshida, Tadao, "Simulation of Non-Azide Gas Generant for Automotive Air Bag Inflators," Proceedings Int. Pyrotech. Seminar, Vol. 19, (1994).

47. Kee, R. J., Rupley, F. M. and Miller, J. A., "The Chemkin Thermodynamic Data Base," Sandia Report SAND87-8215B.UC-4, (Feb. 1992).

48. "1995 Ford Taurus Air Bag Specification Sheet," Breed Technologies, Inc., Boonton, NJ.

49. Rink, K. K., "Autoignition of a Fluid Fueled Inflator," U.S. Patent No. 5.494,312, (Feb. 1996).

50. Frantom, R. L., "Hybrid Airbag Inflator Technology,, Airbag 2000 --- International Symposium on Sophisticated Car Occupant Safety Systems, Karlsruhe, Germany, (1992).

51. Fried, L. E., "CHEETAH 1.39 --- User's Manual," Lawrence Livermore National Laboratory, (Mar. 19, 1996).

52. Hanna, M. and Karim, G. A., "The Combustion of Lean Mixtures of Methane and Air – A Kinetic Investigation," Journal of Energy Resources Technology, Vol. 108, (Dec. 1986).

53. Di Blasi, C. et al., "Numerical Simulation of Forced Ignition of Methane-oxygen Mixtures," Rev. Gen. Therm., (Dec. 1984).